1970

# An Adaptive Redundancy Reduction Technique

Seon J. Chung

# AN ADAPTIVE REDUNDANCY REDUCTION TECHNIQUE

BY

SEON J. CHUNG

A thesis submitted
in partial fulfillment of the requirements for the
degree Master of Science, Department of
Electrical Engineering, South Dakota
State University

1970

**AN ADAPTIVE**
**REDUNDANCY REDUCTION TECHNIQUE**

This thesis is approved as a creditable and independent investigation by a candidate for the degree, Master of Science, and is acceptable as meeting the thesis requirements for this degree, but without implying that the conclusions reached by the candidate are necessarily the conclusions of the major department.

Thesis Advisor _____ Date _____

Head, Electrical Engineering Department _____ Date _____

ACKNOWLEDGEMENTS

The author wishes to express his appreciation and gratitude to Dr. D. E. Sander, whose guidance and advice made this investigation possible and to Mr. Edward Quade who helped the author with computer programming.

S. J. C.

TABLE OF CONTENTS

Chapter Page

LIST OF FIGURES

Figure Page

# LIST OF TABLES

# CHAPTER I

## INTRODUCTION

In telemetry systems, the limited power available from the RF transmitter imposes a constraint on the data transmission rate. For example, a spacecraft's ability to communicate with a ground receiving station decreases with the square of the distance, and electrical power to operate the system increases with the data transmission rate. To solve this problem, considerable attention has been devoted toward improving the efficiency of telemetry systems by selecting advantageous coding, modulation and reconstruction techniques.[10, 23]

One technique which is used to achieve this goal is to design a telemetry system which transmits only the significant information contained in the source data instead of transmitting all of the data so that the system capacity is maximized while the power requirements and size of the system is minimized. This technique is called data compression. Data compression reduces the bandwidth needed to transmit a given amount of information in a given time or it can reduce the time needed to transmit a given amount of information in a given bandwidth.[11]

While basic data compression techniques have been applied for many years in the off-line processing of data and by human analysts in seeking significant changes in data, their application to on-line service and particularly to space vehicles has been quite recent.

Such compression must be accomplished without sacrificing the information requirements of the user. The performance enhancement of a basic data acquisition system by incorporation of data compression can be manifested in a variety of ways, depending on the manner in which the data compressor is utilized in the system and the performance desired. As shown in Figure 1-1, the engineer has the option of incorporating data compression into either the transmitter or the receiver portions of the system. Four basic categories of data handling come under this definition: parameter extraction, adaptive sampling, redundancy reduction and coding. Figure 1-2 shows a schematic classification of data compression techniques by category.[11]

Parameter Extraction

Parameter extraction is a technique that reduces the bandwidth required to transmit a given data sample by means of an information-describing irreversible transformation. These transformations are considered irreversible because, while they provide useful descriptions of the input signal, they so distort the signal that it is impossible to reconstruct the original waveform. Signal conditioning devices producing reductions in source information bandwidth are in this category. Spectrum analyzers, peak detectors, phase comparators, and the like are typical examples of the virtually unlimited number of techniques that have been used or could be devised.

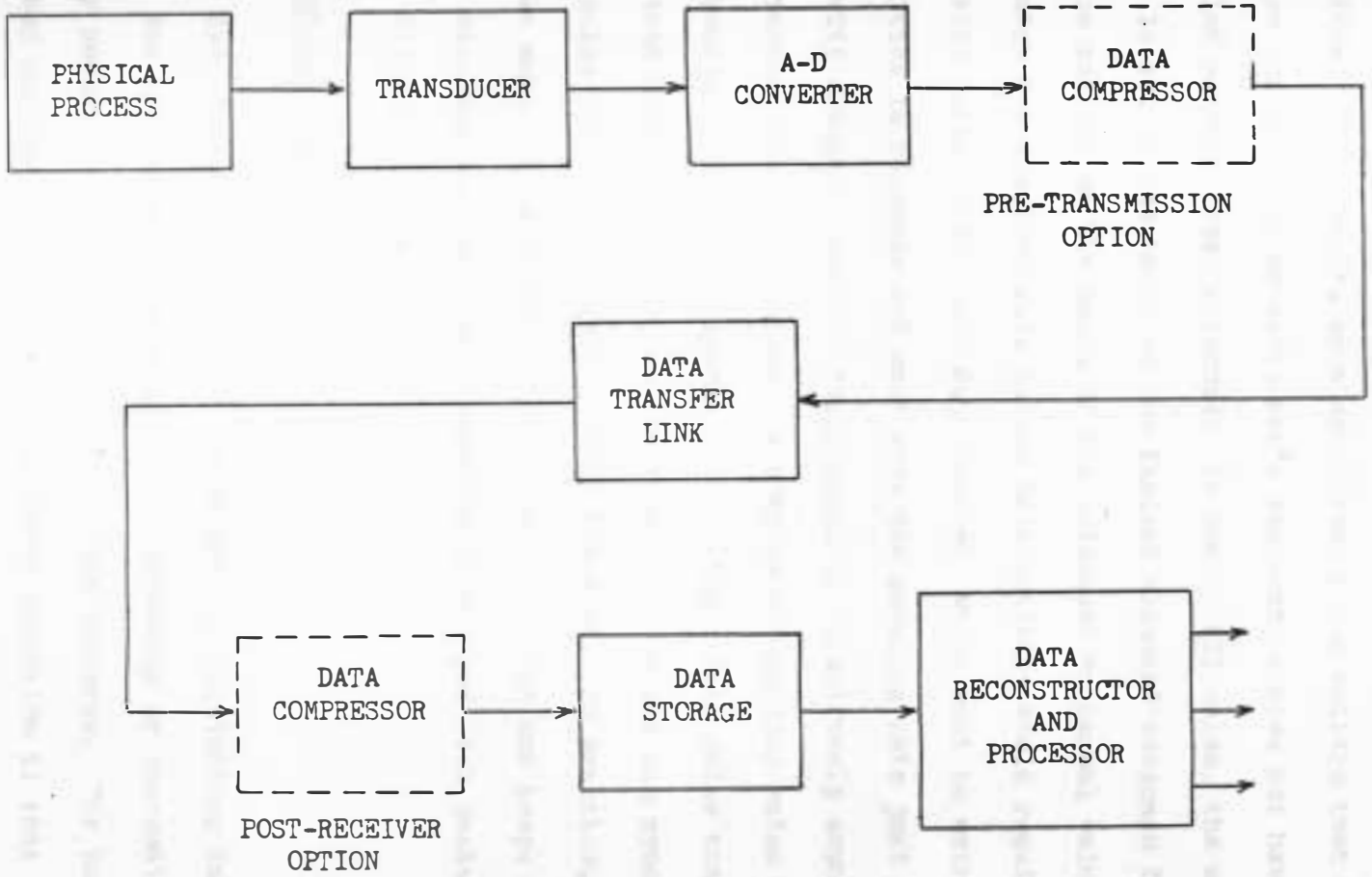


Figure 1-1. Basic data acquisition system block diagram showing integration of data compression.[4]

## Adaptive Sampling

Most of the time, present telemetry systems greatly oversample the data. For example, on a satellite, a d-c voltage that does not change for days, or an astronaut's temperature does not have to be sampled several times a second. In nearly all cases, the sampling rate is set on the basis of the fastest expected response from the source and not on the basis of the quiescent or normal value. However, to match the sampling rate to the data activity would require an activity detector for each data channel, which nust be extremely sensitive in response and must vary the sampling rate just before the activity changes. Another requirement is an extremely sophisticated programmer which will intermix a complex of sampling rates from many independently varying channels into a single data pulse train having a constant output rate so that the receiving station can synchronize with the pulse train and thereby recover the data. In practice, such a system makes the most effective use of bandwidth and keeps the sampling rate at a minimum, both on a per-channel and per-link basis, but is very difficult to implement.[11]

## Redundancy Reduction

Redundancy reduction is a technique for eliminating data samples that can be implied by examination of preceding or succeeding samples or by comparison with arbitrary reference patterns. The basic difference between adaptive sampling and redundancy reduction is that in adaptive

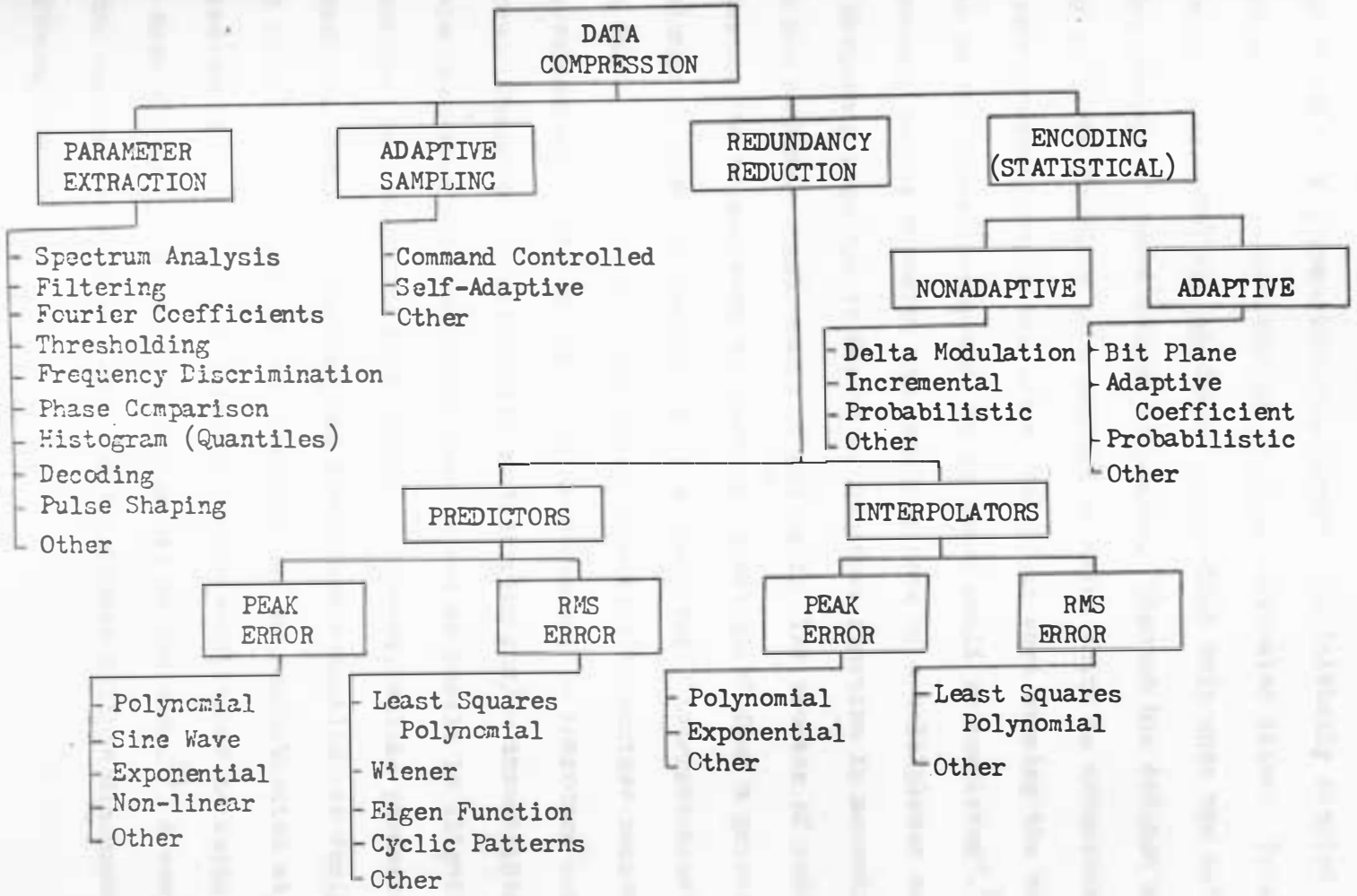


Figure 1-2. Classification of data compression models.[11]

sampling, the sampling rate of the original data waveform is varied, while in redundancy reduction the waveform is initially sampled at a constant rate and nonessential samples eliminated later. Thus, as in adaptive sampling, an output is provided only when the data change exceeds a predetermined tolerance. Shannon has defined redundancy as "that fraction of a message or datum which is unnecessary and hence repetitive in the sense that if it were missing the message would be essentially complete, or at least could be completed".[11] Redundancy exists whenever the sampling rate of a multiplexer exceeds the frequency required to describe the input function in accordance with the accuracy requirements of the user. The process of redundancy reduction can be achieved by means of "prediction" from a priori knowledge of previous sample, or by a posteriori "interpolation" from future samples. For redundancy reduction to achieve reasonable compression efficiencies, it is often necessary to introduce certain errors. These errors are caused by filtering and/or thresholding within the redundancy reduction process and do result in slight reductions in the source data entropy. However, unlike parameter extraction, adaptive sampling and redundancy reduction are designed such that the original source waveforms can be reconstructed with a guaranteed fidelity. This fidelity can be established to supply the data within the accuracy requirements of the user.[11] A review of the various redundancy reduction techniques will be discussed in the following chapter.

## Encoding

Encoding is a technique for transforming a given message into a corresponding sequence of code words. As in the cases of adaptive sampling and redundancy reduction, an effective coding technique requires sequential message words to exhibit a high average correlation. Consequently to achieve the desired coding it is necessary to know the source statistics. If statistics are stationary and are known a priori, a nonadaptive encoding procedure can be specified. In many cases, however, the statistics are not well-known to the experimenter, and/or the statistics of the measurement source may be nonstationary. Under these conditions a nonadaptive encoding procedure can result in a bandwidth expansion instead of a reduction. To solve this problem, adaptive encoding techniques can be devised whereby the code assignments are based upon the most recent statistics measured by the encoder itself.[11]

The purpose of this work is to analyze, by computer simulation, a redundancy reduction technique which was proposed by Sander in (18). A function of time is sampled and a redundancy reduction technique is applied that determines the sampling instants by holding constant or fixing the sampled amplitude changes from one non-redundant sampling instant to the next. This redundancy reduction technique reduces the number of samples needed to reproduce the function from sampled data within acceptable accuracy limits, thereby decreasing memory requirements in computers and data storage systems. The technique

will be advantageous for large volume data storage, function modeling, sampled data control systems, and bioengineering problems dealing with both measurements and simulation.[18]

Results of the analysis will be compared with those of the conventional technique. Therefore, the analysis of the redundancy reduction technique will consist of studies concerning the effects of parameters such as sampling rate, quantization level size and number of quantization levels, on peak error, mean square error, variances of error, compression ratio and the signal-to-noise ratio for various conditions and signals.

Chapter II of this dissertation contains a general review of technical literature associated with redundancy reduction, while Chapter III deals with the analysis and practical application of the new technique. A zero-order reconstruction scheme is used and will be discussed in the following chapters. A unit amplitude sine wave is applied as a test input signal and electrocardiogram (ECG) data recorded on magnetic tape is applied as a practical source input signal. An IBM 360/30 computer system is used for simulation. Chapter IV deals with a modified redundancy reduction technique which improves a noise difficulty experienced with the proposed redundancy reduction technique and Chapter V contains conclusions obtained from the results.

# CHAPTER II

## REVIEW OF TECHNICAL LITERATURE

The modulation systems in communication are classified into two categories; "continuous wave" and "discrete wave" systems. Linear and exponential modulations are continuous wave, and pulse modulation is discrete wave. In discrete wave systems, the carrier is composed of a train of discrete pulses or short bursts. In all modulation systems, the message function is sampled at regular intervals and the samples are used to modulate the carrier pulses, therefore, it is valuable to consider first the sampling principle.

### A. Sampling Principle

It has been mentioned that in pulse modulation systems the message function is sampled and the samples are used to modulate some parameter of the carrier pulses. The advantage derived from transmitting only periodic samples of the message function and not the complete signal is the conservation of time, whereby the time saved may be used to transmit samples from other independent signal sources and thereby realize a time-division multiplex system. At the receiver it is possible to reconstruct the continuous message signal from its periodic samples.

At this point, the question arises; How often must the continuous message signal be sampled in order to be assured that the receiver reconstruct the original waveform? This is the sampling theorem in

the time domain.

A restricted but widely used form of the sampling theorem states: If a signal f(t), a real function of time, is sampled instantaneously at regular intervals and at a rate slightly higher than twice the highest significant signal frequency, then the samples contain all the information of the original signal. Thus, if $f_s$ denotes the sampling rate, and $f_m$ is the highest significant frequency of the signal f(t), then

$$f_s > 2f_m \qquad (2\text{-}1)$$

This theorem is also frequently stated as follows: Any function of time f(t) which is band-limited to B(or $f_m$) cycles/second is completely described by its sample values at every $\frac{1}{2}B$ second, the samples extending throughout the time domain. A corollary is that a channel B cycles wide can be used to transmit 2B independent samples/second. There is theoretically no upper limit on $f_s$. However, as $f_s$ is increased, the available time between samples is decreased and fewer channels can be multiplexed. The lower limit on the sampling frequency is highly significant. There is evidently a relation between the rate at which a signal varies and the number of samples needed to reproduce it exactly, for if the sampling rate is too low, the signal may change radically between sampling times, resulting in a loss of information. Besides this, practically, system errors make it necessary to increase the lower limit of sampling rate higher than $2f_m$ for reliable reproduction of the signal

without distortion. These errors will be discussed later.[12, 16]

B. Delta Modulation (DM)

The delta modulation method is employed in the proposed redundancy reduction technique which this dissertation analyzes, and it is desirable to review literature on the DM principle. Delta modulation uses only one digit code for the input message information. The transmitted pulses carry the message information corresponding to the derivative of the amplitude of the message function, and at the receiving end these pulses are integrated to obtain the original waveform. There are several variations of DM, such as delta-sigma modulation and high information delta modulation, which overcome some of the deficiencies of ordinary delta modulation.

Theory of DM:[16]

In a DM system, instead of the absolute signal amplitude being transmitted at each sampling instant, only the changes are transmitted. The principle of operation of DM can be described with reference to Figure 2-1. It is essentially a quantized feedback system consisting of a pulse generator, a pulse modulator, an integrator, and a difference circuit or comparator. In the encoder, the pulses from the pulse generator are modified by the modulator, which delivers positive pulses if the sign of the difference signal $\in(t)$ is positive and otherwise delivers negative pulses. As shown in Figure 2-2, the transmitted pulse train $e_2(t)$ of positive and negative pulses at the

output of the encoder can be assumed to be generated at a constant clock rate. The difference circuit or comparator at the transmitter decides based on feedback whether the output pulse should be positive or negative. The difference signal from the comparator is derived in the following manner. The delta-modulated output pulse train $e_2(t)$ is synthesized by passing it through the integrating network of the feedback loop, and the resulting waveform $e_1(t)$, which consists of a series of unit steps up and down, is then compared with the original message signal $e_o(t)$ by the comparator. The output of the comparator $\epsilon(t) = e_o(t) - e_1(t)$ decides what the polarity of the output pulse should be in order to correct for the difference between the two voltages. The feedback system tends to reduce the difference, so that the synthesized signal $e_1(t)$ in the form of a step wave follows the message signal $e_o(t)$. In practice, the negative pulses of the output signal $e_2(t)$ may be omitted in the transmission path without affecting the signal-to-noise ratio at the receiving end. This is accomplished by adding a periodic series of positive pulses to $e_2(t)$. The addition of a periodic series of positive pulses to the original pulse series of $e_2(t)$ has only the effect of raising the d-c level by doubling the amplitude of the positive pulses and deleting the negative ones, as all other frequencies are cut off by the low-pass filter.

In the following discussion, however, the approximation signal will be considered to be generated by narrow positive and negative pulses. In the decoder, the delta-modulated pulse train $e_2(t)$

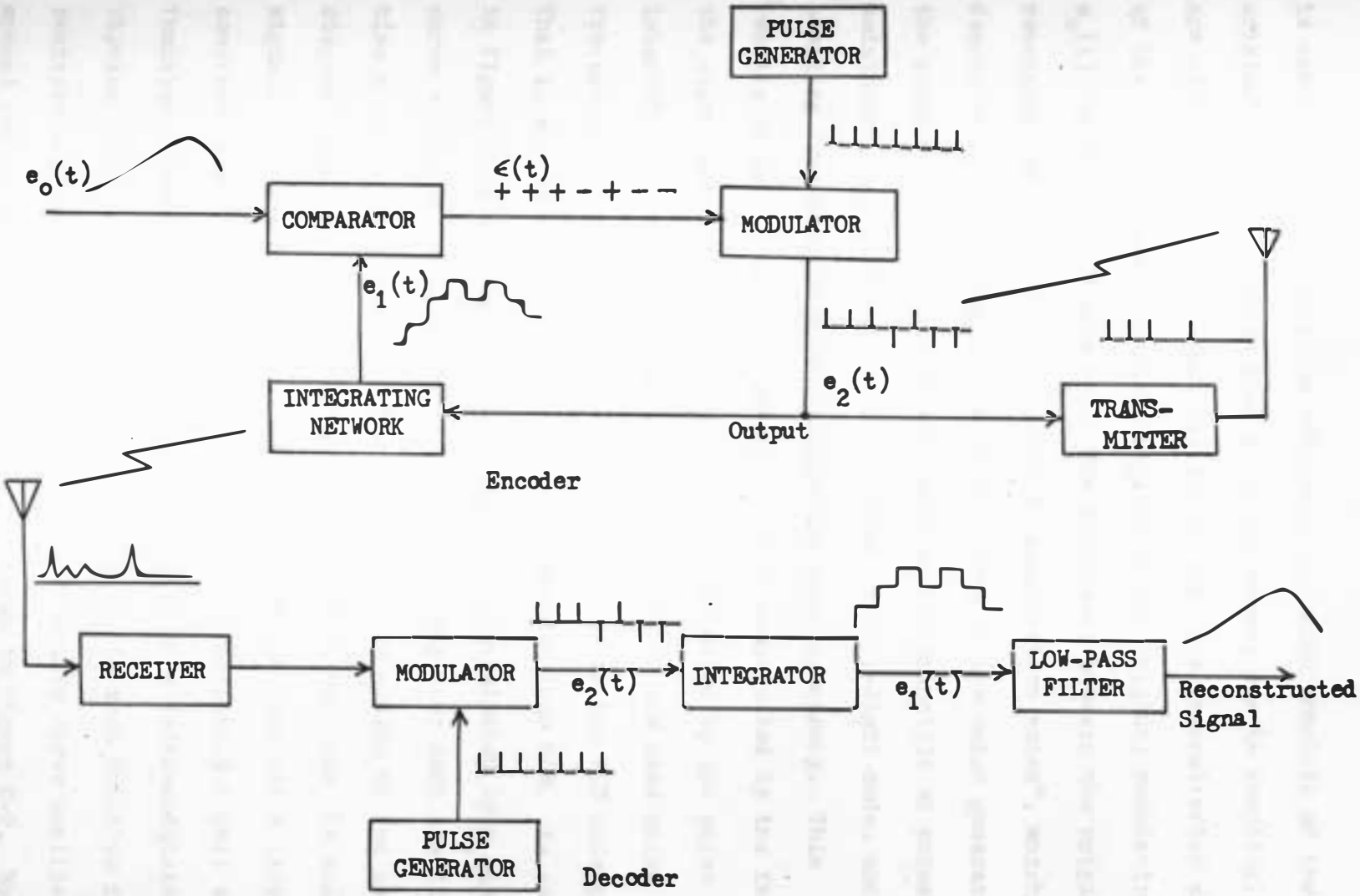


Figure 2-1. Basic circuit for DM.[16]

is again integrated into the voltage $e_1'(t)$ which consists of the original message function plus noise components due to sampling. These are eliminated by a low-pass filter, so that the reconstructed signal of the final output is a close replica of the original modulating signal $e_o(t)$, as shown in Figure 2-2. The difference between the original and reconstructed signals give rise to a "quantization noise", which can be decreased by increasing the pulse frequency of the pulse generator in the encoder. In contrast to the quantization principle of pulse code modulation, the information is quantized in an 1-digit code, and the sampling frequency is made equal to the pulse frequency. This results in very rough quantizing, which is compensated by the fact that the signal samples are taken as often as indicated by the pulse interval and thus n times as often as for PCM at the same pulse frequency, where n equals the number of pulses in the PCM code group. That is why DM requires so much wider bandwidth than PCM. As seen in Figure 2-2, the message signal $e_o(t)$ is approximated by a step curve $e_1(t)$, which is constructed in such a way that each sampling time a unit step upward or downward is made, depending on the synthesized stepped signal at the encoder being lower or higher than the message signal. The integrating network in the feedback loop has a large time constant, and the response to an impulse is practically a unit step function. The input to the integrator $e_2(t)$ is a delta-modulated bipolar pulse train. The output signal $e_1(t)$ is then built up from positive and negative pulses in the form of a step curve oscillating around the information signal $e_o(t)$, as shown in Figure 2-2. By

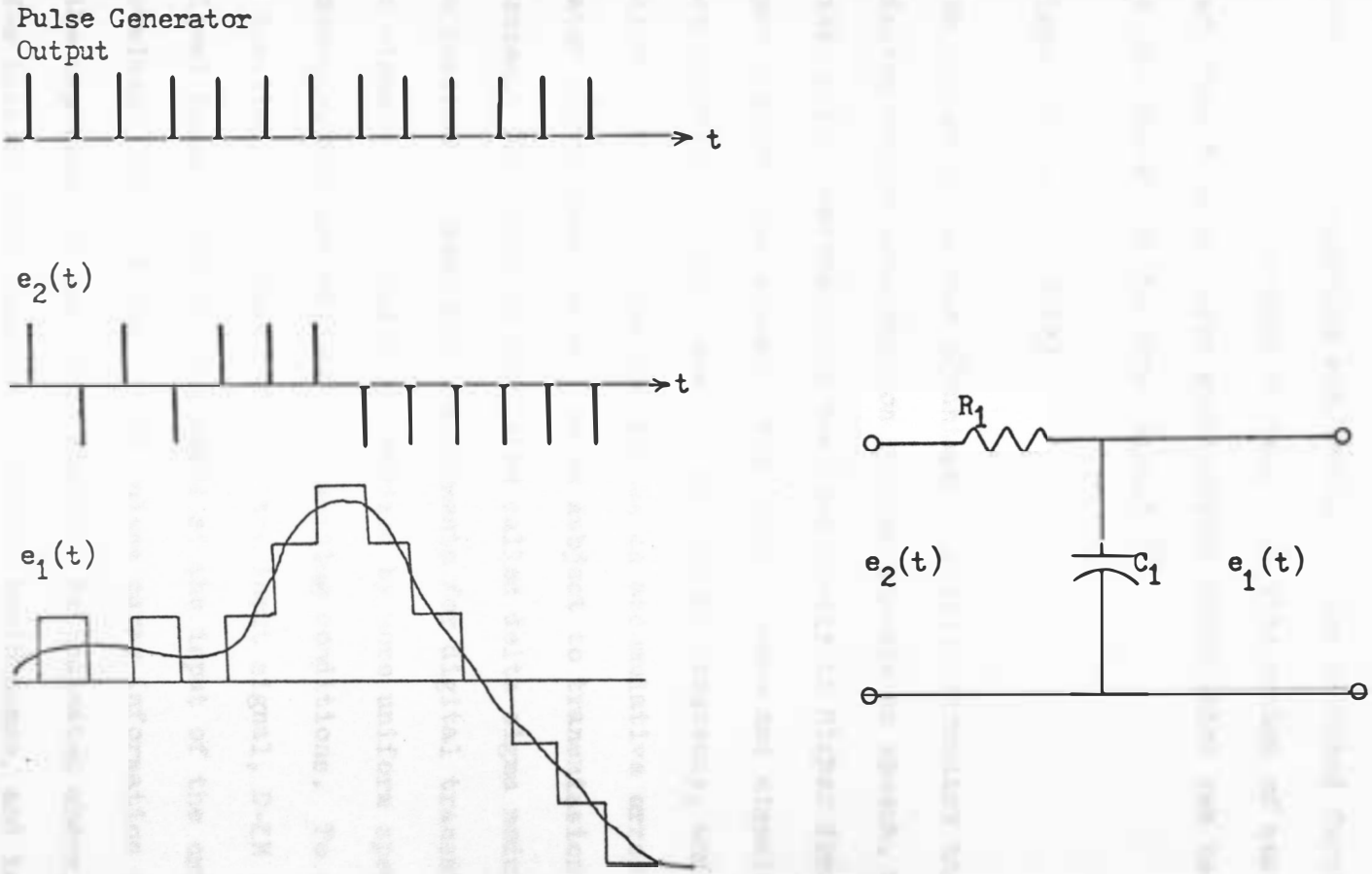


Figure 2-2. DM waveforms using single integrator.

applying the same bipolar pulse train to another integrating network at the decoder, the same approximate replica of the message signal is obtained at the receiving end, which is then smoothed further by passing it through a low-pass filter. But this method of quantization is coarse, resulting in large quantization noise which can be considered as noise correlated to the input signal.[19]

Delta-Sigma Modulation (D-ΣM):

Even though DM has the advantage of simpler circuitry than PCM, it is limited to the transmission of such signals as speech, which does not contain a d-c component and has less energy in higher frequencies. DM can not transmit d-c signals, its dynamic range and signal-to-noise ratio are inversely proportional to the signal frequency, and the integration at the receiving end causes an accumulative error in the demodulated signal when the system is subject to transmission link disturbances. The modified DM system called delta-sigma modulation has been designed to meet the requirements for digital transmission of video signals, which are characterized by more uniform spectra with d-c components, through adverse transmitting conditions. To compensate for the inevitable differentiation of the input signal, D-ΣM system has a signal integration process added at the input of the original delta-modulator, so that the output pulses carry information corresponding to the amplitude of the input signal. As indicated above, D-ΣM offers d-c transmission capability, stable performance, and independence of signal-to-noise ratio from signal frequency. Figure 2-3

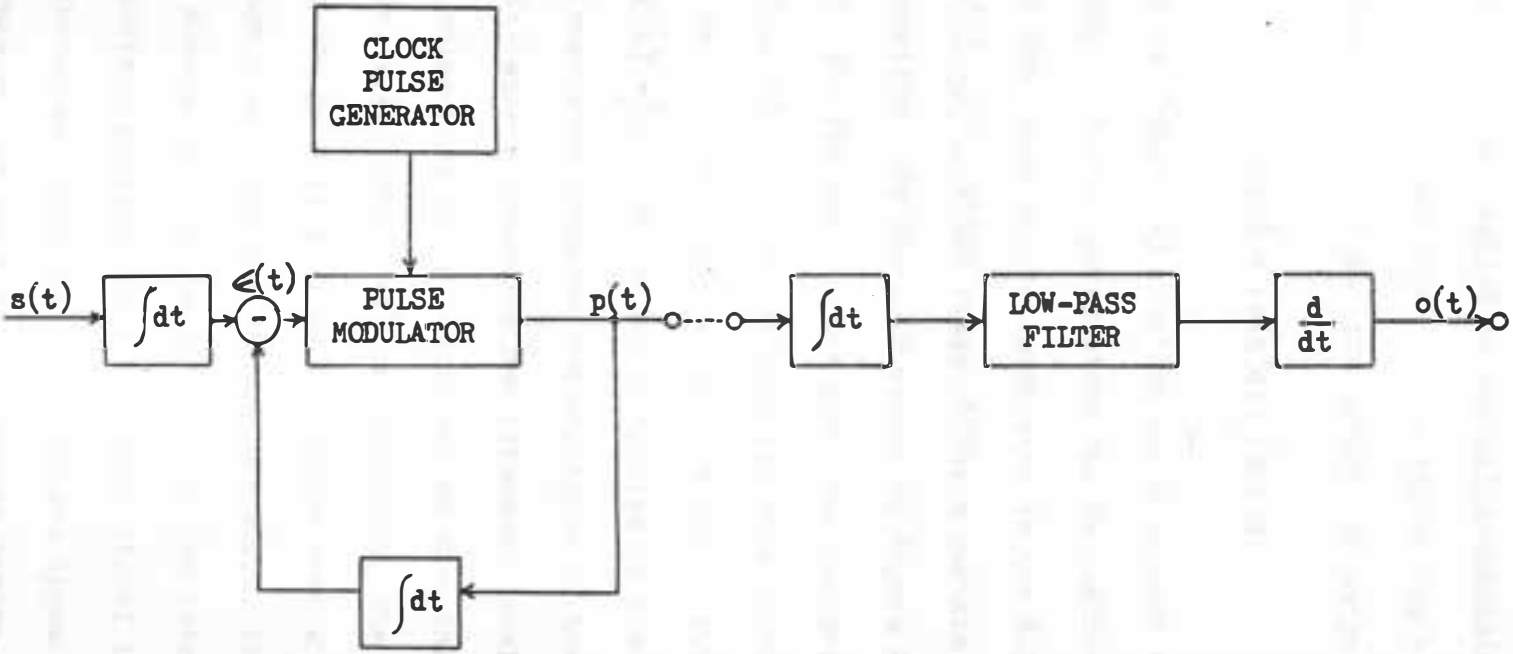


Figure 2-3. Block diagram of Delta-Sigma Modulator.[16]

illustrates delta-sigma modulator. The message signal s(t) is first integrated and then applied to the delta-modulator so that the input to the pulse modulator $\in(t)$ is the difference between the integrated message signal $\int s(t)dt$ and the integrated output pulses $\int p(t)dt$,

$$\in(t) = \int s(t)dt - \int p(t)dt \qquad (2\text{-}3)$$

The system in Figure 2-3 requires an integrator with a very large dynamic range, the two integrators can be combined as shown in Figure 2-4, where the input to the integrator is the difference signal $\Delta(t) = s(t) - p(t)$, which stays within a certain limit for proper system operation. In the D-ΣM system of Figure 2-4, the output pulses p(t) are fed back to the input and subtracted from the input signal s(t), which varies sufficiently more slowly than the sampling pulses. The difference signal $\Delta(t) = s(t) - p(t)$ is integrated to produce $\in(t) = \int \Delta(t)dt$, which is applied to the pulse modulator. The pulse modulator compares the amplitude of the integrated difference signal $\in(t)$ with a predetermined reference level and opens the gate to pass a pulse from the pulse generator when the polarity of $\in(t)$ is positive, i.e., when $\in(t)$ is larger than the reference level, and closes the gate to inhibit the pulses when $\in(t)$ is negative. Thus through this negative-feedback procedure, the integrated difference signal is always kept in the vicinity of the reference level of the pulse modulator, provided that the input signal is not too large. It follows, therefore, that the output pulses appear more frequently as the amplitude of the input signal becomes larger. In other words, the

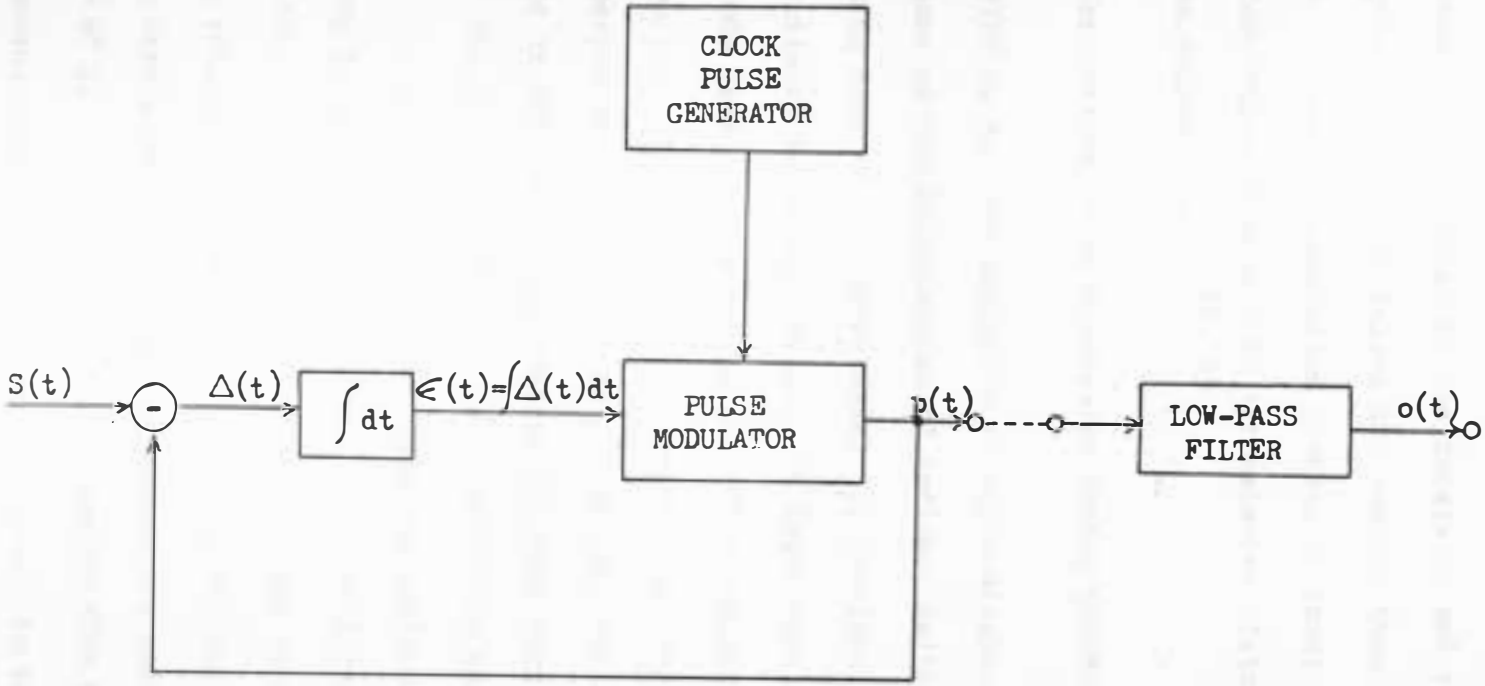


Figure 2-4. Block diagram of the Delta-Sigma Modulator with combined integrator.[16]

output pulses carry the information corresponding to the input-signal amplitude. Demodulation in the receiving end is performed by reshaping the received pulses and passing them through a low-pass filter. Since no integration process is involved in the demodulation, no accumulative error due to transmission disturbances results in the demodulated signal.[16, 25]

High-Information Delta Modulation System (HIDM):

HIDM is another variation of delta-modulation designed to overcome some of the deficiencies of ordinary delta-modulation while retaining most of its advantages. It provides a greater dynamic range than ordinary delta-modulation. In delta-modulation, there is one amplitude level change per pulse. This suggests that with a sequence of n pulses, all of the same polarity, the level change could vary with proper instrumentation as $2^n$, or exponentially. This is accomplished in HIDM where the changes in level vary exponentially with time. The essential difference between HIDM and ordinary delta-modulation is in the manner of counting amplitude levels. In HIDM, counting is performed in binary steps, resulting in an exponential variation of $2^n$ of the amplitude levels due to a sequence of pulses of one polarity such as 1, 2, 4, 8, 16, 64, etc. Should the increment be too large, the pulse direction reverses, reducing in magnitude by a factor of 2. The method of instrumenting HIDM is similar to that for delta-modulation except for the difference in the demodulator.[16, 24]

## C. Redundancy Reduction Scheme

Many redundancy reduction schemes are possible; however, at present those most effective and widely useful are the polynomial predictors and interpolators. Other mathematical forms such as sine waves and exponentials, are more complex and generally not as efficient as the polynomials for most telemetry applications. Among the polynomial predictors, the zero-order predictor is the simplest of all the variable sampling rate techniques. It is used in this dissertation, and therefore, will be discussed in greater detail.[1,4,8,10]

### Zero-Order Predictor :

A predictor is an algorithm that estimates the value of each new data sample based on past performance of the data. If the new value falls within the tolerance range about the estimated new value, it is rejected as redundant since it is known that the data value can be reconstructed within the specific tolerance. Polynomial predictors are based on a finite difference technique which permits an nth-order polynomial to be calculated in successive time increments producing a predicted data point at each increment. A polynomial of the type

$$X(t) = a_0 + a_1 t + a_2 t^2 + \ldots\ldots + a_n t^n \qquad (2\text{-}4)$$

may be fitted to the data points by means of a difference equation,

$$\bar{X}(t) = X_{t-1} + \Delta X_{t-1} + \Delta^2 X_{t-1} + \ldots\ldots + \Delta^n X_{t-1} \qquad (2\text{-}5)$$

where

$\bar{X}(t)$ = predicted value at time t

$X_{t-1}$ = data sample value at one sample period prior to t

$\Delta^{n+1}X_t = \Delta^n X_t - \Delta^n X_{t-1}$

$\Delta X_t = X_t - X_{t-1}$

Here, the n+1 various values, $X_{t-1}$, $X_{t-2}$, $X_{t-3}$, ..... $X_{t-(n+1)}$ are known and $X_t$ is to be predicted.

The simplest predictor is the zero-order predictor which is obtained by letting n equal zero in equation (2-5), as follows

$$X_t = X_{t-1} \tag{2-6}$$

It is important to realize that if $X_{t-1}$ were always taken to be the actual data value, each time a data sample were not transmitted, the value predicted for the next sample could shift up or down, and would become equal to the discarded sample value. If no transmissions occurred over relatively long periods of time, this variation of the predicted values could result in large and uncontrollable errors in the post-transmission reconstruction of the data samples, even though the actual data sample fell each time within the predescribed aperture. In order to avoid these errors, $X_{t-1}$ in (2-6) must be interpreted as the actual sample value only if that value was transmitted, but as the value which was predicted if no transmission occurred. The new predicted value thus becomes the last transmitted value. If this is done, the post-transmission reconstruction of the data sample can be accomplished with a maximum error of K merely by setting each missing sample equal to the one

most recently transmitted. There are three versions of the zero-order predictor; fixed-aperture, floating-aperture and zero-order offset predictor.

In the fixed-aperture version, apertures of width 2K are assigned to the amplitude scale as shown by the dotted lines in Figure 2-5. A sample value is transmitted if it falls outside the aperture belonging to the last transmitted sample. As shown in Figure 2-6, the floating-aperture of the zero-order predictor always positions an aperture of width 2K symmetrically about the last transmitted data point. If each new data point lies within the aperture placed about the last transmitted data point, the new data point is not transmitted. If the new data point lies outside the aperture, then the point is transmitted, the 2K aperture is placed about it, and the process is repeated. Thus, the aperture is in effect "floating" with the last transmitted sample. Medlin gives a simple implementation for both the fixed-aperture and floating-aperture versions of the zero-order predictors. The zero-order offset predictor is a modification of the floating-aperture zero-order predictor, which attempts to take advantage of knowledge of the data trend established at the time of the last transmitted sample. As before, the predicted value remains constant as long as a sample is not transmitted. However, in this case the floating-aperture is offset from the previously transmitted value by a fixed, pre-determined amount. The sign of the offset is determined by noting the sign of the most recent out-of-tolerance deviation of the data. The offset would be in the positive direction if the deviation

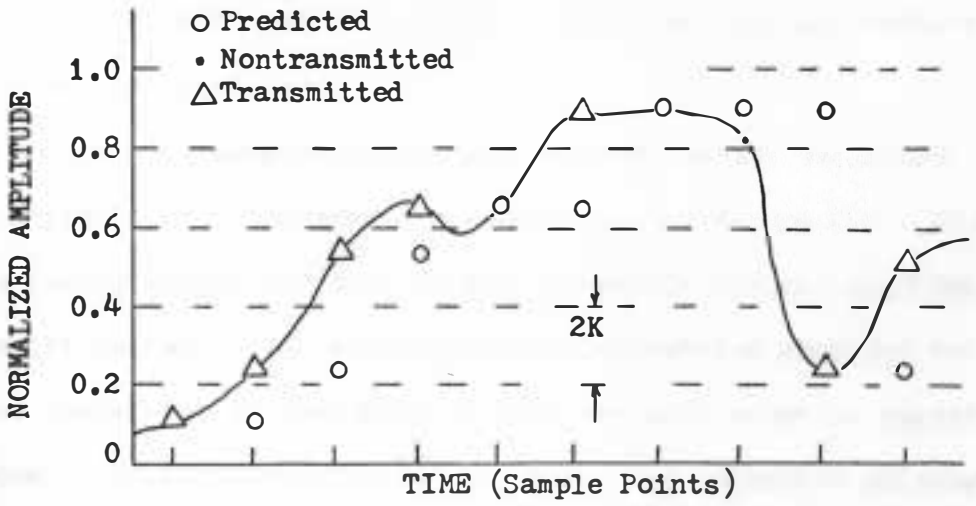


**Figure 2-5. Data Sampling and Selection; Fixed-Aperture Zero-Order Predictor.**

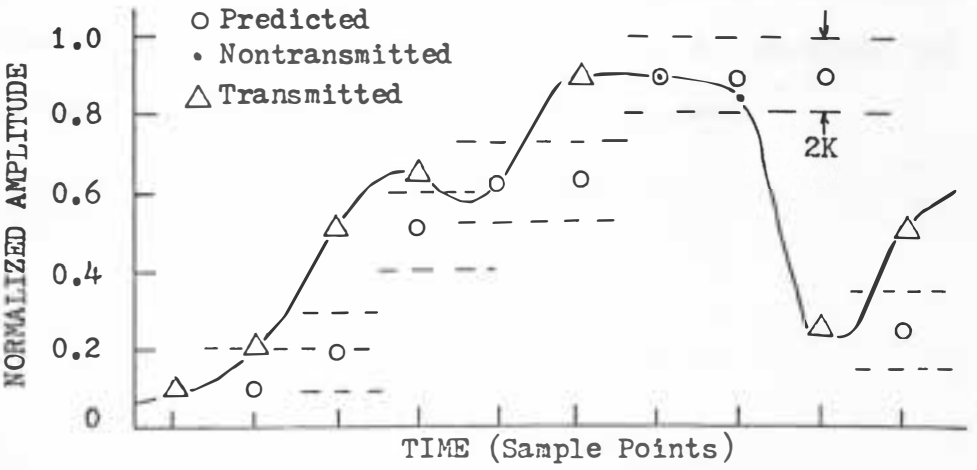


Figure 2-6. Data Sampling and Selection; Floating-Aperture Zero-Order Predictor.

showed a positive trend and vice versa. The fixed-aperture version is used in this dissertation.

For any of the redundancy reduction algorithms the essential components required to implement them are shown in Figure 2-7. The reference memory stores the data values, tolerance limits, algorithm selection (if needed), plus any additional information required to enable the comparator to determine if each new data value is significant or redundant. If the new value is redundant, the reference information is returned to the reference memory and the next data value is examined. However, if a new value is significant, the reference information is updated and returned to the reference memory. At the same time the significant data value is inserted into the buffer memory and stored until it can be read out. The buffer is required in most systems to accept significant data points at an irregular rate and submit the data to a data link at a constant rate.[11]

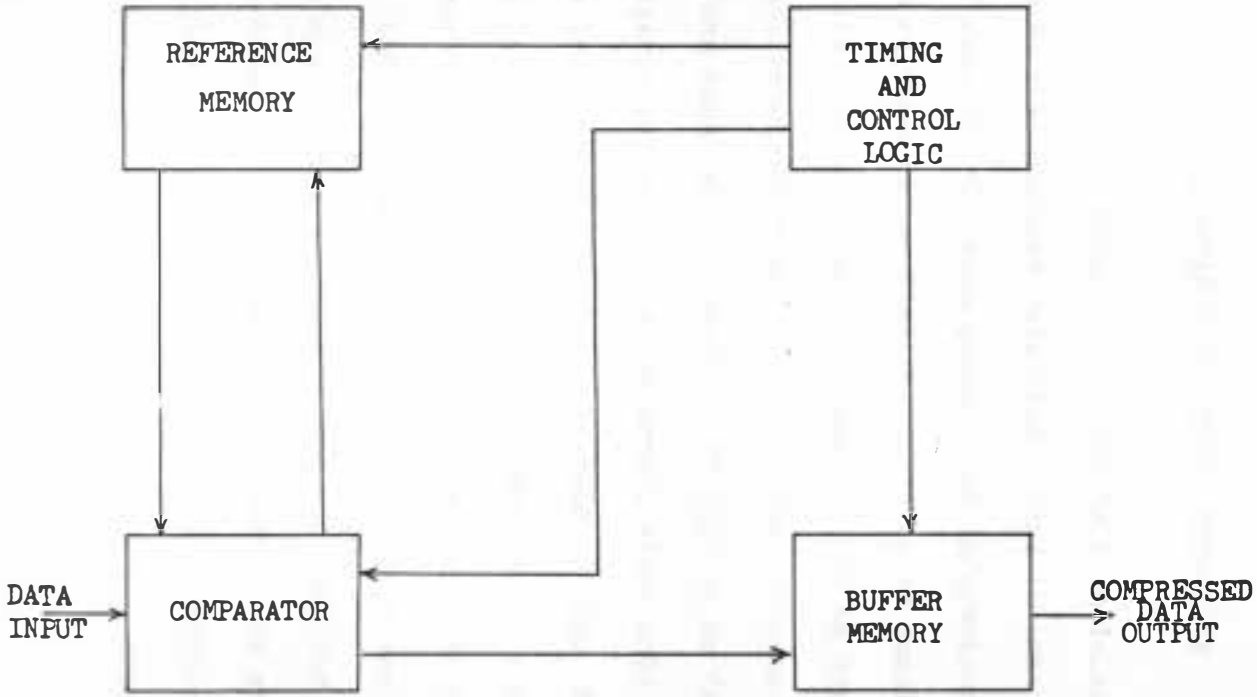


Figure 2-7. Simplified block diagram of a redundancy reduction type data compressor.[11]

# CHAPTER III

## A REDUNDANCY REDUCTION TECHNIQUE

The significant advantage of the delta-modulation (DM) technique as a redundancy reduction scheme is that DM decreases the amount of data for the same quantity of information by transmitting only time difference information, while other modulation techniques transmit time and amplitude information. If an equal number of samples are transmitted and stored as two different types of output data, DM has much better reduction efficiency as far as bandwidth and storage requirements are concerned, since only one type of data has to be transmitted and stored instead of two. But DM has no capability of transmitting the d-c component in a signal because of the differentiation and subsequent integration in the modulation process. Delta-Sigma-Modulation, (D-ΣM), improves this problem by integrating the input in the modulator so that the d-c component is not lost; however, the implementation problem is greater than that for DM. Thus, there is a need for an easily implemented redundancy reduction technique, employing DM, that utilizes data in the form,

$$t = F(Y) \tag{3-1}$$

instead of in the usual form,

$$y = g(t) \tag{3-2}$$

A redundancy reduction technique with the above mentioned

characteristics would be varied in its application. In digital computer applications, it would reduce the number of samples to be stored in function modeling situations, data storage, or other related problems. It could be especially advantageous for function modeling in a rapid-access memory when large computer programs are being used and memory space is critical.

Computer programs for problems of large dimension can occupy a great deal of storage to manipulate a large number of equations describing a single system. These programs process the data which is in storage and produce a desired output. The redundancy reduction technique proposed reduces the number of data points needed to reproduce the stored function within a desired accuracy limit, thereby increasing the memory space available for program instructions and other additional data.

This technique is also advantageous for data storage and processing in bio-medical research. An application would be in recording and processing of electrocardiograms (ECG). The ECG waveform is characterized by a portion of rapidly changing amplitude followed by a period of relative inactivity. The rapidly changing portion of the waveforms relays the most information to a physician while the inactive portion relays very little information unless abnormal activity is present in this portion. If abnormal activity does occur in the inactive region, the proposed redundancy reduction technique will preserve the waveform since it can be designed to be sensitive to any significant amplitude changes. Therefore, many

unnecessary sample points can be omitted and more memory space is made available, while all meaningful data are still preserved.[18]

A. Theory of Operation

The proposed redundancy reduction technique is outlined in block diagram form in Figure 3-1. The signal, f(t), is first fed through a sample-and-hold unit which samples at a uniform and predetermined rate. This rate is fast enough to satisfy the Sampling Theorem.[12] Figure 3-2 shows the input to the sample-and-hold unit, while Figure 3-3 shows its output. The signal is then passed to a combination analog-to-digital (A-D) converter and quantizer. This unit converts the analog signal to digital form and quantizes the digital signal. The amplitude values of the sample points can only take on a set of discrete values that are the quantization levels. The output of this unit is shown in Figure 3-4. The quantization level or the actual digital output value the quantizer assumes, is a function of the quantizer. This will be discussed in Section (B) of this chapter. The choice of quantization interval size or step, R(M), for the quantizer will be discussed in Section (B) of this chapter.

The comparator takes the quantized-amplitude value of the present sample and compares it to the quantized amplitude value of the previous sample which was in storage. The comparison is actually a subtraction of $\bar{f}^*(t_i) - \bar{f}^*(t_{i-1})$. If $\bar{f}^*(t_i)$ is not equal to $\bar{f}^*(t_{i-1})$, the value of the time difference of the two samples,

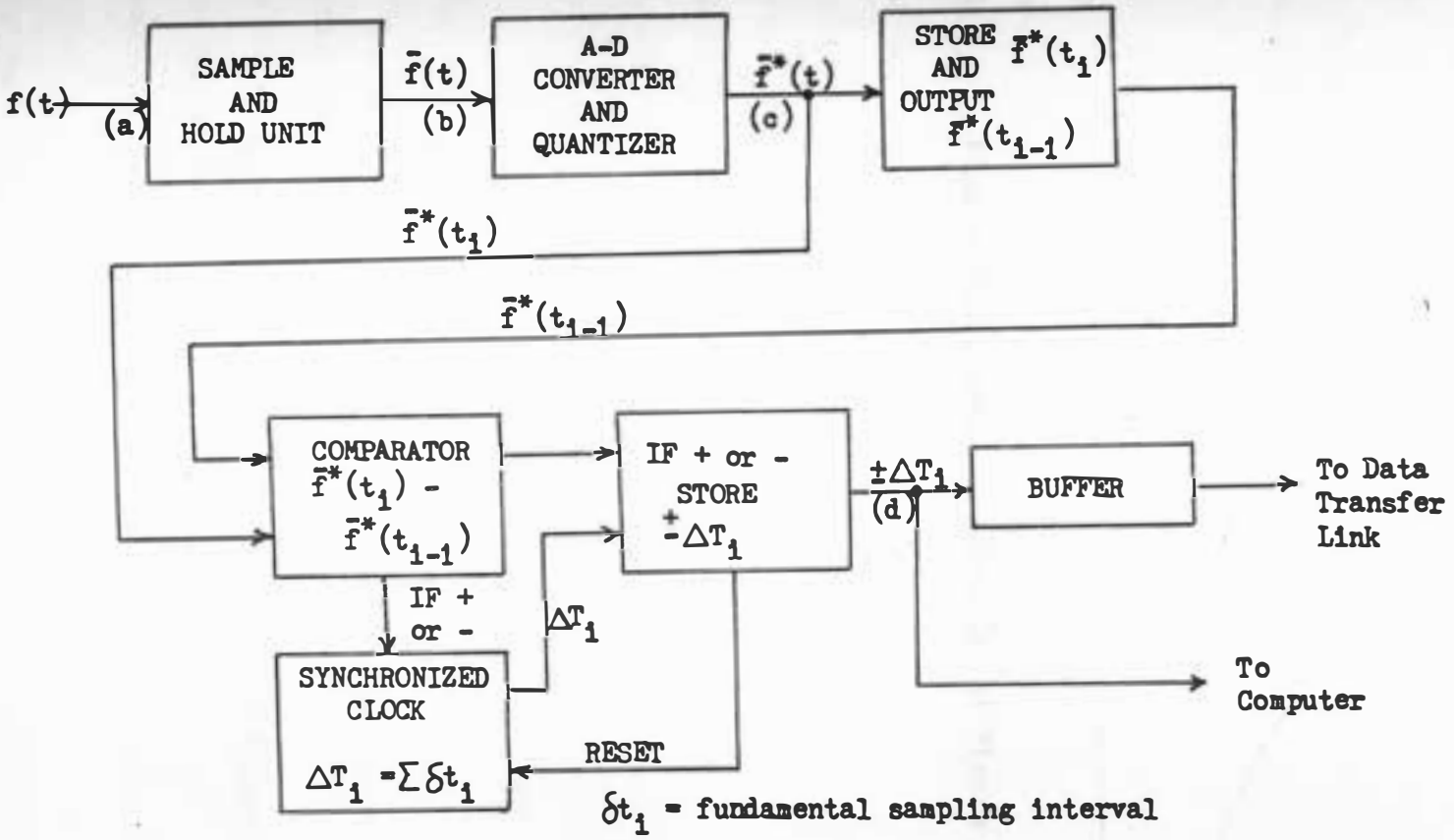


Figure 3-1. Block Diagram of Data Compressor for the Redundancy Reduction Technique.

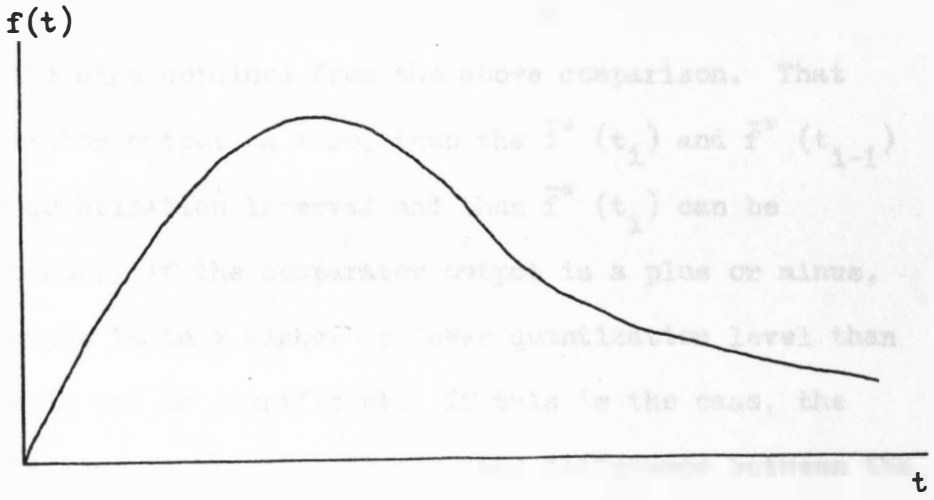


Figure 3-2. Signal at point (a) of Figure 3-1.

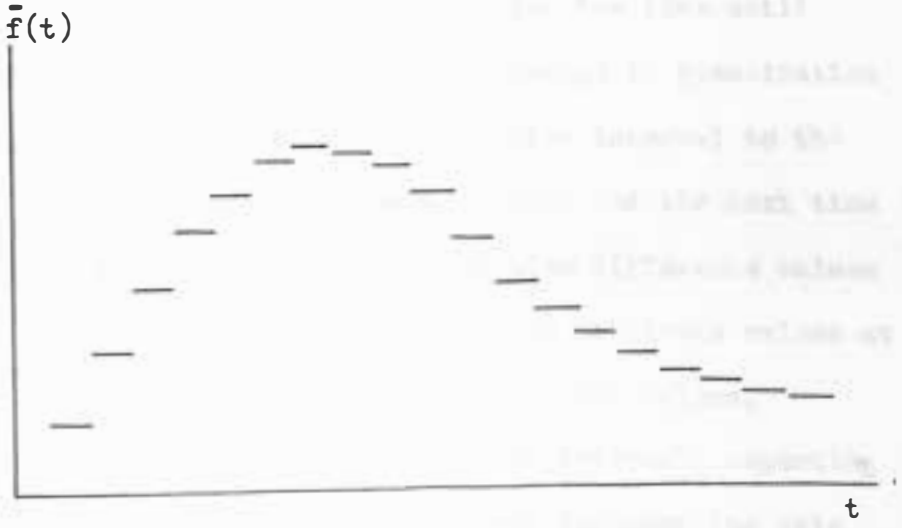


Figure 3-3. Signal at point (b) of Figure 3-1.

$$\Delta T_i = t_i - t_j \qquad \begin{matrix} 1 \leq i \leq N \\ j < i \end{matrix} \qquad (3\text{-}3)$$

is stored with the sign obtained from the above comparison. That is, if the comparator outputs a zero, then the $\bar{f}^*(t_i)$ and $\bar{f}^*(t_{i-1})$ are in the same quantization interval and thus $\bar{f}^*(t_i)$ can be considered redundant. If the comparator output is a plus or minus, then the last sample is in a higher or lower quantization level than the previous sample and is significant. If this is the case, the sign of the comparison is attached to the time difference between the two non-redundant samples. The time difference, $\Delta T_i$, is obtained from the sum of $\delta t_i$ intervals which correspond to the sampling rate of the sample-and-hold unit. Starting with the last compared sample value that was plus or minus, the clock evaluates the time until another pulse from the comparator indicates a change in quantization levels for $\bar{f}^*(t_i)$. The clock then outputs a time interval to the storage unit and is automatically set back to zero and the next time interval value $\pm\Delta T_i$ is evaluated, the stored time difference values along with the corresponding non-redundant sample amplitude values at point (d) of Figure 3-1 are shown in Figure 3-5. The values, $\pm\Delta T_i$, are output by the "IF" block at irregular intervals depending on the shape of the waveform, the step size, and the sampling rate. The buffer stores this time information and outputs it at a uniform rate to the data transfer link. The $\pm\Delta T_i$ values may also be sent directly to a computer, which may not need the information at a uniform rate for further processing or reconstruction.

The reconstruction of the signal is achieved as shown in

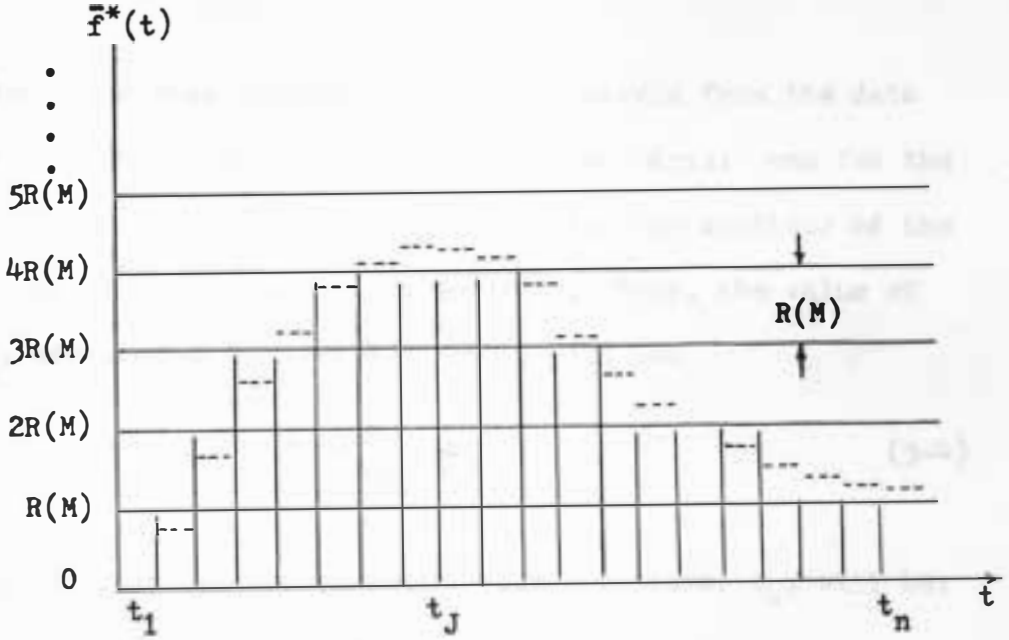


Figure 3-4. Signal at point (c) of Figure 3-1.

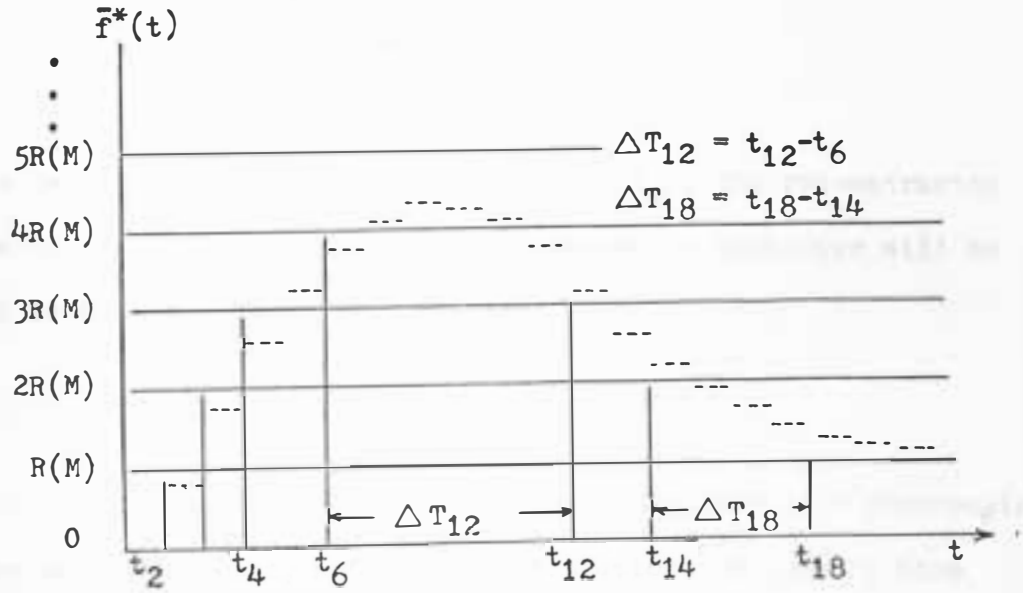


Figure 3-5. Time difference, $\Delta T_i$, stored in the buffer of the system in Figure 3-1.

Figure 3-6. The time information, $\pm\Delta T_i$, travels from the data transfer link to an adder. The adder has two parts: one for the addition of the amplitude portion and one for the addition of the time portion of the reconstructed waveform. Thus, the value of time, $t_k$, computed at the reconstructor, will be:

$$t_k = \sum_{i=1}^{k} \Delta T_i \quad . \tag{3-4}$$

The amplitude value of the quantized signal at time, $t_k$, will be:

$$F(t_k) = R(M) \cdot \sum_{i=1}^{k} (\text{sign of } \Delta T_i) \cdot 1.0 \tag{3-5}$$

where

$$R(M) = \text{quantization step size} \ .$$

Using the two pieces of information, $t_k$ and $F(t_k)$, the reconstructor reconstructs the input signal. The reconstruction technique will be discussed in Section (B) of this chapter.

## B. Computer Simulation

The digital computer makes it possible to analyze data compression techniques easily via many arithmetic calculations in a short time interval. The computer used for simulation is the IBM 360/30, and the programs are written in Fortran IV programming language.

A unit amplitude sine wave signal is generated in the computer and used as a standard test signal, which is statistically stationary and uniformly distributed. An input signal of practical importance

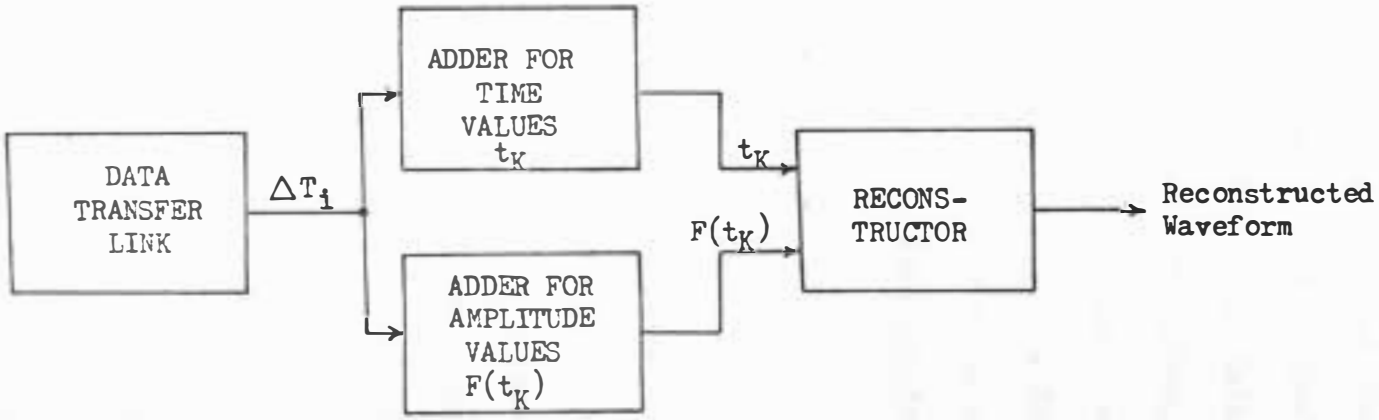


Figure 3-6. Simplified block diagram of the reconstructor for the DM redundancy reduction technique.

is the electrocardiogram (ECG). The ECG data, which is used, has been recorded in digital form on magnetic tape. It is transformed to binary digits by an assembler program and these binary numbers are converted to actual voltage levels. The original ECG data is recorded in the form of consecutive sets of X, Y, Z, data points separated by a time interval of 0.004 seconds. Therefore, the maximum sampling rate for this ECG signal cannot be more than 1 sample per 0.004 seconds or 250 samples per second. Thus, the ECG signal used here is not in analog form, but has been sampled previously. Specific information concerning the ECG data used is detailed in Appendix A.

Sampling Rate and Quantization Interval Size:

The key criteria of a redundancy reduction scheme are quantization step size, R(M), and the constant sampling rate associated with the sample-and-hold unit. The quantization step size, R(M), is varied from 0.01 to 0.5 amplitude units for each individual sampling rate used. The input signal is normalized to restrict the data to a unit amplitude or less. The independent variable, M, is the number of quantization steps in the positive half plane. Twice that number gives the total number of quantization levels in both positive and negative half planes. Therefore, there is a maximum of 100 quantization levels and a minimum of 2 quantization levels in the positive half plane. This gives a maximum of 200 quantization levels and a minimum of 4 quantization levels in the entire plane. Hereafter, when referring to the number of quantization levels, the number used

will be only those in the positive half plane with the understanding that an equal number exist in the negative half plane.

When parameters such as mean square error, variance of error, etc., are obtained, they are computed for 35 different quantization levels, M is varied from 2 to 20 by 1's and from 25 to 100 by 5's.

The sampling rate for the sine wave input is varied by changing the radian angle interval, which is equivalent to a degree/sample interval, from 2 to 36. For the ECG signal, the sampling rate is limited to the range from 1 sample per 0.004 seconds to 1 sample per 0.032 seconds. The lowest rate was chosen such that the sampled data points would not miss the actively changing region of the ECG waveform.

Quantizer:

An equal increment quantizer is used in this redundancy reduction technique. Referring to Figure 3-7, R(M) is defined as the quantizer step size. As shown in Figure 3-7, the characteristic of the quantizer is such that for an input source signal, f(t) whose normalized maximum amplitude is 1.0, when

$$0 \leq f(t) < \frac{R(M)}{2}$$

then, the output, F(t), is equal to zero.

And, if the input, f(t), satisfies the following,

$$\frac{R(M)}{2} \leq f(t) < \frac{3}{2} R(M) \qquad (3\text{-}7)$$

then the output, F(t), is equal to R(M).

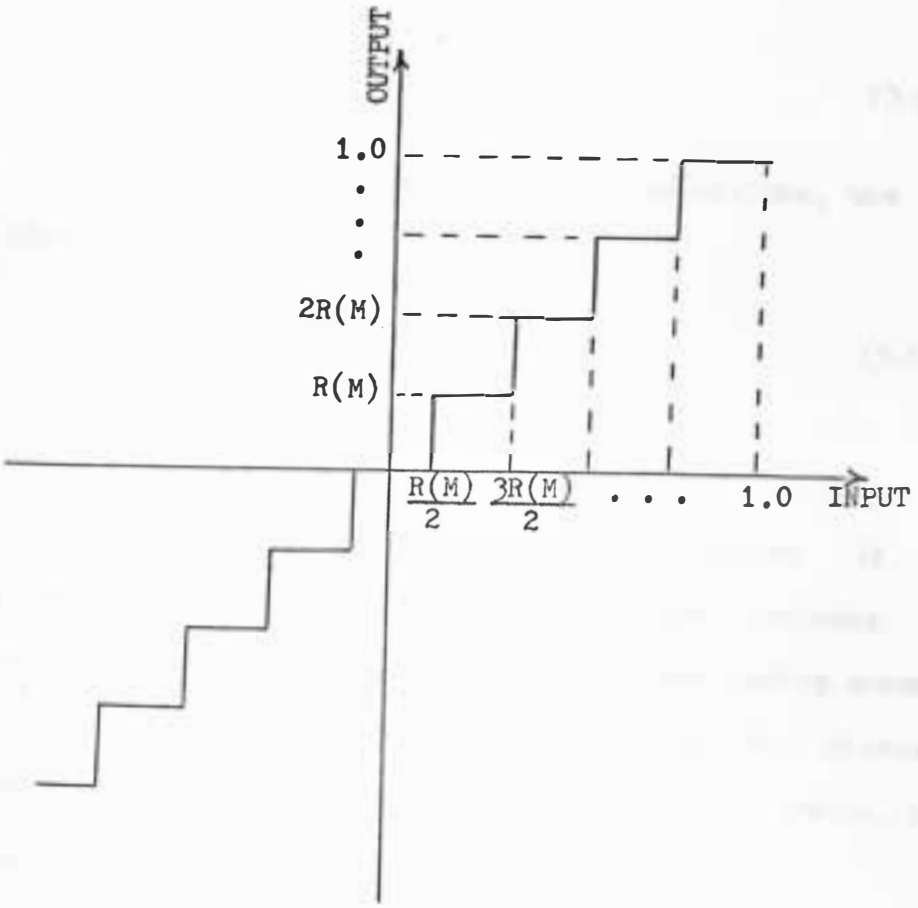


Figure 3-7. Quantizer used for the system in Figure 3-1.

In general, for any input value f(t), where,

$$\left(\frac{2k-1}{2}\right) \cdot R(M) \leq f(t) \leq \left(\frac{2k+1}{2}\right) \cdot R(M) \qquad (3\text{-}8)$$

the output, F(t), is

$$F(t) = K \cdot R(M) ,$$
$$K = 0, \pm 1, \pm 2, \ldots . \qquad (3\text{-}9)$$

Since the inputs are normalized to unit maximum excursions, the following inequality holds,

$$\left| K \cdot R(M) \right| \leq 1.0 \qquad (3\text{-}10)$$

C. Noise Analysis

There are many sources of noise in a telemetry system. In general, noises can be classified into two categories: process noise such as sampling noise, quantization noise, and coding error, and transmission noise such as system errors and electrical disturbances from outside of the system. In the redundancy reduction system, the following types of noise are important.

Sampling noise:

Two types of errors are introduced by the sampling system; errors in signal amplitude and errors in timing. If x(t) is a continuous parameter signal which is being sampled at discrete multiples of the period T, then the samples

$$f^*(t) = f(nT) \qquad (3\text{-}11)$$

provide a discrete-parameter process.

In the physical application of the sampling theory, an attempt is made to sense the signal f(t) at t = nT, and to regenerate f(t) from the samples f(nT). In real problems, the sampled numbers are $f(nT - \mu_n)$ where $\mu_n$ are the deviations of the sampling times from nT, and the problem is to determine f(t) in terms of $f(nT - \mu_n)$.[2]

The time jitter error introduced by data transmission media can be eliminated if it is sufficiently small with respect to the sampling rate of the sample-and-hold unit. This is because the basic sampling rate of the sample-and-hold unit is known and it is the time information, not the amplitude information, that is transmitted through the data transfer link. The time information could be in error up to 1/2 of a sampling interval without introducing error due to time jitter, since the basic sampling rate is also known at the reconstruction end of the process.[15, 17]

Another error in the sampling process is aliasing. An aliasing error happens when the spectrum of a continuous waveform which is to be sampled contains some power at frequencies higher than 1/2 of the sampling frequency. Figure 3-8 illustrates the problem. In Figure 3-8 (a) the sampling frequency is eight times the frequency of the sine wave. The set of sample values bears an obvious resemblance to the continuous waveform, and it is possible to reconstruct the original signal. In Figure 3-8 (b), however, the sampling frequency is only 8/7 times that of the frequency of the sine wave signal being

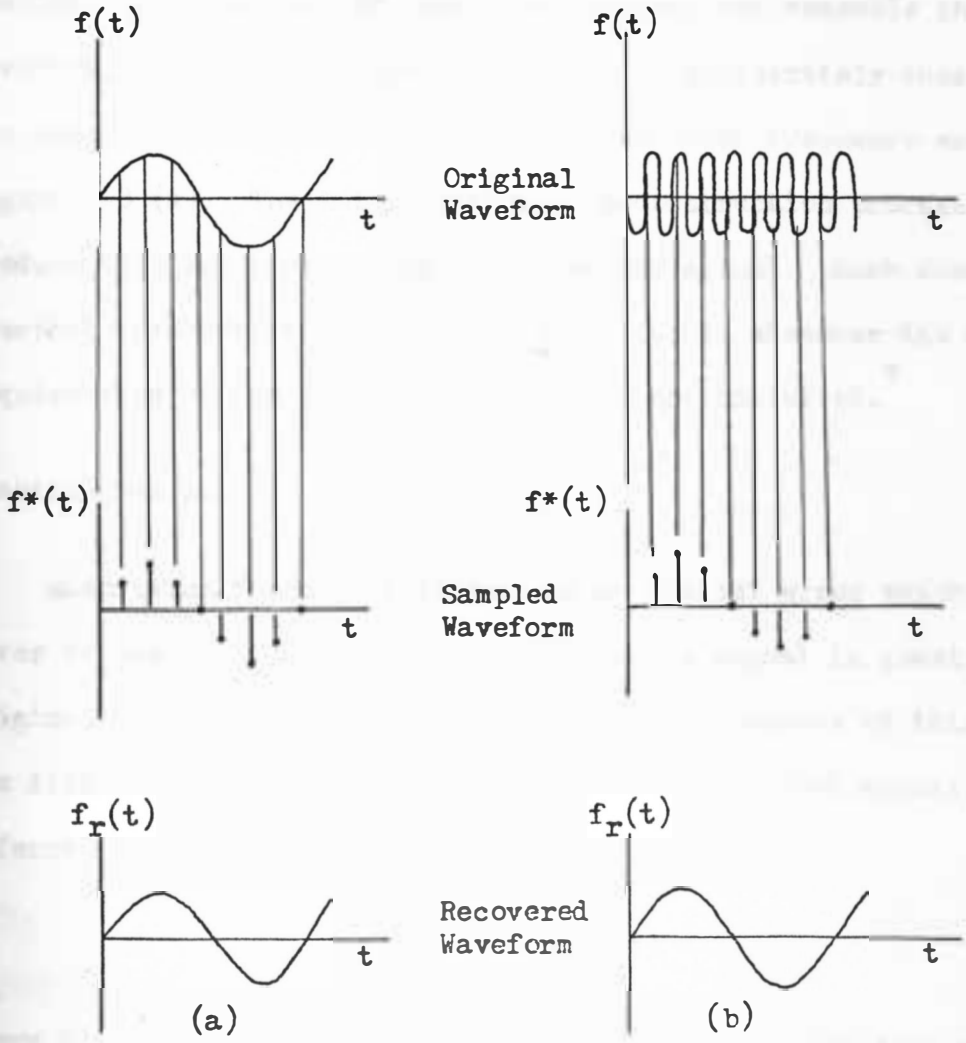


Figure 3-8. Aliasing. Waveform (a) has a sampling frequency 8 times the signal frequency and waveform (b) has 8/7 of the signal frequency.[7]

sampled. Now, the set of sample values does not resemble the continuous waveform; in fact, the higher frequency is deliberately chosen so that the samples appear to be derived from the lower frequency wave of Figure 3-8 (a). The interpolation or reconstruction process will produce this lower-frequency signal as any output. Such downward spectral transposition of message power occurs whenever the minimum requirements of the sampling theorem are not satisfied.[7]

Quantization Noise:

Quantizing the signal introduces an initial error which can never be removed from that point on. Once a signal is quantized, the original signal cannot be recovered perfectly because of this error. The difference between the input signal and quantized signal, is referred to as the quantization noise;

$$q_n(t) = f(t) - f_q(t) \qquad (3\text{-}12)$$

where $f(t)$ is the original input and $f_q(t)$ is the quantized output signal. The unique feature of this noise is that its magnitude is always less than one-half a quantization step size,

$$q_n(t) < \frac{R(M)}{2} \qquad (3\text{-}13)$$

This is distinctly different from transmission noise that could theoretically take on all possible amplitudes. Bennet and others have shown that quantization noise in a pulse code modulation system is similar to an additive random component with a zero mean and a

r.m.s. value determined by the quantization step size.[16]

When a signal is reconstructed from quantized samples, the original signal plus noise having a uniform power spectrum over the bandwidth of the signal is obtained. Based on the assumption that, over a long period of time, all values of error voltage in the range $(-\frac{R(M)}{2}, \frac{R(M)}{2})$ appear the same number of times, the mean squared value of the error will be

$$q_n^2 = \frac{1}{R(M)} \int_{-\frac{R(M)}{2}}^{+\frac{R(M)}{2}} q_n^2 \, dq_n = \frac{R^2(M)}{12} \quad . \qquad (3\text{-}14)$$

With the assumption made that the average value of the error is zero, the r.m.s. fluctuation error is $1/\sqrt{12}$ times the height of a single quantization step. This r.m.s. error voltage then represents the effect of quantization noise at the output of a pulse code modulation system.[21]

Slope Overload Noise:

Slope overload error occurs when the steepest reproducible slope of the redundancy reduction system employing the delta-modulation method is not as steep as the slope of the input signal. Figure 3-1 shows that the output of the analog-to-digital converter is set to within one quantum level of the actual input signal. Thus, adjacent significant samples may be any number of quantums apart. The input to the buffer is $+\Delta T_i$ or $-\Delta T_i$. From this point on, the adjacent

significant samples are interpreted as being only one quantum level apart, either the next one higher or lower. This process, in the transmission of only $\pm\Delta T_i$, introduces the possibility for slope overload error. The maximum slope producible between adjacent significant samples is

$$S_m = \frac{R(M)}{I} \tag{3-15}$$

where

$S_m$ = maximum slope

$R(M)$ = one quantum

$I$ = fundamental sampling interval

Thus, in order for slope overload not to occur in the reconstruction process, the following condition must be satisfied:

$$\frac{R(M)}{I} = S_m \geq \left| f'(t) \right| \tag{3-16}$$

where

$\left| f'(t) \right|$ = magnitude of the input signal derivative with respect to time.

In the example illustrated in Figure 3-9 the noise $n(t)$, which is defined as

$$n(t) = f(t) - F(t) \tag{3-17}$$

where

$f(t)$ = input signal

$F(t)$ = reconstructed signal

is due to quantization before time $t_0$. For time greater than $t_0$,

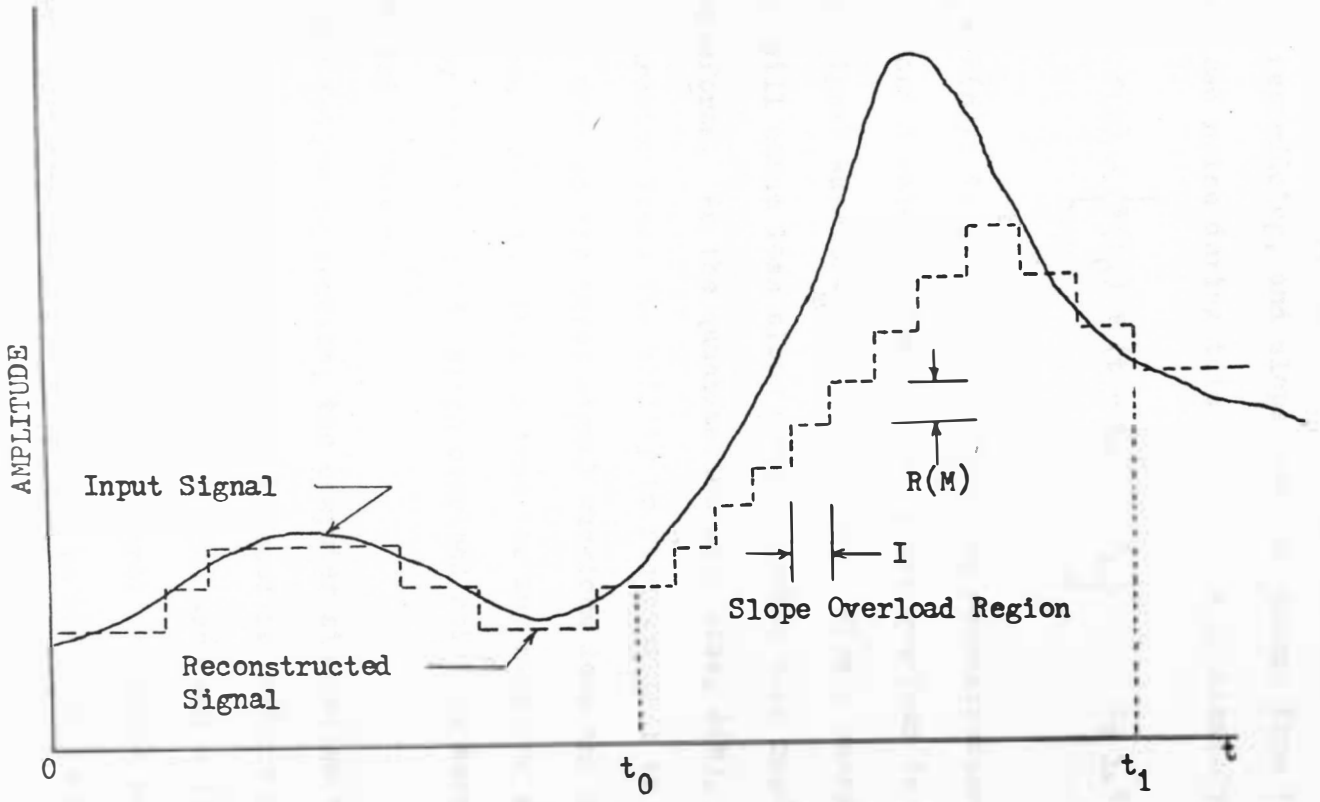


Figure 3-9. Input signal and reconstructed output signal showing region of slope overload noise ($t_0 \leq t \leq t_1$).

the input signal, f(t), exceeds that which the reconstructor is capable of reproducing, and slope overload occurs from $t_0$ to $t_1$. The slope overload noise during this period is approximately,

$$n(t) = f(t) - \left\{F(t_0) + (t - t_0) \cdot S_m\right\}, \qquad t_0 \leq t \leq t_1 \tag{3-18}$$

where $S_m = R(M)/I$ is the maximum slope the reconstructor can trace with given R(M) and I values. Definitely, slope overload is dependent upon the input signal waveform characteristics. Slowly changing signal waveforms will cause less slope overload noise than rapidly fluctuating signal waveforms. As the quantization step size, R(M), is decreased, the reconstructor loses its ability to rise and fall in one sampling interval as much as the input signal waveform does and slope overload noise becomes dominant. This is true for any sampling rate. As indicated by equation 3-15, slope overload noise is dependent upon both R(M) and I values.[15]

In the following section, the computer simulation results using the conventional technique and the proposed redundancy reduction technique to sample and reconstruct a sine wave and a representative ECG waveform will be discussed. The signal generated by the zero-order-hold with a constant sampling rate will be referred to as the conventional technique.

## D. Experimental Results

The discussion of experimental results contains analysis and comparison of four sets of output data; two input signals are applied

to each of two techniques. The techniques are the conventional technique, and the DM technique which indicates the proposed redundancy reduction technique employing the delta-modulation scheme. This technique transmits only time information. Since the output data received at the reconstructor using the conventional technique is the same as the signal data produced by the quantizer and A-D converter unit of the system in Figure 3-1, the computer programs are written to compute the parameter data for each of the two techniques at the same time.

In the parameter curve-plotting, the quantization step size, R(M), and sampling interval size, I, are used as independent variables. The sample interval size, I, specifies the number of original sample intervals between each sample used. Thus, if I equals 6, the sample interval size for the ECG signal will be 6 times 0.004 or 0.024 seconds. For the ECG data input, 2, 4 and 6 intervals per sample are used. R(M) values range from 0.01 to 0.5 on the normalized abscissa scale. Since all signals are constrained to have a maximum amplitude of unity, R(M) is equivalent to 1/M, where M is the number of quantization steps.

a. Waveform Plot

Visual comparison of the reconstructed output waveform with the original input signal waveform is done by plotting two waveforms on the same axis using the x-y plotter of the computer system. One cycle of sine wave is used for various values of I and R(M), while 636 data values are used for the ECG data input. Figure 3-10 shows

the original input and reconstructed output sine waveforms using the conventional technique, while Figure 3-11 shows that by the DM technique. Both results are for I = 12 and R(M) = 0.1. The conventional technique introduces only quantization noise while the DM technique introduces slope overload noise. Figures 3-12 and 3-13 show another comparison for R(M) = 0.0142. Obviously the reconstructed waveform of the conventional technique represents the input signal better as the quantization step size, R(M) decreases, while the DM technique increases the error. This is a natural result because the R(M) value is directly related to quantization noise, as shown in Equation 3-14, and with slope overload noise as shown in Equation 3-16. The cut-off of the output waveform peaks for the sine wave input in Figures 3-10 and 3-11 is caused by the quantizer, which restricts the maximum amplitude of the output signal to unity. For small R(M), this cut-off error is negligible, but, for large R(M), it is significant. The DM technique reproduces the input reasonably well for R(M) values from 0.05 to 0.083, while the conventional technique reproduces more accurately as R(M) decreases or the number of the quantization levels, M, increases. The DM technique produces slope overload noise for all R(M) values smaller than the minimum mean-square error point while quantization noise is dominant for all larger R(M) values. Thus, the transition point exists at the minimum mean-square error point of R(M), and it has significance in that it determines the optimum sampling conditions for the DM technique.

Figures 3-14 and 3-15 show the results for the ECG data input.

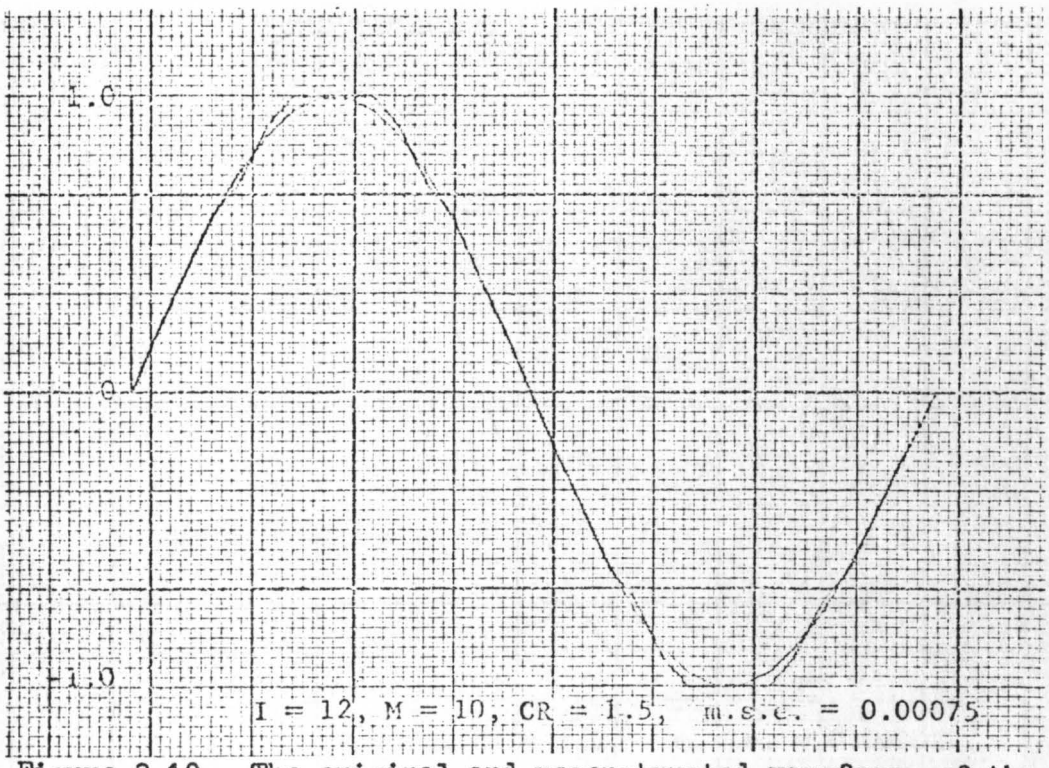


Figure 3-10. The original and reconstructed waveforms of the sine wave input by the conventional technique.

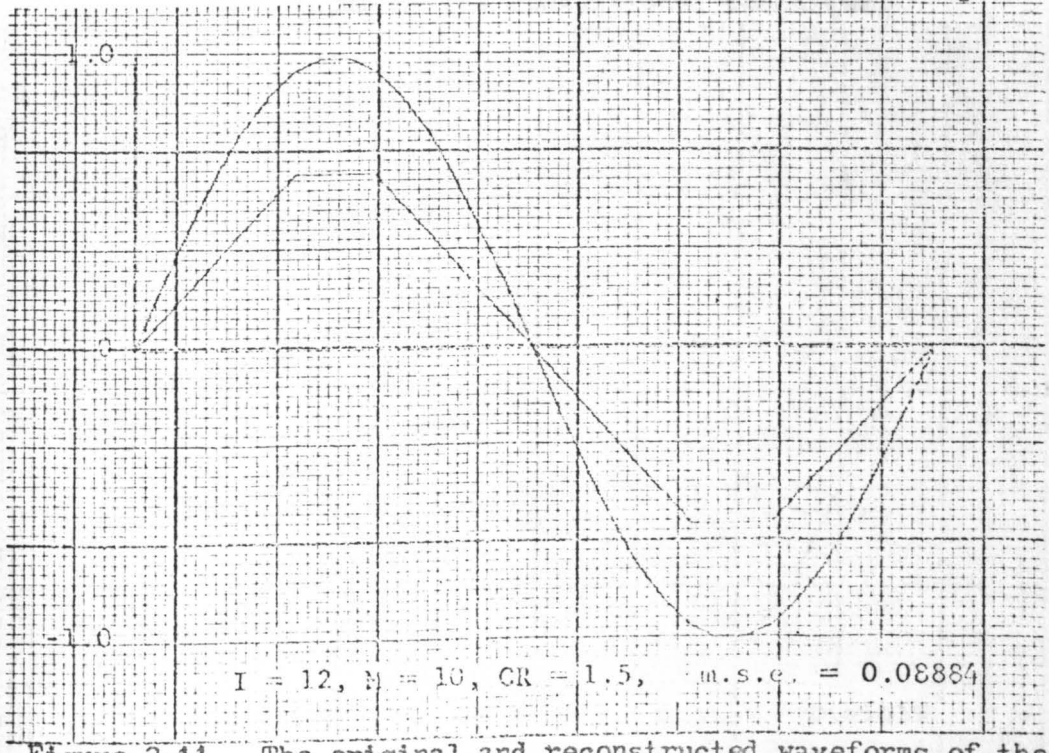


Figure 3-11. The original and reconstructed waveforms of the sine wave input by the DM technique.

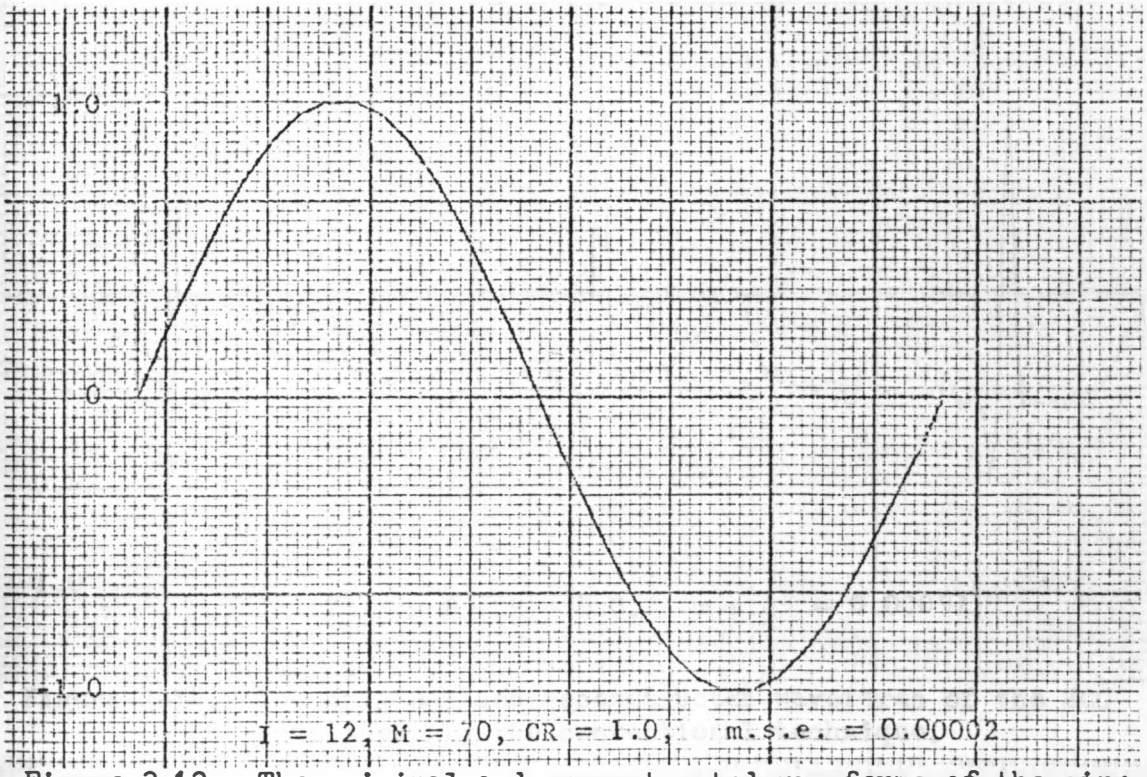


Figure 3-12. The original and reconstructed waveforms of the sine wave input by the conventional technique.

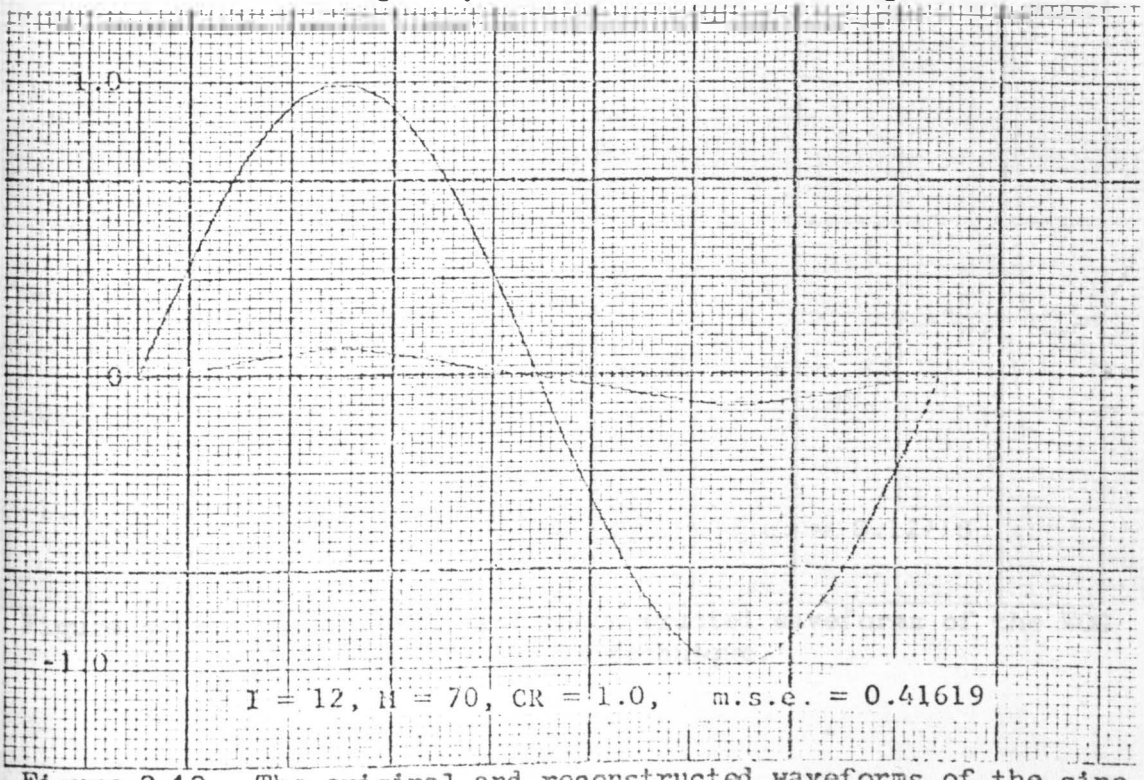


Figure 3-13. The original and reconstructed waveforms of the sine wave input by the DM technique.

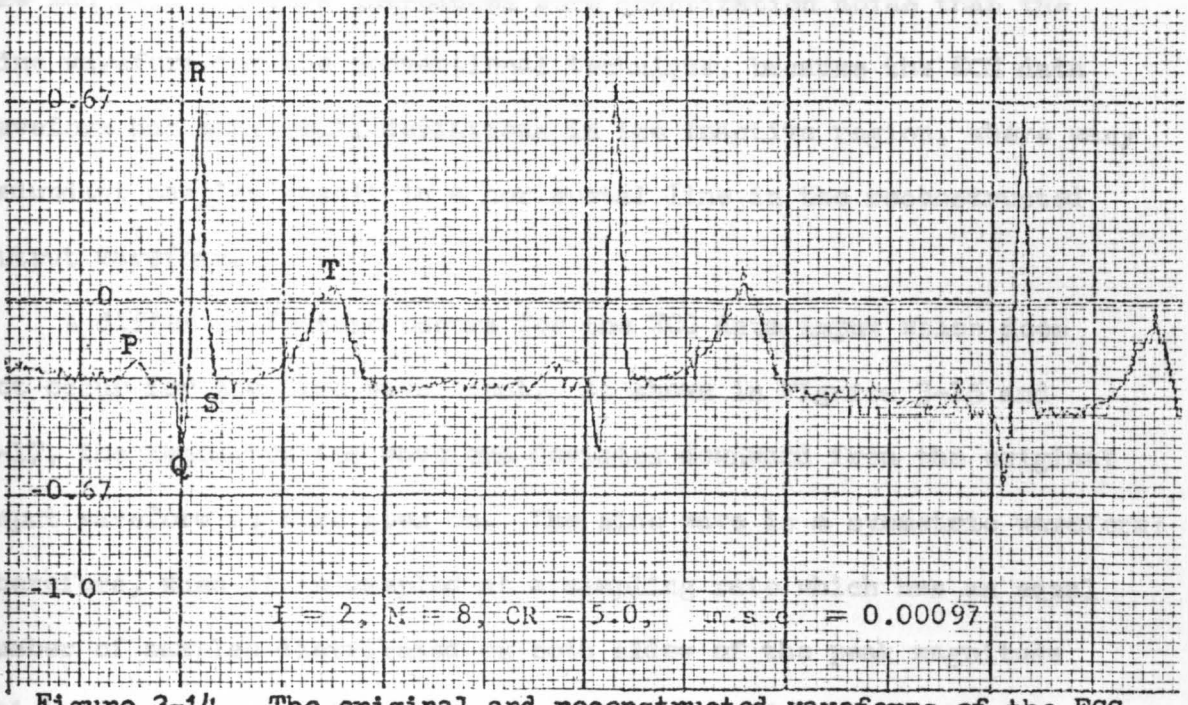


Figure 3-14. The original and reconstructed waveforms of the ECG data input by the conventional technique.

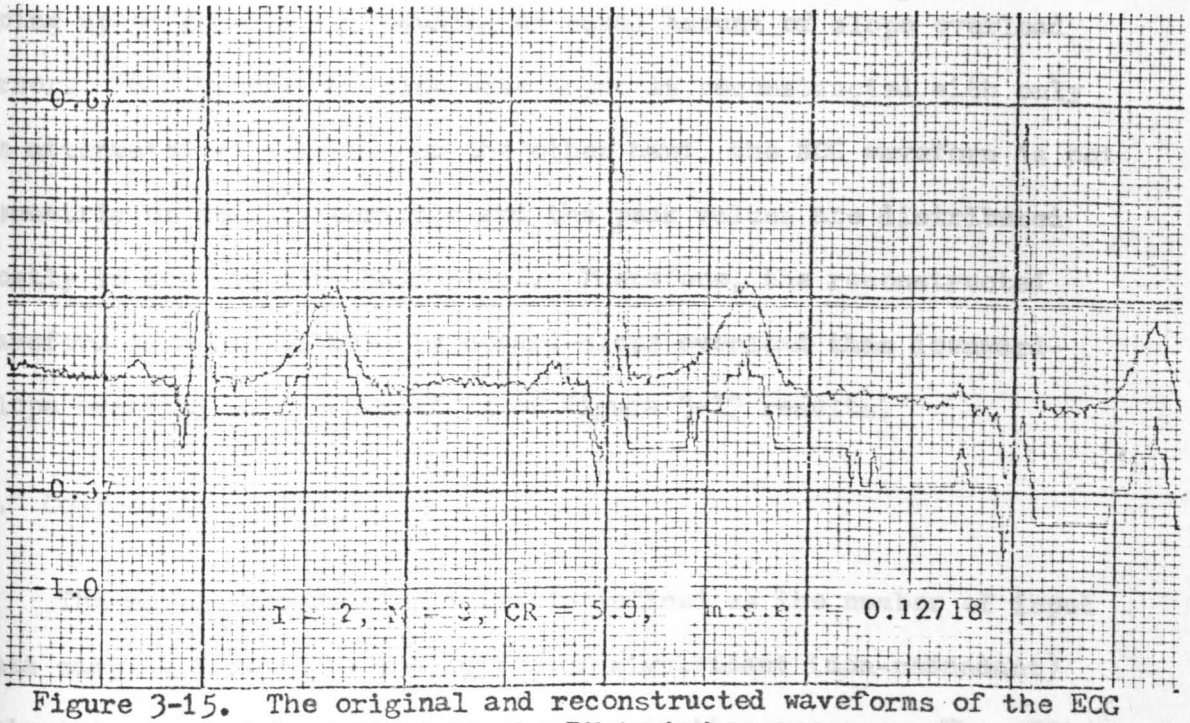


Figure 3-15. The original and reconstructed waveforms of the ECG data input by the DM technique.

The ECG data waveform introduces more quantization noise than the sine waveform for the conventional technique, because the ECG data waveform has many small deviations in the inactive region, where many redundant samples result in a horizontal line in the reconstructed output waveform.

A different feature occurs for the ECG data input which does not occur for the sine wave input. As shown in Figures 3-15 and 3-17, the reconstructed waveform deviates downward from the original input waveform as time goes on. The sine wave is a symmetric waveform: therefore, when it is sampled at a sampling rate which has an equal number of samples distributed on both sides of the peak magnitude point, the reconstructor, has an equal number of quantization steps going up or going down, causing an equal amount of slope overload error. This is why the sine wave input is reconstructed with only an attenuated waveshape. On the other hand, the ECG waveform is not symmetric or exactly periodic and the peak values are distributed mostly in the positive half plane. Therefore, the reconstructed waveform is affected more by upward-slope overload than downward-slope overload and the waveform of Figure 3-17 results.

b. Compression Ratio

The sample compression ratio is defined as the number of input data samples divided by the number of significant (non-redundant) output data samples of the redundancy reduction process. The efficiency of a redundancy reduction technique can be established by

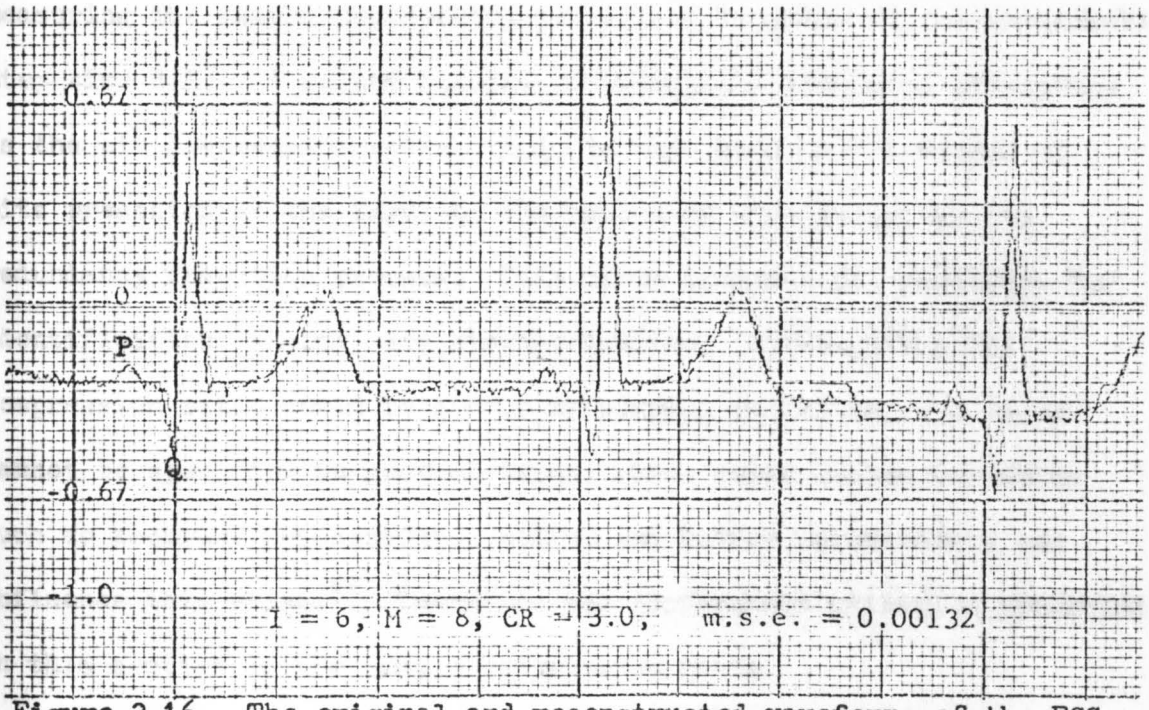


**Figure 3-16.** The original and reconstructed waveforms of the ECG data input by the conventional technique.


**Figure 3-17.** The original and reconstructed waveforms of the ECG data input by the DM technique.

measuring the sample compression ratio as a function of the quantization step size R(M). A second measure of redundancy reduction efficiency is the bit compression ratio. This is the ratio of the number of bits presented at the input to the number of bits output by the redundancy reduction process. This ratio includes all penalties for identification, timing, and synchronization. Although the bit compression ratio would be a more meaningful parameter, its value cannot be specified in general terms, since other system variables such as accuracy requirements, coding and buffer requirements can influence this value.[11] Therefore the performance criterion presented in this section is the sample compression ratio.

Figures 3-18 and 3-19 show sample compression ratios for the sine wave input and the ECG data input for each of the two techniques. The sine wave input is sampled at the rate of one sample every 6, 12, and 18 degrees, which is equivalent to 60, 30, and 20 samples per cycle. Since the ECG data signal waveform has narrow, sharp pulses in the active regions, each of which contains less than 8 discrete data samples, the minimum sampling rate is limited to 1 sample per 0.024 seconds. The compression ratios increase as the sampling rate increases because high sampling rates produce many redundant samples. In general, for the values of R(M) less than 0.05 the compression ratios are nearly equal and constant. Because of the waveform characteristics, the compression ratios of the ECG data input have different values than the sine wave as shown in Figure 3-19. Even though the ECG data signal waveform is not exactly periodic, its

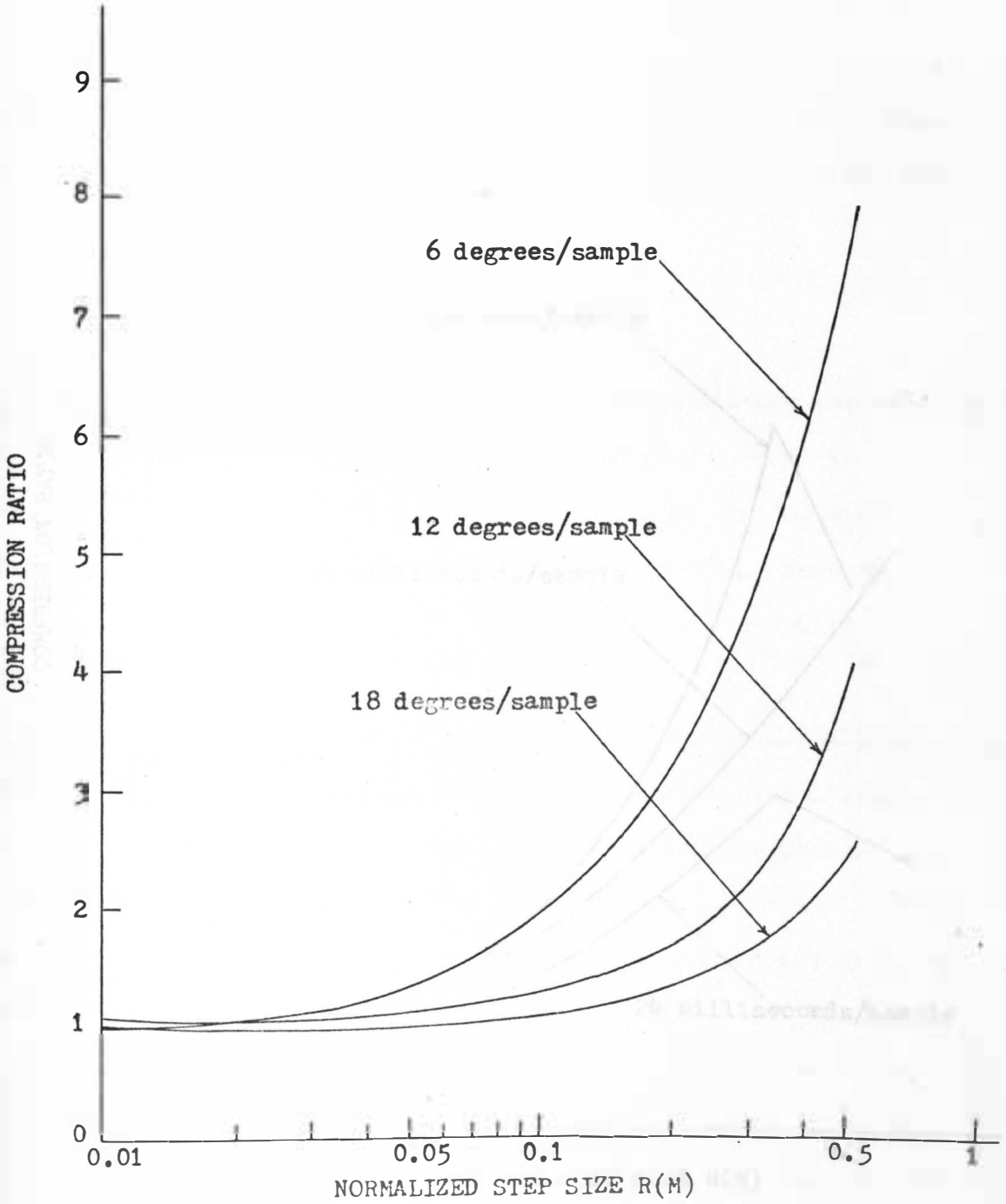


Figure 3-18. Compression ratio versus normalized step size, R(M), for the sine wave input.

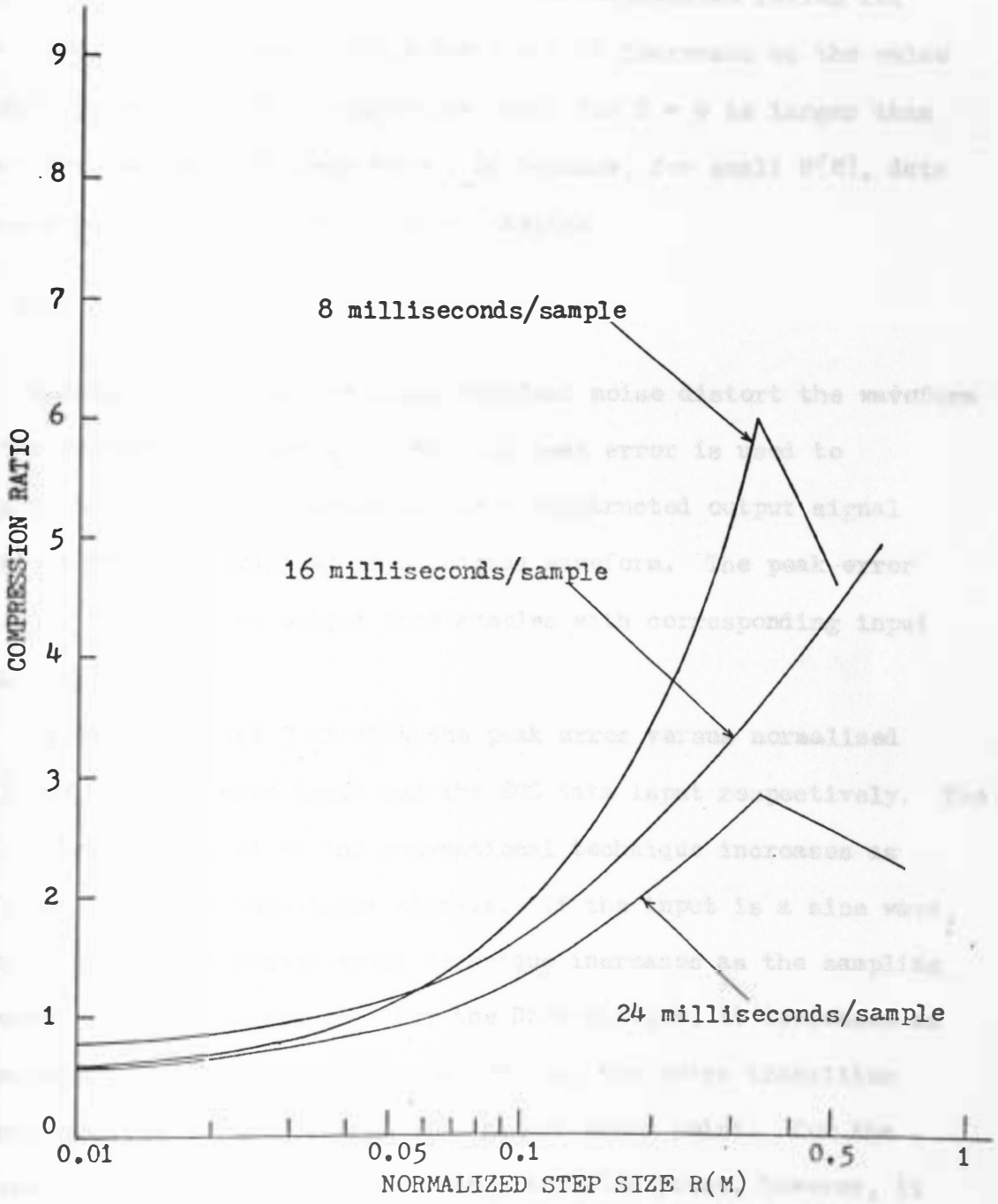


Figure 3-19. Compression ratio versus normalized step size R(M) for the ECG data input.

ripples and peak pulses appear in an approximately periodic manner, and a certain sampling rate will sample more peak values of the ripples and pulses than others. Thus the compression ratios for I = 2 and I = 6 decrease, while for I = 4 it increases as the value of R(M) increases. The compression ratio for I = 4 is larger than the other two for R(M) less than 0.06 because, for small R(M), data sampled at I = 4 has more redundant samples.

c. Peak error

Quantization noise and slope overload noise distort the waveform of the reconstructed output signal and peak error is used to measure the maximum deviation of the reconstructed output signal waveform from the original input signal waveform. The peak error is found by comparing output data samples with corresponding input data samples.

Figures 3-20 and 3-21 show the peak error versus normalized R(M) for the sine wave input and the ECG data input respectively. The peak error introduced by the conventional technique increases as R(M) increases for both input signals. If the input is a sine wave, peak error for the conventional technique increases as the sampling interval size, I, decreases. For the DM technique, it decreases as I decreases for values of R(M) smaller than the noise transition point, which is at the minimum mean-square error point. For the values of R(M) larger than the noise transition point, however, it increases as I decreases. In other words, as I decreases the

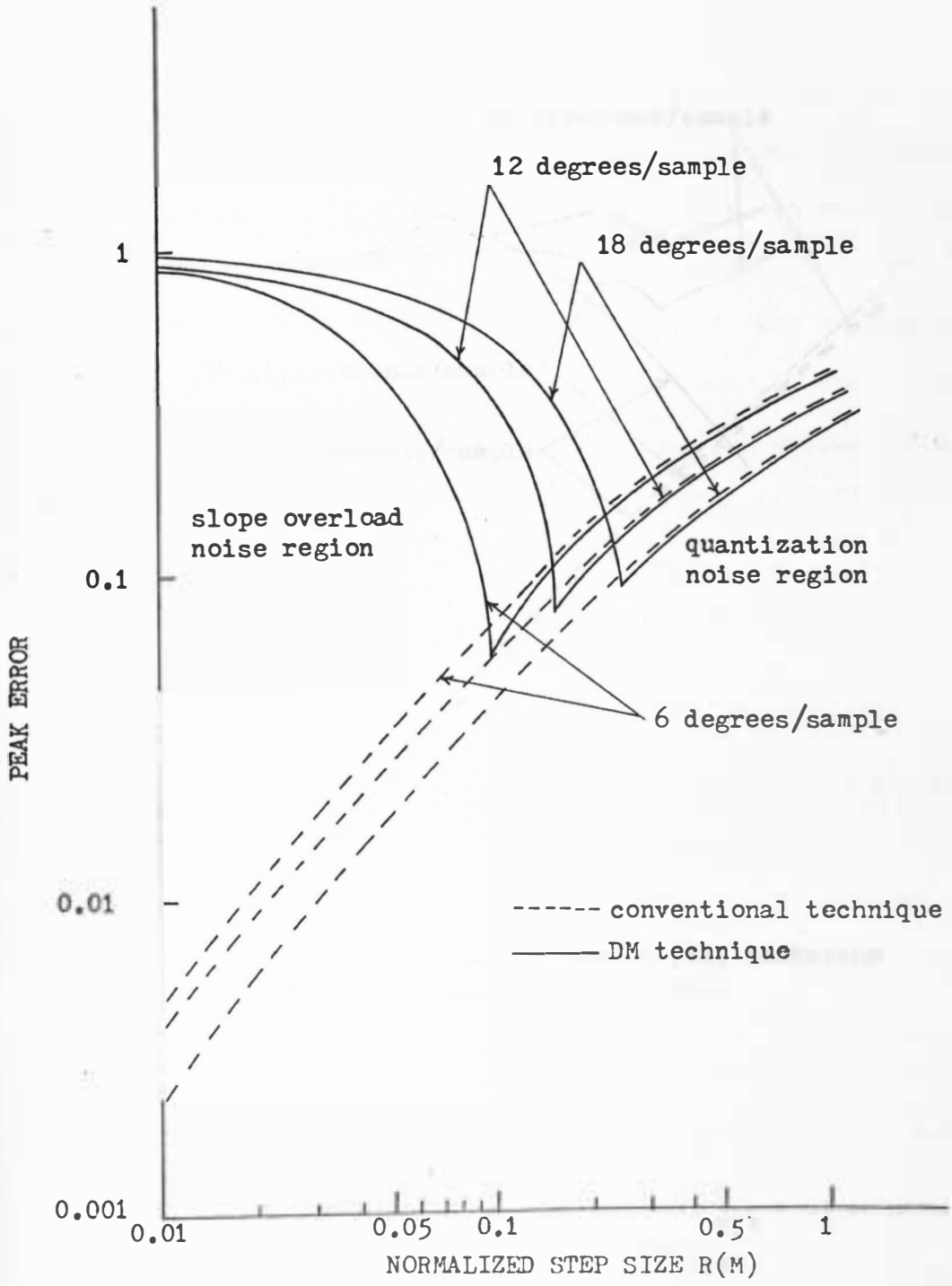


Figure 3-20. Peak error versus normalized R(M) for the sine wave input.

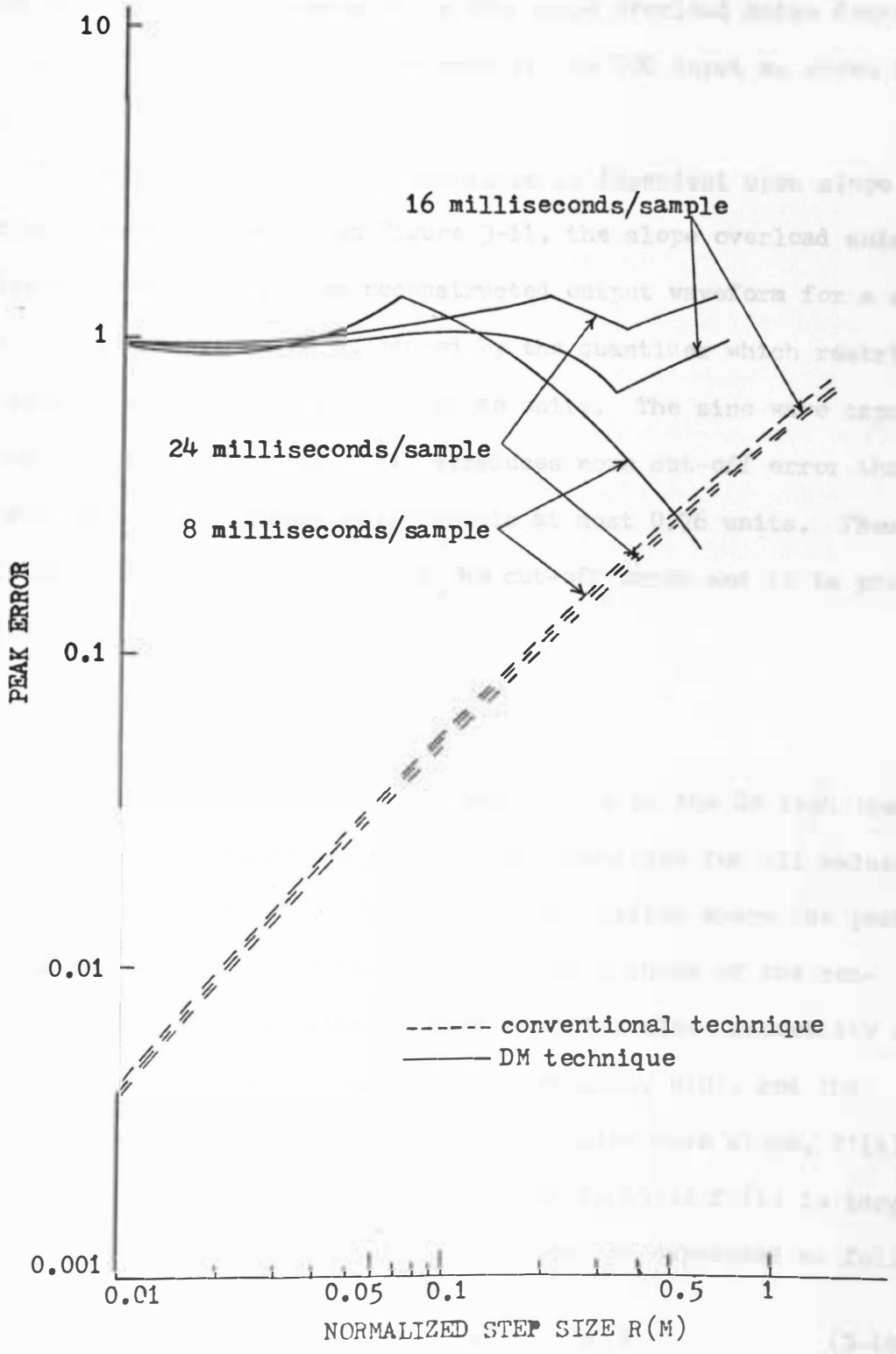


Figure 3-2i. Peak error versus normalized R(M) for the ECG data input.

quantization noise increases while the slope overload noise decreases. This is true also for the peak errors of the ECG input as shown in Figure 3-21.

The peak error for the DM technique is dependent upon slope overload noise. As shown in Figure 3-11, the slope overload noise produces attenuation in the reconstructed output waveform for a sine wave. This cut-off error is caused by the quantizer which restricts the maximum amplitude of the output to unity. The sine wave input has an amplitude of unity, this introduces more cut-off error than the ECG data whose maximum amplitude is at most 0.76 units. Thus the slope overload noise contains the cut-off error and it is proportional to the value of R(M).

d. Slope overload noise in the ECG output

Referring to Figure 3-21, the peak errors by the DM technique are larger than those by the conventional technique for all values of R(M), from 0.01 to 0.5. There is no R(M) region where the peak error values of the DM technique coincide with those of the conventional technique. Equation 3-16 relates the slope capability of the reconstructor, $S_m$, to quantization step size, R(M), and the fundamental sampling interval size, I. The sine wave slope, f'(t), is smaller than $S_m$ for large R(M) and small I, while f'(t) is larger than $S_m$ for small R(M) and large I. This can be expressed as follows

$$\frac{R(M)}{I} > f'(t) \qquad \text{for } R(M) > K \qquad (3\text{-}19)$$

and

$$\frac{R(M)}{I} < f'(t) \qquad \text{for } R(M) < K \qquad (3\text{-}20)$$

where

K = constant equivalent to R(M) value at the transition point

and I is assumed to be fixed at a given value. Equation 3-19 indicates the quantization noise region and Equation 3-20 indicates the slope overload noise region. Thus, the sine wave input has both regions, in one, quantization noise is dominant, and in the other, the slope overload noise is dominant.

On the other hand, the ECG data signal has an extremely steep slope at the leading edge and trailing edge of the R-wave, which is followed by inactive regions. The R-wave portion of the ECG is noted on the first cycle of Figure 3-14. Therefore, f'(t) of the ECG signal can be large unless the data sampling interval lies within the inactive region. For example, if I is limited to 6 input data-intervals per sample, the magnitude of f'(t) can be calculated using two adjacent sampled-data values; one sample at the peak of the pulses and another sample which is within the 6th data interval before or after the peak data sample. Actual data values for the R-wave of the ECG data input are shown in Table 3-1. The values of f'(t) for each sampling interval size are as follows:

for $I = 6$, $f(t) = \frac{X(nT) - X((n \pm 6)T)}{I}$

$$= \frac{1}{0.024} \cdot (0.755626 - (-0.358281))$$

$$= 46.3$$

| n | nT | X(nT) |
|---|---|---|
| • | • | • |
| • | • | • |
| 280 | 1.120 | -0.500800 |
| 281 | 1.124 | -0.499885 |
| 282 | 1.128 | -0.358281 |
| 283 | 1.132 | -0.143129 |
| 284 | 1.136 | 0.115968 |
| 285 | 1.140 | 0.349736 |
| 286 | 1.144 | 0.548408 |
| 287 | 1.148 | 0.722056 |
| 288 | 1.152 | 0.755626 |
| 289 | 1.156 | 0.592354 |
| 290 | 1.160 | 0.300907 |
| 291 | 1.164 | -0.020142 |
| 292 | 1.168 | -0.138857 |
| 293 | 1.172 | -0.177004 |
| 294 | 1.176 | -0.252079 |
| • | • | • |
| • | • | • |

Table 3-1. Original data composing a peak pulse of ECG data input signal.

For $I = 4$,

$$f'(t) = \frac{X(nT) - X((n \pm 4)T)}{I}$$

$$= \frac{1}{0.016} \cdot (0.755626 - (-0.138857)$$

$$= 56.0$$

For $I = 2$,

$$f'(T) = \frac{X(nT) - X((n \pm 2)T)}{I}$$

$$= \frac{1}{0.008} \cdot (0.755626 - 0.300907)$$

$$= 56.8$$

The above f'(t) values represent the slope of the R-wave for three sampling interval sizes.

In Table 3-2, possible $S_m$, or maximum slope values for the reconstructor, are shown for different values of R(M) and I. By comparing these $S_m$ with the f'(t) values found above, the points at which slope overload will occur can be found.

| I \ R(M) | 0.5 | 0.4 | 0.3 | 0.2 | 0.1 |
|---|---|---|---|---|---|
| 2 | 62.5 | 50.0 | 37.5 | 25.0 | 12.5 |
| 4 | 31.3 | 25.0 | 18.8 | 12.5 | 6.3 |
| 6 | 20.8 | 16.7 | 12.5 | 8.3 | 4.1 |

Table 3-2. Slope capability of reconstructor for various quantization step sizes and sampling interval sizes.

The comparison shows that the slope capability of the reconstructor, $S_m$, is smaller than the slope of the ECG waveform except for R(M) = 0.5 and I = 2. Therefore, slope overload noise is present for most R(M) and I values when using ECG data. This results in larger errors with the DM technique than the conventional technique as shown in Figure 3-21.

e. Mean-Square Error

To overcome the difficulty of cancellation of positive with

negative errors, mean-square error is used as an error criterion. The absolute difference between the input signal data and the corresponding reconstructed output signal data is found and these differences are squared. The squared differences are summed for the entire waveform and divided by the total number of data sample points, Then the mean-square error is,

$$M.S.E. = \frac{1}{N}\left( \sum_{n=0}^{N-1} (f(nT) - F(nT))^2 \right) \qquad (3\text{-}21)$$

where

$n = 0, 1, 2, 3, \ldots N-1$

$T$ = sampling period

$N$ = total number of samples

$f(nT)$ = nth sample of the input signal

$F(nT)$ = nth value of the reconstructed output signal

For sine wave input, 20 cycles are sampled and for every 5 cycles the M.S.E. value is tested for its convergence to the deviation limit of 1%. The ECG data used consisted of 1050 samples from the X-lead of the Frank lead system. (Appendix A).

Figures 3-22 and 3-23 show the M.S.E. versus normalized R(M) for the sine wave input and ECG data input. Different M.S.E. values are obtained for both the conventional and the DM techniques when each is applied to the sine wave input or the ECG data input. For all R(M) values, the conventional technique introduces much smaller M.S.E. than the DM technique. This is because slope overload noise is present for all regions of R(M) for the ECG data. Curves for the DM

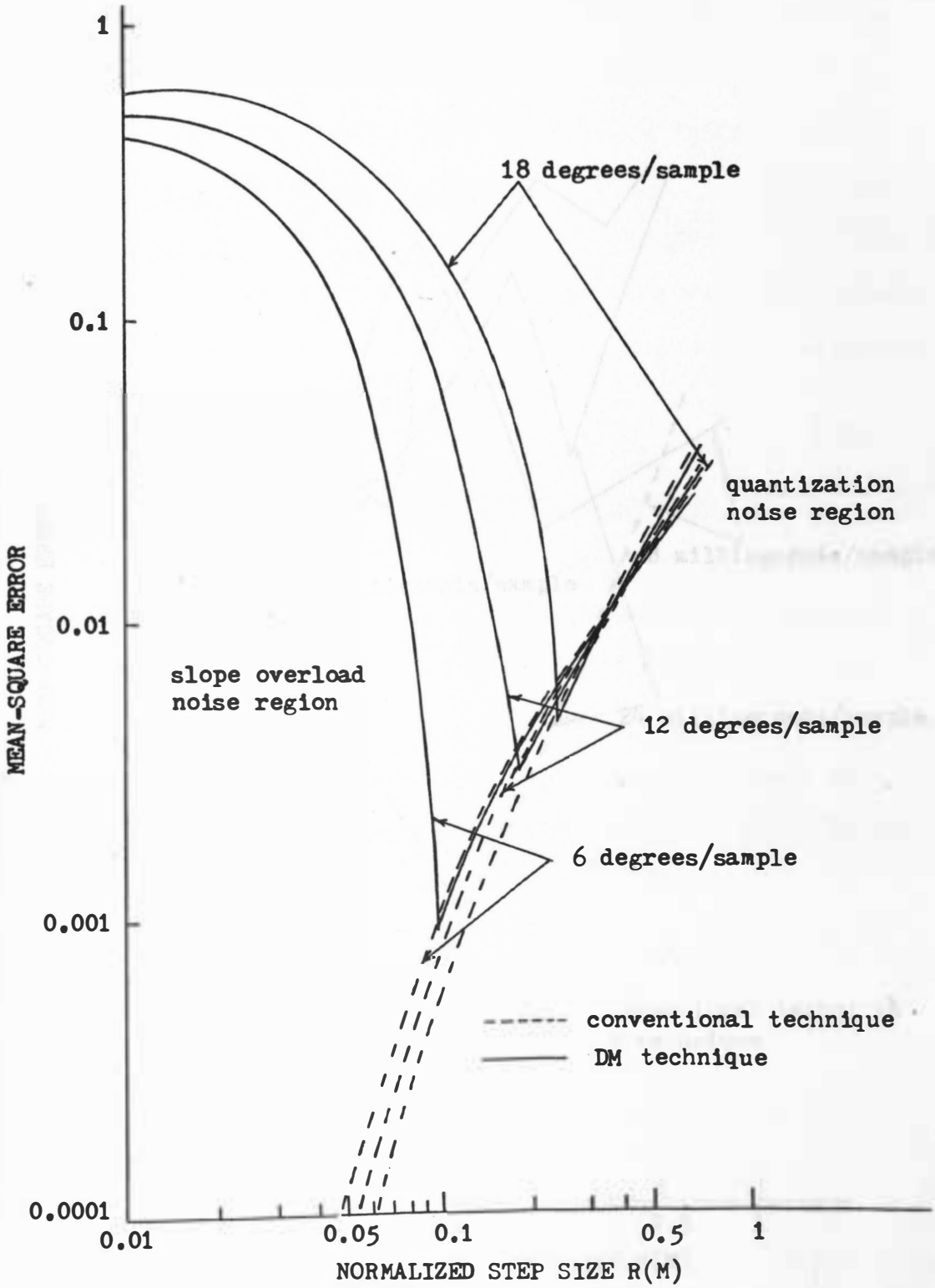


Figure 3-22. M.S.E. versus normalized R(M) for the sine wave input.

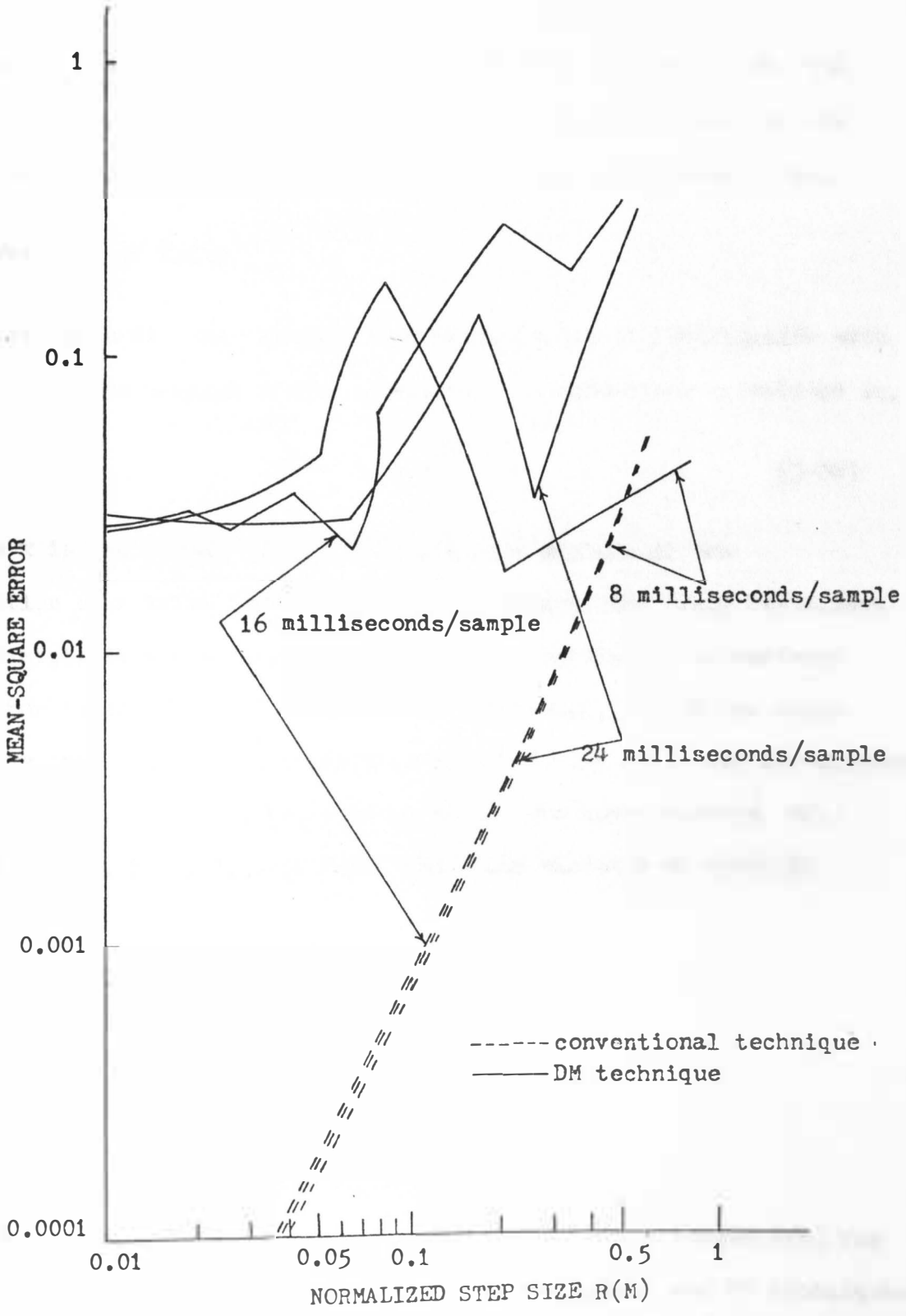


Figure 3-23. M.S.E. versus normalized R(M) for the ECG data input.

technique are random for large R(M), while they approach 0.026 for small R(M)'s. The randomness is due to the characteristics of the ECG data signal and is dependent upon the sampling interval size.

f. Variance of Error

Variance of error is used to measure the error distribution with respect to the average error. Variance of a variable x is defined as,

$$\sigma^2 = \overline{(x - \bar{x})^2} \qquad (3\text{-}22)$$

where $\bar{x}$ is the average of x. Variance is a measure of the deviation of a value from its mean that augments the large deviations and diminishes the small ones by a squaring process. The variance of error is an important parameter of dispersion. Since the error for the analog signal is defined as e(t) = f(t) - F(t), for the discrete signal input, time t is replaced by the sample time sequence, nT, where n is 0, 1, 2, 3, .... N-1. Thus, the variance of error is

$$\sigma^2 = \frac{1}{N} \sum_{n=0}^{N-1} \left( (e(nT) - \bar{e})^2 \right)$$

where

e(nT) = error for the nth sample

$\bar{e}$ = average error for N samples.

Figures 3-24 and 3-25 show the variance of error versus R(M) for the sine wave and ECG data input for the conventional and DM techniques. The variance values decrease as R(M) decre es for the conventional

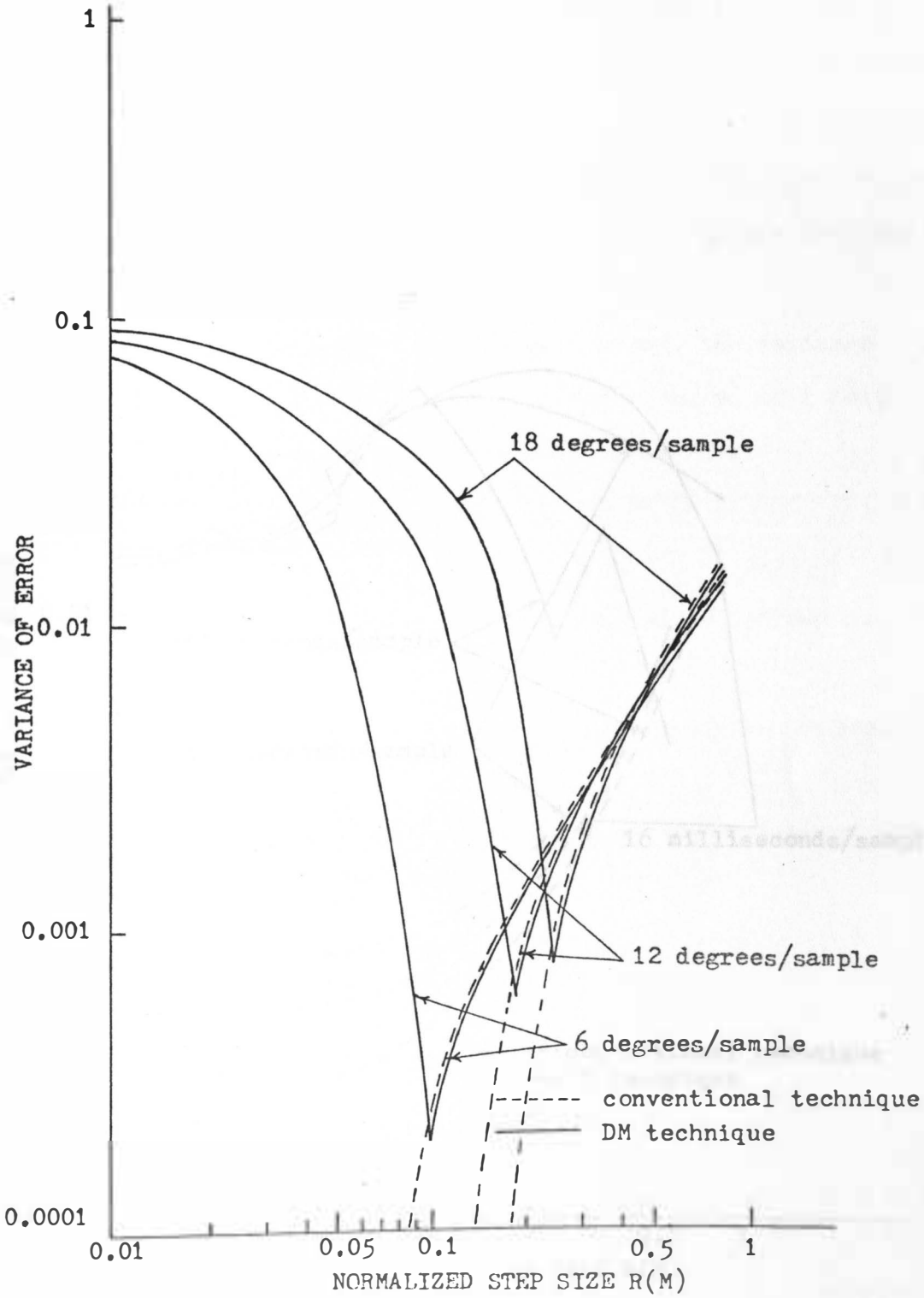


Figure 3-24. Variance of error versus normalized R(M) for the sine wave input.

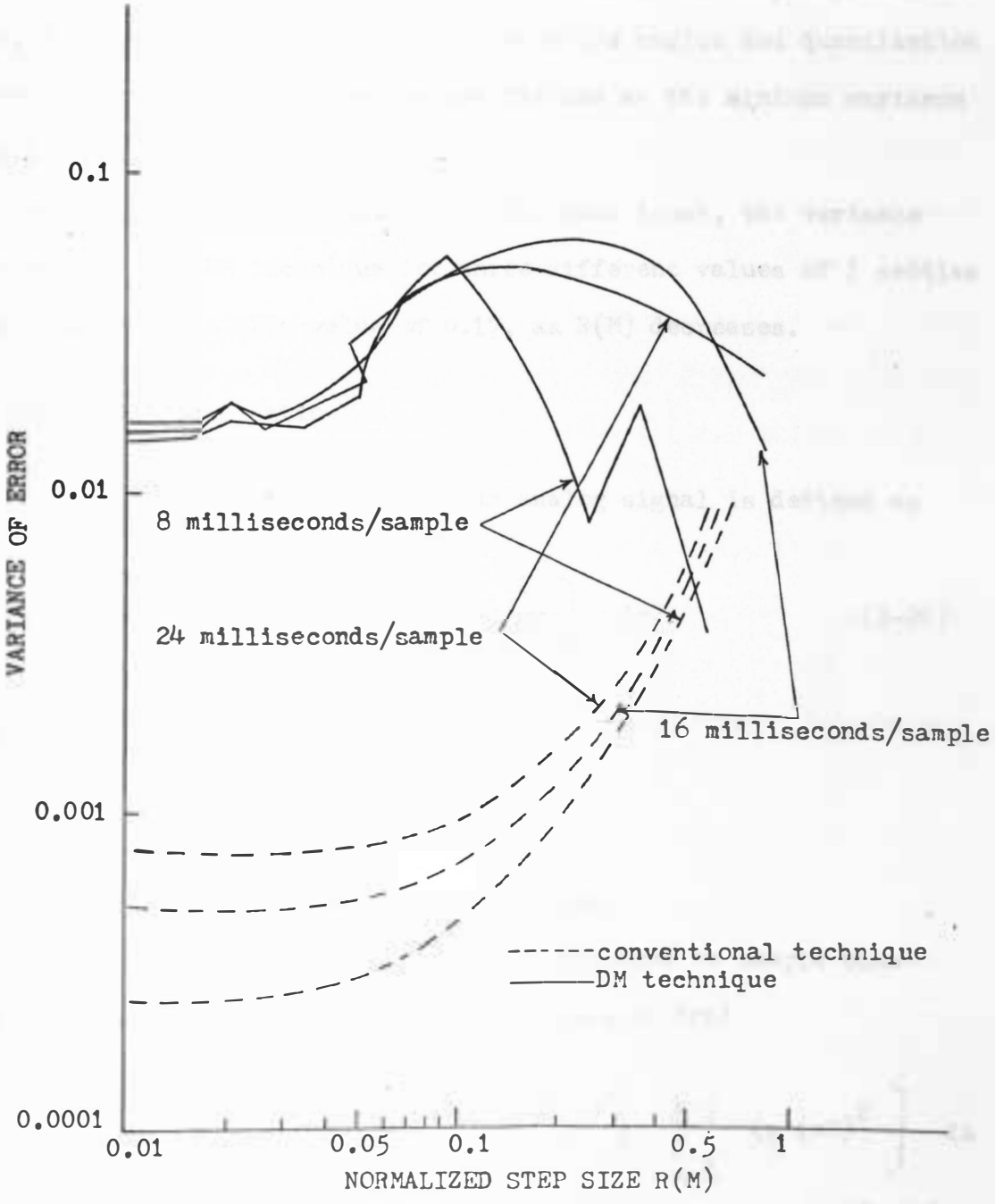


Figure 3-25. Variance of error versus normalized R(M) for the ECG data input.

technique and the sine wave input because the quantization noise is distributed within the length of 1/2 R(M). The conventional technique introduces a smaller variance as R(M) decreases and sampling interval size, I, increases. The slope overload noise region and quantization noise region of the DM technique are divided at the minimum variance points.

Figure 3-25 shows that, for the ECG data input, the variance of error for the DM technique for three different values of I settles down to a nearly stable value of 0.17, as R(M) decreases.

g. Signal-to-Noise Ratio

The signal-to-noise ratio for an analog signal is defined as

$$S/N = 10 \text{ Log}_{10} \left[ \frac{F(t)^2}{n'(t)^2} \right] \quad \text{db} \qquad (3\text{-}24)$$

where

$n'(t) = f(t) - F(t)$

$f(t)$ = input signal

$F(t)$ = reconstructed output signal.

For the discrete input signal, t is replaced by sample time sequence nT, where n is 0, 1, 2, 3, .... N-1, so that

$$S/N = 10 \text{ Log}_{10} \left[ \frac{1}{N} \sum_{n=0}^{N-1} (F(nT)^2 \Big/ \frac{1}{N} \sum_{n=0}^{N-1} (n'(nT)^2 \right] \quad \text{db} \qquad (3\text{-}25)$$

is an average S/N ratio.[16]

Figure 3-26 and 3-27 shows S/N ratios versus normalized R(M) values for the sine wave and ECG data inputs for the two techniques.

For a sine wave input, the conventional technique has a better signal-to-noise ratio for small values of R(M) than the DM technique. This holds for all three sampling rates. In the quantization noise region both techniques have the same signal-to-noise ratios for small sampling interval size, I, and quantization step size, R(M). But, for the ECG data input, the conventional technique has better signal-to-noise ratios than the DM technique over most of the values of R(M) and I. Since the slope overload noise attenuates the output signal amplitude, the signal-to-noise ratio in the slope overload noise region is smooth. The curves show a slight randomness in the quantization noise region because the quantization noise is not proportional to the amplitude and slope of the input signal and the slope overload noise in the ECG data input is very large because of the R-waves.

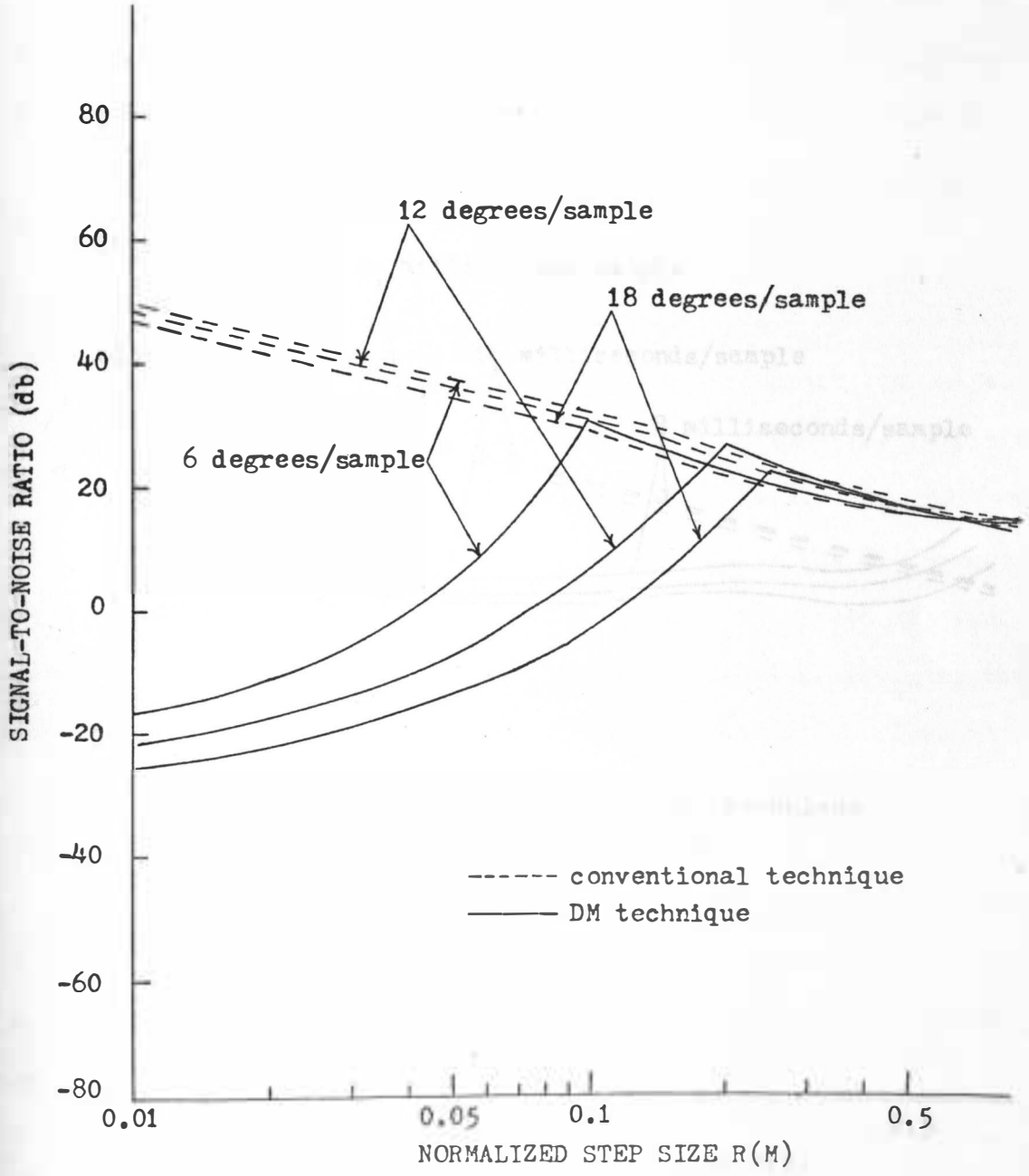


Figure 3-26. Signal-to-noise ratio versus normalized R(M) for the sine wave input.

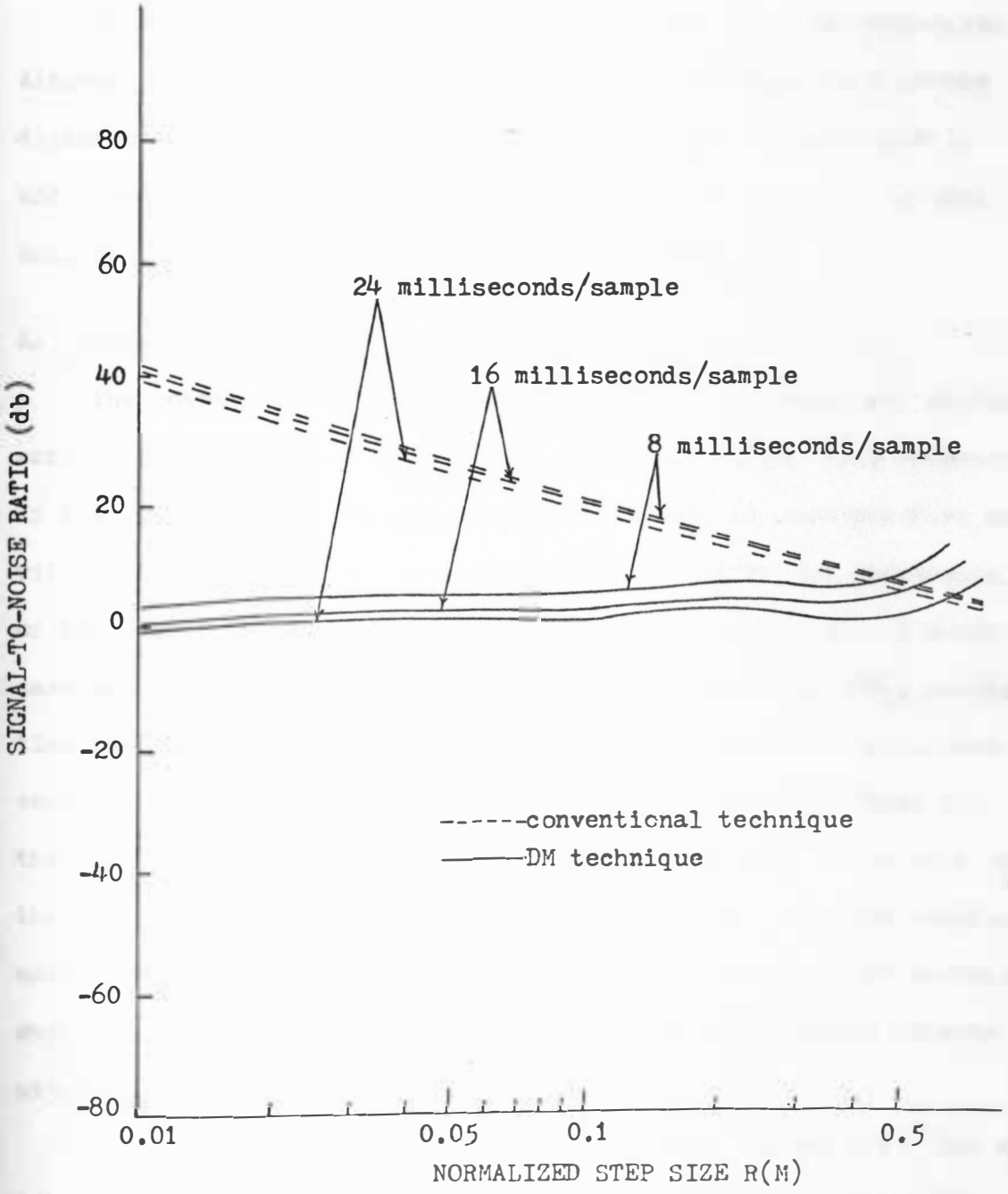


Figure 3-27. Signal-to-noise ratio versus normalized R(M) for the ECG data input.

# CHAPTER IV

## A MODIFIED REDUNDANCY REDUCTION TECHNIQUE

In Chapter III a redundancy reduction technique was discussed. Although it has some advantages, slope overload noise is a severe disadvantage. To eliminate this difficulty, the DM technique is modified by using an adaptive scheme for reconstruction. In this chapter the modified DM technique will be discussed.

### A. Slope Detection

The comparator in the system of Figure 3-1 compares two adjacent samples and determines the sign to be attached to the time information. If the difference is positive, the sign of $\triangle T_i$ is also positive and vice versa. However, the comparator never computes the difference or the number of magnitude levels, R(M) which are between adjacent samples. Since the magnitude of the time information, $\triangle T_i$, is the time interval size between two adjacent non-redundant samples, the reconstructor goes up or down only one quantum size and holds for the period of $\triangle T_i$, no matter how large the magnitude difference of the two samples may be. Such a limitation results in slope overload noise. Therefore, to eliminate this error, the modified DM technique employs a scheme which determines the amplitude difference between adjacent significant samples.

The modified form of the system is shown in Figure 4-1. The slope detector is composed of a subtraction and a comparison unit. The subtraction unit computes the magnitude of the difference, D, between

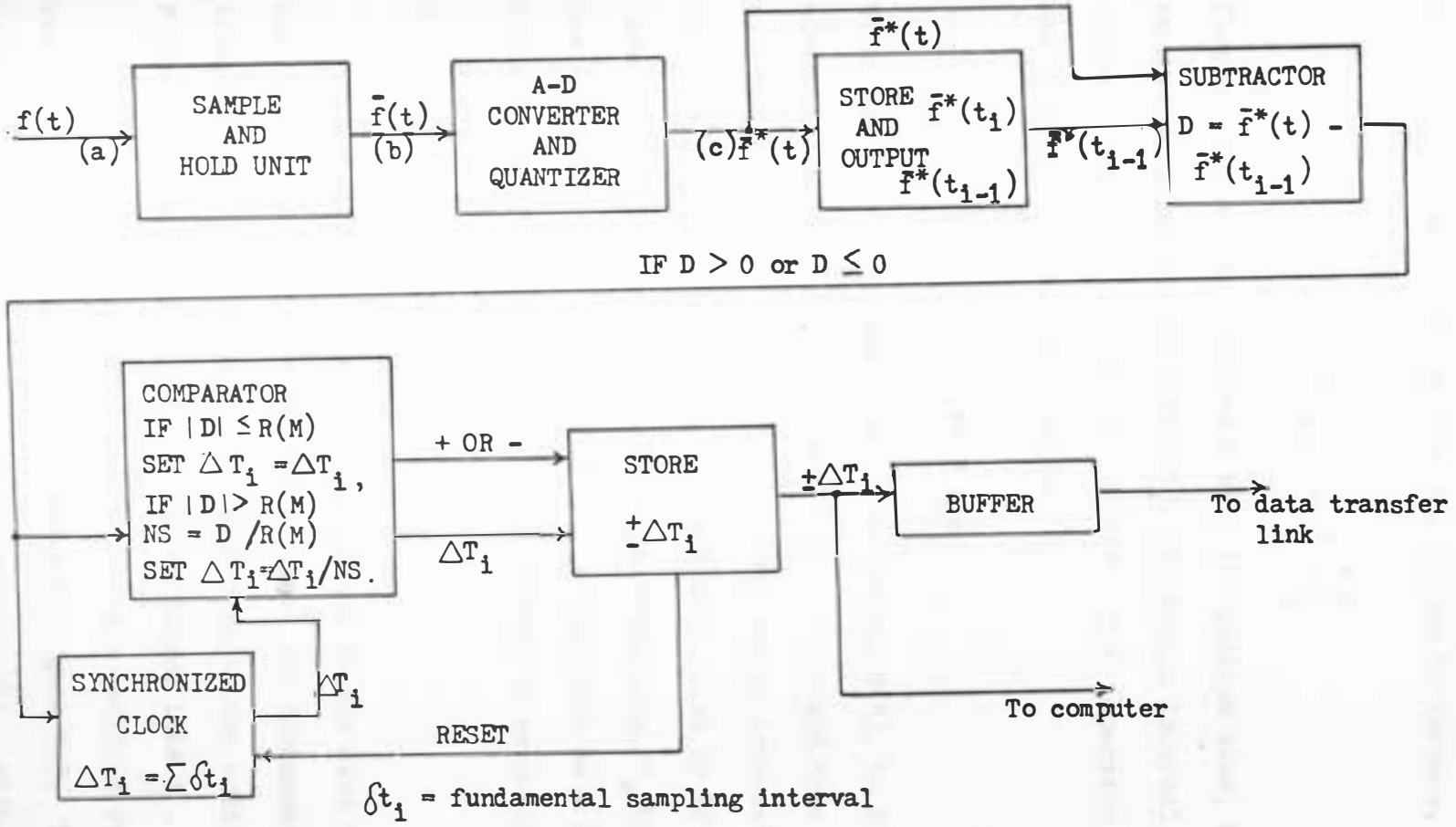


Figure 4-1. Block diagram of data compressor for the adaptive redundancy reduction technique.

the two samples as well as the sign of the difference,

$$\bar{f}^*(t) - \bar{f}^*(t_{i-1}) = \begin{cases} +D \\ -D \\ 0 \end{cases} \qquad (4\text{-}1)$$

Then the comparator compares D with the quantum size, R(M). If D is smaller in magnitude than R(M), the sample interval size is not changed, but, if D is larger than R(M), the comparator computes a new quantity, NS, as shown below,

$$NS = \frac{D}{R(M)} \qquad (4\text{-}2)$$

NS is the number of quantization intervals, R(M), in D and is always an integer number since $\bar{f}^*(t)$ is different from $\bar{f}^*(t_{i-1})$ by K•R(M), K = 0, 1, 2, 3, .... N. The sample interval size, $T_s$, which is actually the same as I, is then divided by NS to replace the time information, $\triangle T_i$, with the subinterval size, $T_s/NS$. As soon as the subinterval size is sent to the storage unit as a $\triangle T_i$ value, the next sample is compared and the process is repeated.

B. Adaptive Reconstructor

The time interval values transmitted by the data transfer link unit in Figure 3-1 are never smaller than the fundamental sampling interval size, $T_s$, while those transmitted by the modified system in Figure 4-1 can be equal to, smaller or larger than $T_s$.

The adaptive reconstructor, which is a modified form of the reconstructor in Figure 3-6, is shown in Figure 4-2. The comparator unit compares the received time information, $\triangle T_i$, with $T_s$ and detects

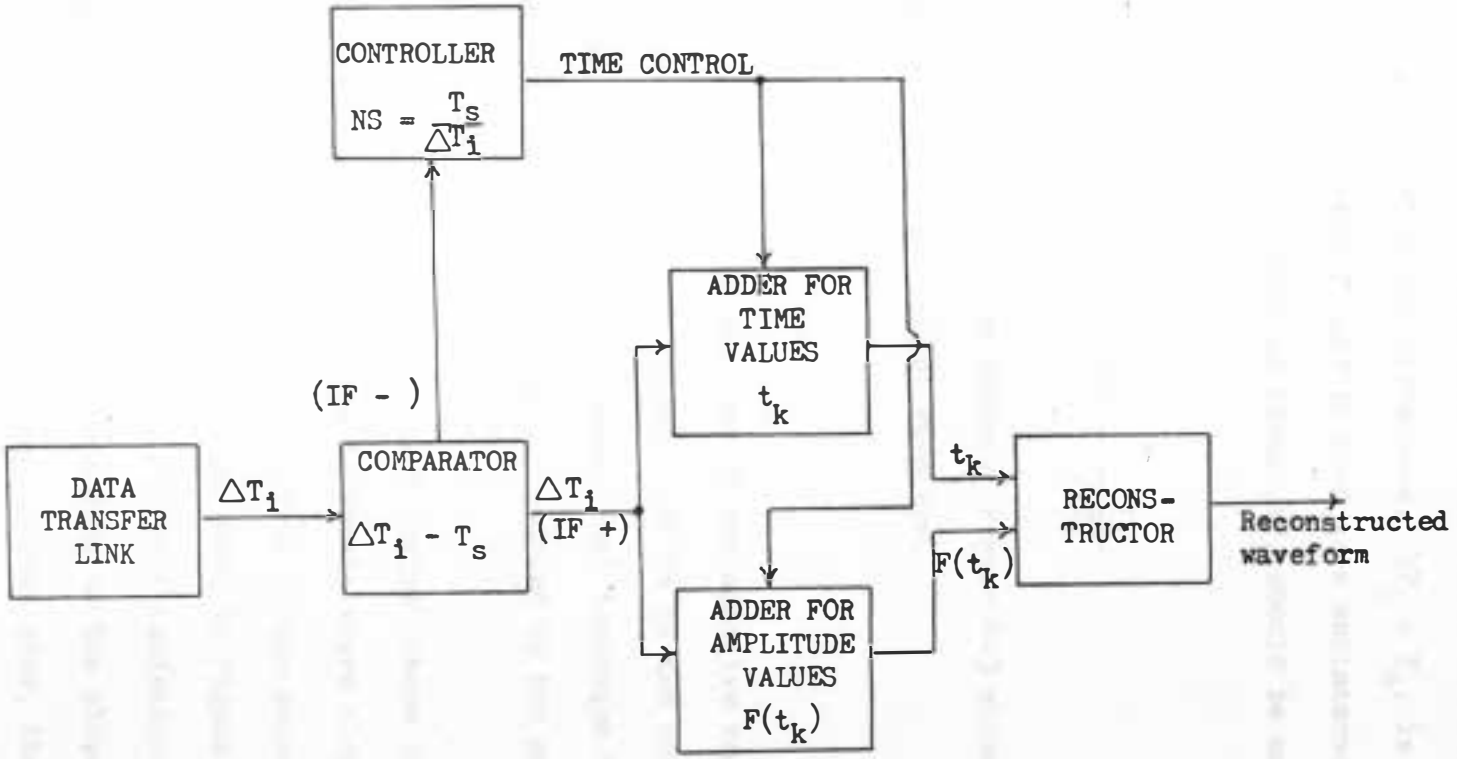


Figure 4-2. Simplified block diagram of the adaptive reconstructor for the modified DM redundancy reduction technique.

when the size of $\triangle T_i$ is smaller than the fundamental sampling interval size. When the difference, $\triangle T_i - T_s$, is negative, then $\triangle T_i$ is smaller than $T_s$ and is used as a subinterval, and the controller unit computes the number of times $\triangle T_i$ should be used as a subdivision, NS, where

$$NS = \frac{T_s}{\triangle T_i} \qquad (4\text{-}3)$$

This is always as integer number. Figure 4-3 shows the adaptive reconstruction of the output waveform.

C. Noise

The reconstructed waveform of the adaptive reconstructor is not the exact replica of the output waveform by the conventional technique. Since the noise due to the conventional technique has been analyzed in Chapter III, only the noise introduced by the adaptive technique will be discussed here.

The noise introduced by the adaptive scheme is mainly due to phase distortion in the sample intervals where slope overload occurs. The phase distortion error is produced by the reconstruction process of the adaptive reconstructor. As shown in Figure 4-3, the 6th sample is divided into 4 subintervals. In each subinterval the output data increases by one step size. Depending on the slope of the input signal waveform and the sampling interval size, the reconstructed output waveform usually lags or leads the original input waveform by some time interval. The phase distortion noise increases as the

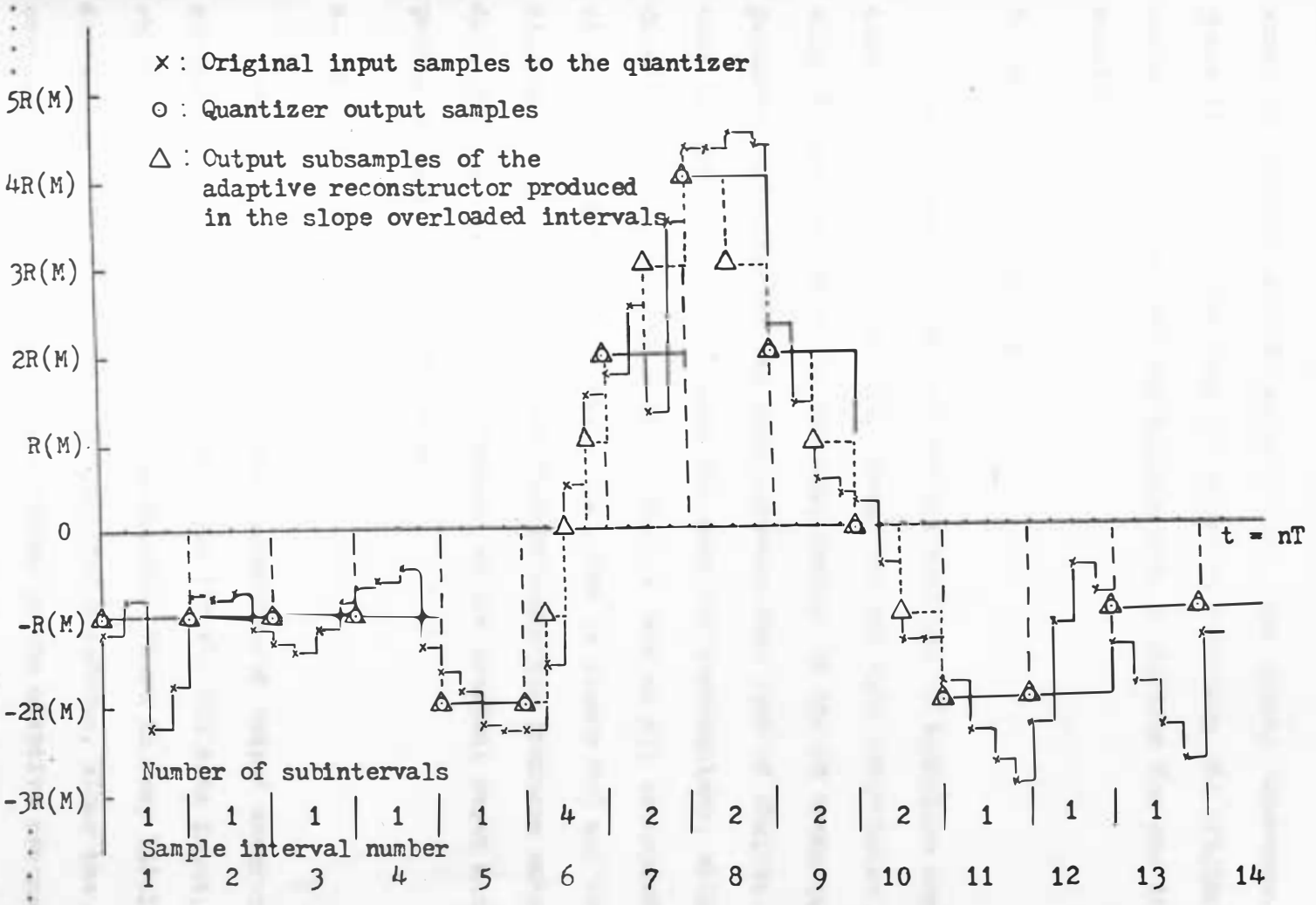


Figure 4-3. Graphical analysis of the adaptive reconstruction by subdividing the slope overloaded input sample intervals.

sampling interval and the slope of the input signal increases. The phase distortion noise does not completely destroy the original input signal waveform because the maximum time distortion for one interval is bounded by $T_s/2$.

D. Experimental Results

The parameters analyzed for the modified DM technique are the same as those of Chapter III, except for the data compression ratio which is not influenced by the modification of the DM technique. The parameter calculations are more accurate than that of Chapter III in that all available data points are used for computations, while in Chapter III only sampled data points are used as all unsampled signal data points are ignored. As shown in Figure 4-3 and the flow diagram in Appendix B, the modified DM technique produces output data which do not exactly correspond to the original input data points in some sample intervals.

a. Waveform Plot

Figures 4-4 and 4-5 show the reconstructed output waveforms by the conventional and modified DM technique for the ECG data input, each of which is plotted for the same conditions. There is very little visual difference between the two reconstructed waveforms, since the slope overload noise is completely eliminated by the adaptive reconstructor. The modified DM technique not only eliminates the slope overload noise, it also reduces the quantization noise introduced by the

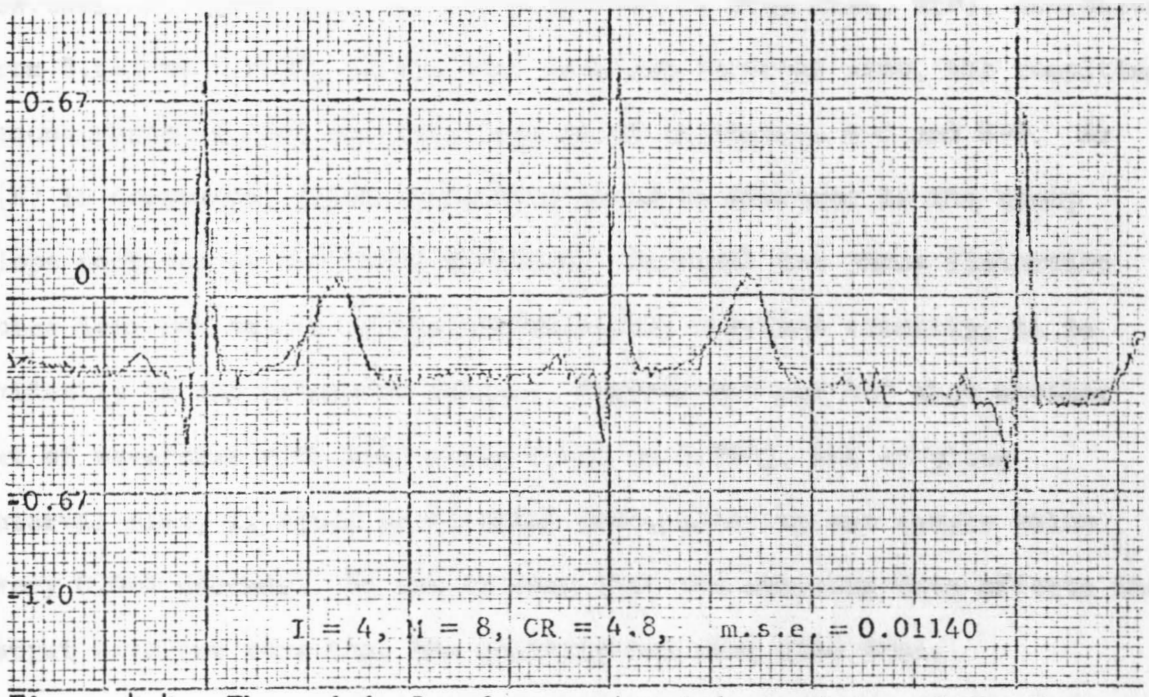


Figure 4-4. The original and reconstructed waveforms of the ECG data input by the conventional technique.

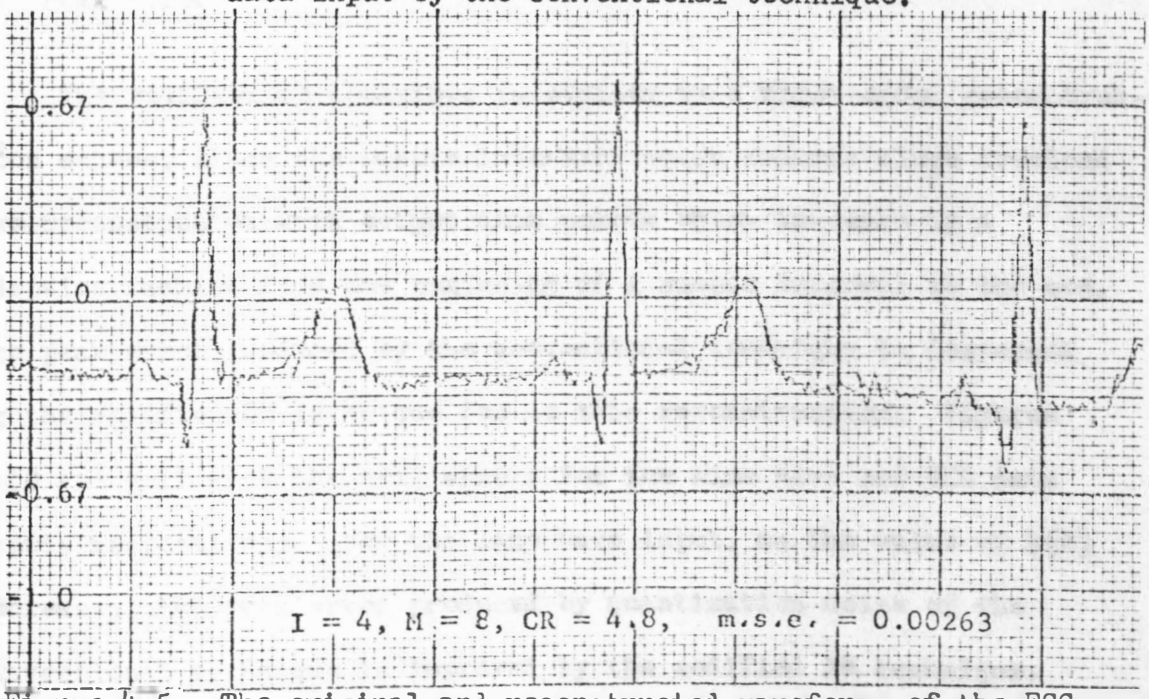


Figure 4-5. The original and reconstructed waveforms of the ECG data input by the modified DM technique.

conventional technique. If the quantization step size, R(M), decreases from 0.125 to 0.0238, at the same sampling interval size, the resulting reconstructed output waveforms are shown in Figures 4-6 and 4-7. As R(M) is decreased, phase distortion noise is produced in the steep slope portions of the input waveform. Although the phase distortion noise does not appear in the reconstructed waveform visually, it is evidently in the parameter values. Figures 4-8 and 4-9 show another set of waveforms with R(M) value equal to 0.0883, and sampling interval size, I, equal to 6, which corresponds to one sample value every 0.024 seconds. It can be seen that the sampling rate affects the output waveform more than the quantization step size does.

b. Peak Error

The modified DM technique is similar to a first-order reconstruction scheme, since the sample intervals which contain slope overload are reconstructed with output data points which increase in a stepwise fashion from the beginning of a sample interval to the end. The peak error produced by the conventional technique is decreased by the modified DM technique due to this reconstruction. Figures 4-10 and 4-11 show the peak errors for the sine wave and ECG data inputs respectively. For the sine wave input, as the value of R(M) decreases, the peak error produced by quantization noise of the conventional technique is improved by the modified DM technique. When R(M) is large and the number of subintervals is very small, the peak error is nearly equal to that of the conventional technique. The peak error for the ECG data input is only slightly affected by the

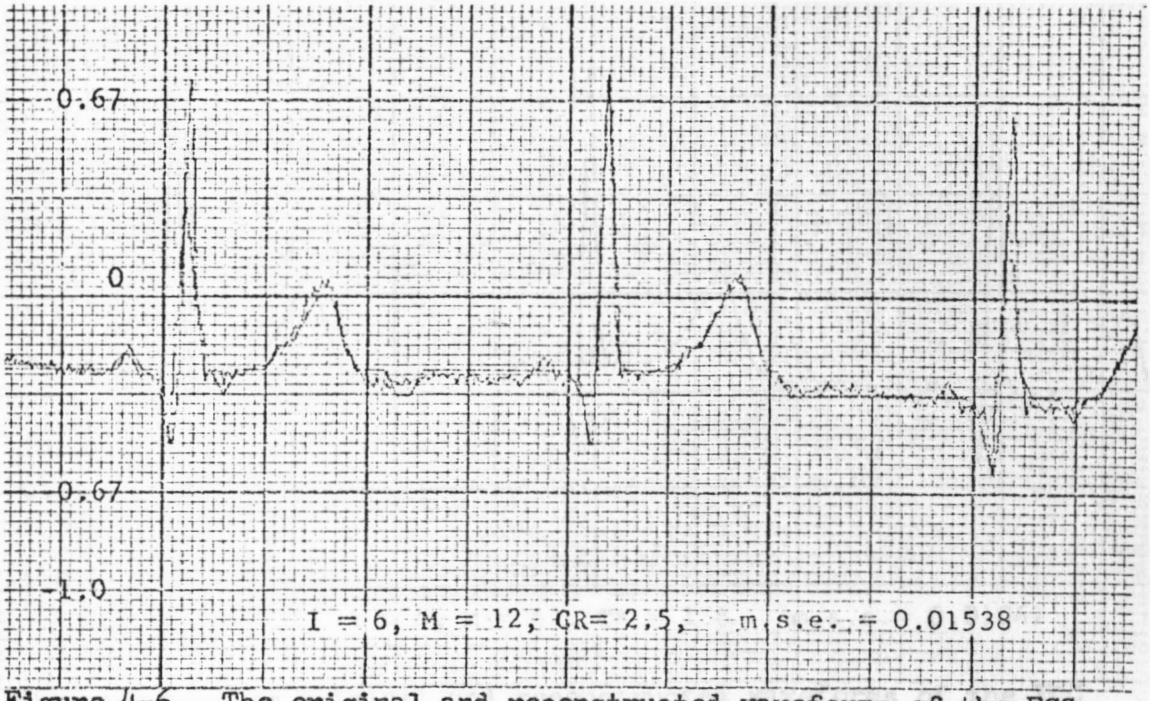


Figure 4-6. The original and reconstructed waveforms of the ECG data input by the conventional technique.

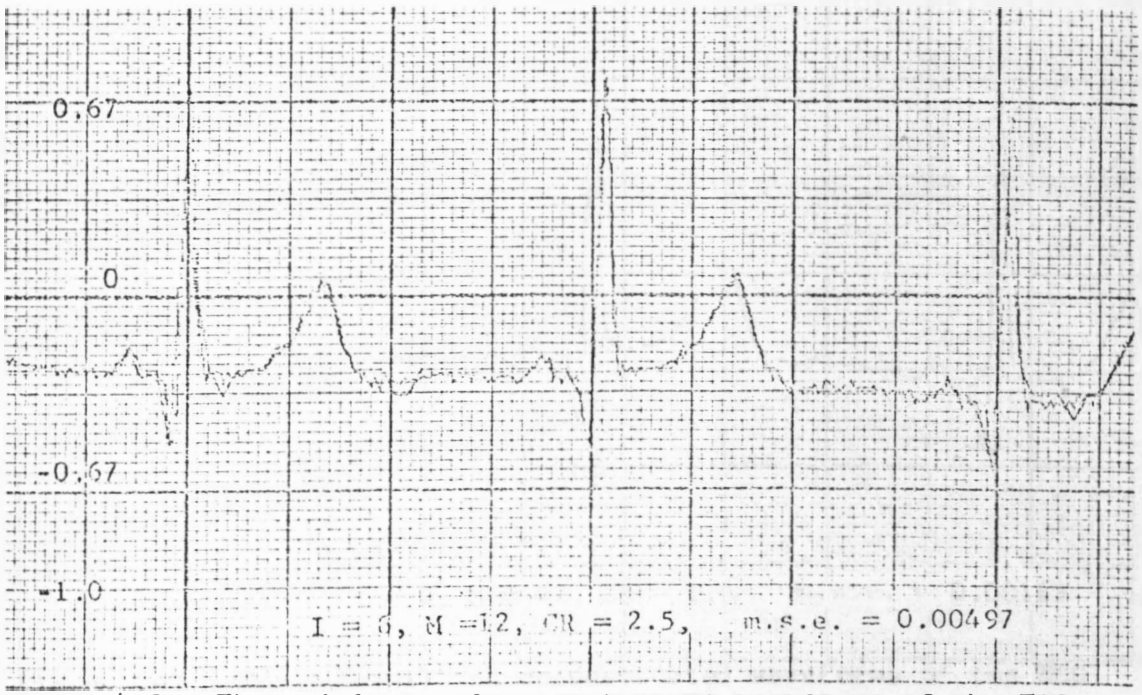


Figure 4-7. The original and reconstructed waveforms of the ECG data input by the modified DM technique.


Figure 4-8. The original and reconstructed waveforms of the ECG data input by the conventional technique.

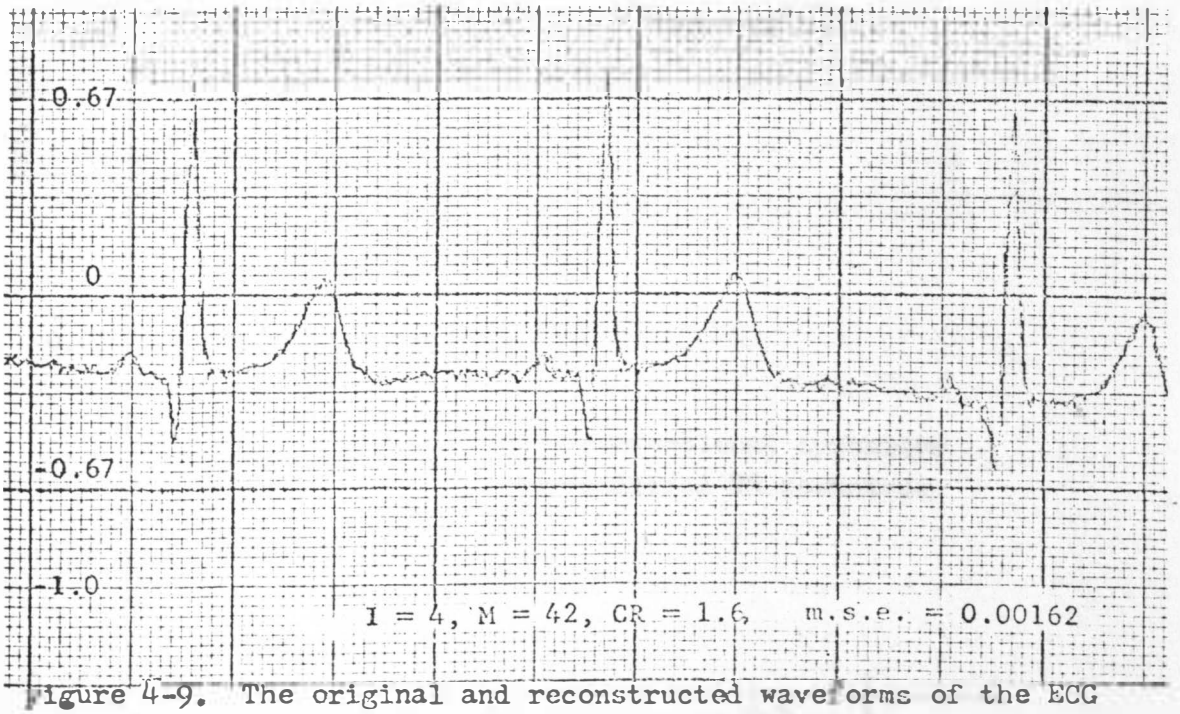


Figure 4-9. The original and reconstructed waveforms of the ECG data input by the modified DM technique.

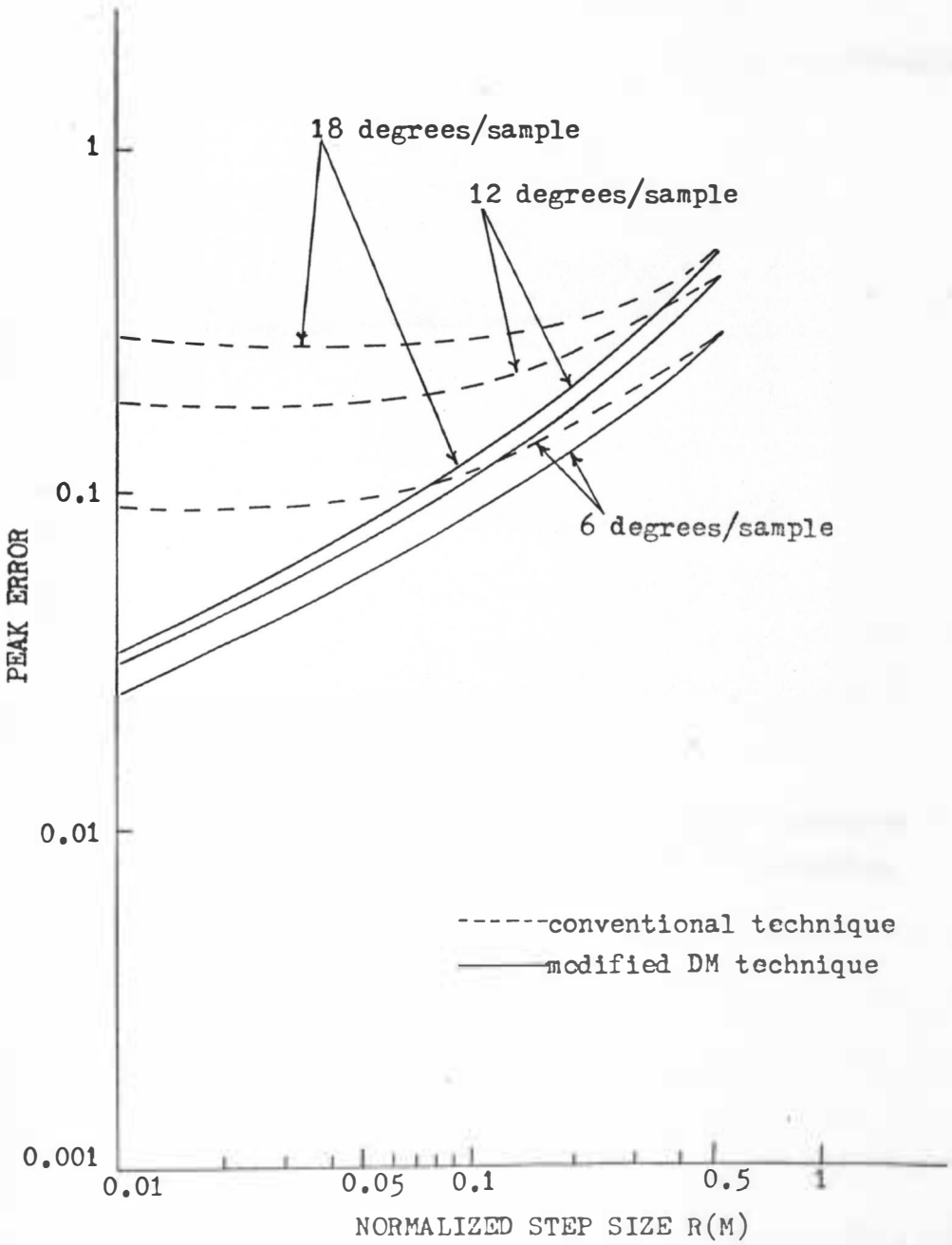


Figure 4-10. Peak error versus normalized R(M) by the conventional and modified DM techniques for the sine wave input.

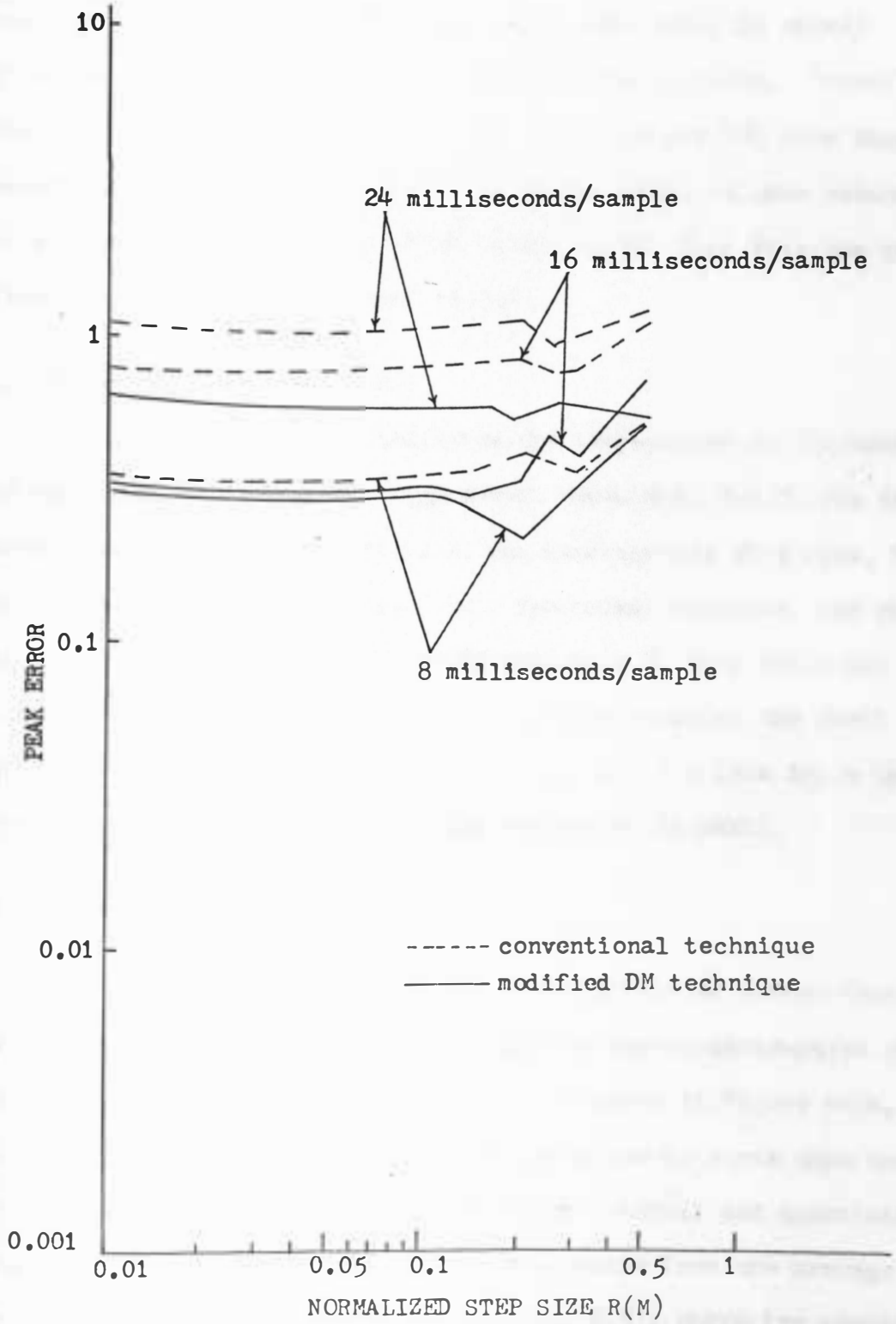


Figure 4-11. Peak error versus normalized R(M) by the conventional and modified DM techniques for the ECG data input.

quantization step size, R(M) because the peak error is mainly produced by the small deviations which are not sampled. Therefore, the sampling rate dominates the peak error for the ECG data input waveform. When the value of R(M) is large, there is some randomness in the peak error activity, which is due to the fact that the quantization noise is dominant in that region.

c. Mean-Square Error (M.S.E.)

The mean-square error indicates the improvement of the modified DM technique more clearly. Figure 4-12 shows that M.S.E. for the sine wave input decreases very fast, as the quantization step size, R(M), decreases. Since the sine wave is a symetrical function, the phase distortion error of the modified DM technique is very small and the quantization noise is reduced to the minimum value at the small values of R(M). Referring to Figure 4-13, the ECG data input introduces phase distortion noise in the range where R(M) is small.

d. Variance of Error

Since the variance of error is the deviation of errors from the average of errors, it shows the fidelity of the reconstruction of the input signal. For the sine wave input, as shown in Figure 4-14, the variance of error for the modified DM technique is worse than the conventional technique for larger sampling interval and quantization step sizes. This means that the errors deviate from the average error more actively in the region of large R(M), where the quantization noise is large. The error deviation from the average error value for

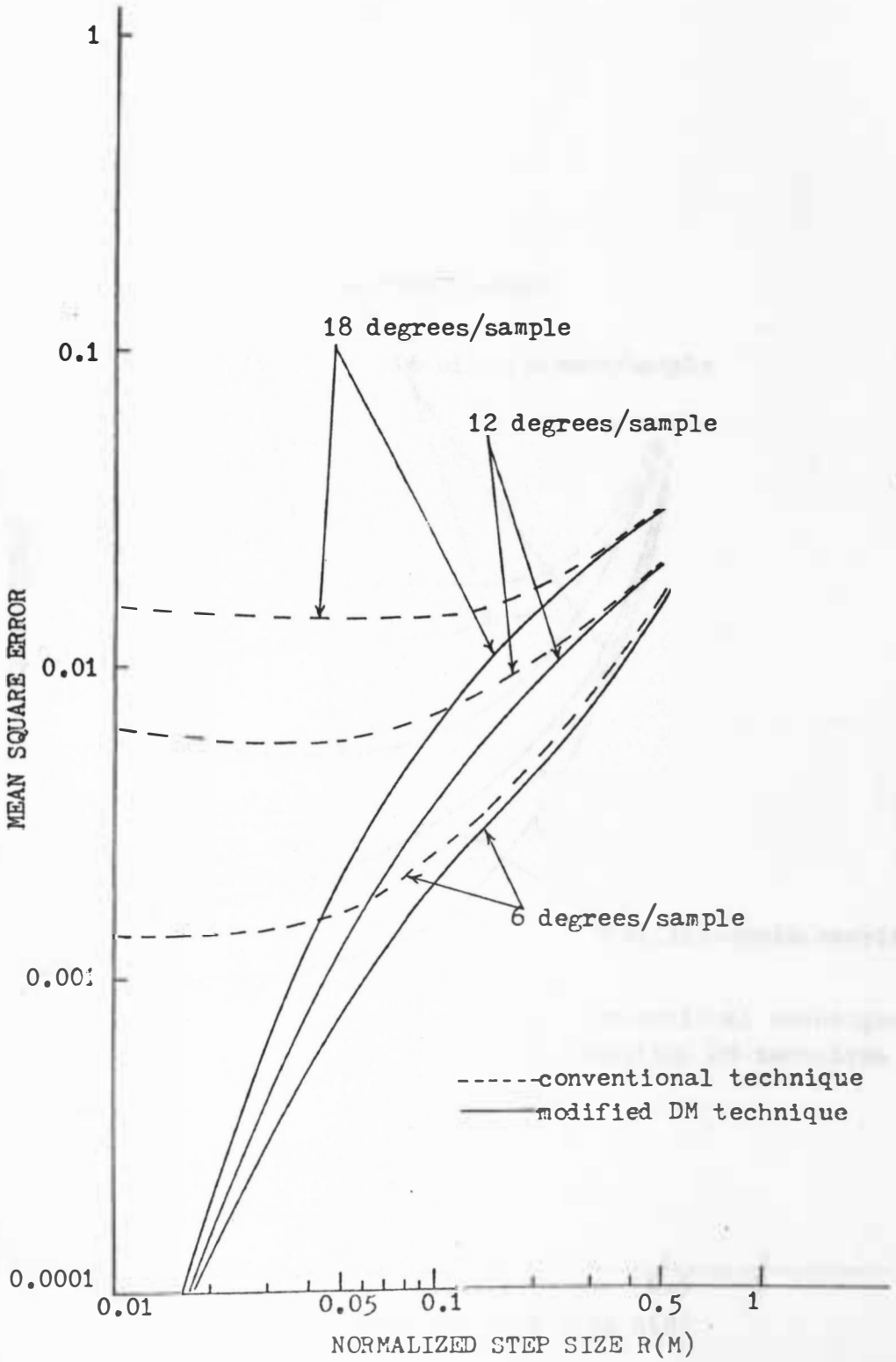


Figure 4-12. M.S.E. versus normalized R(M) by the conventional and modified DM techniques for the sine wave input.

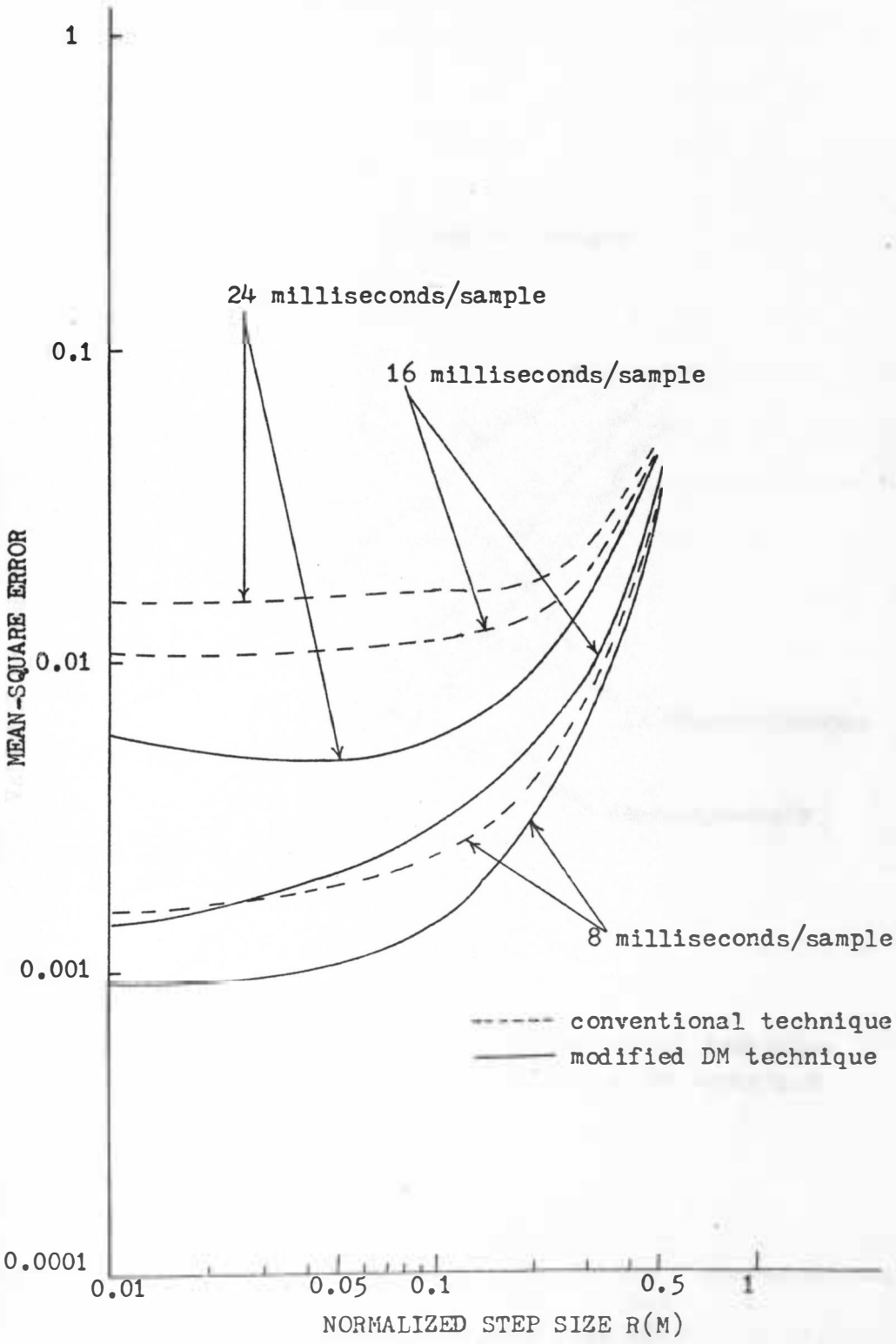


Figure 4-13. M.S.E. versus normalized R(M) by the conventional and modified DM techniques for the ECG data input.

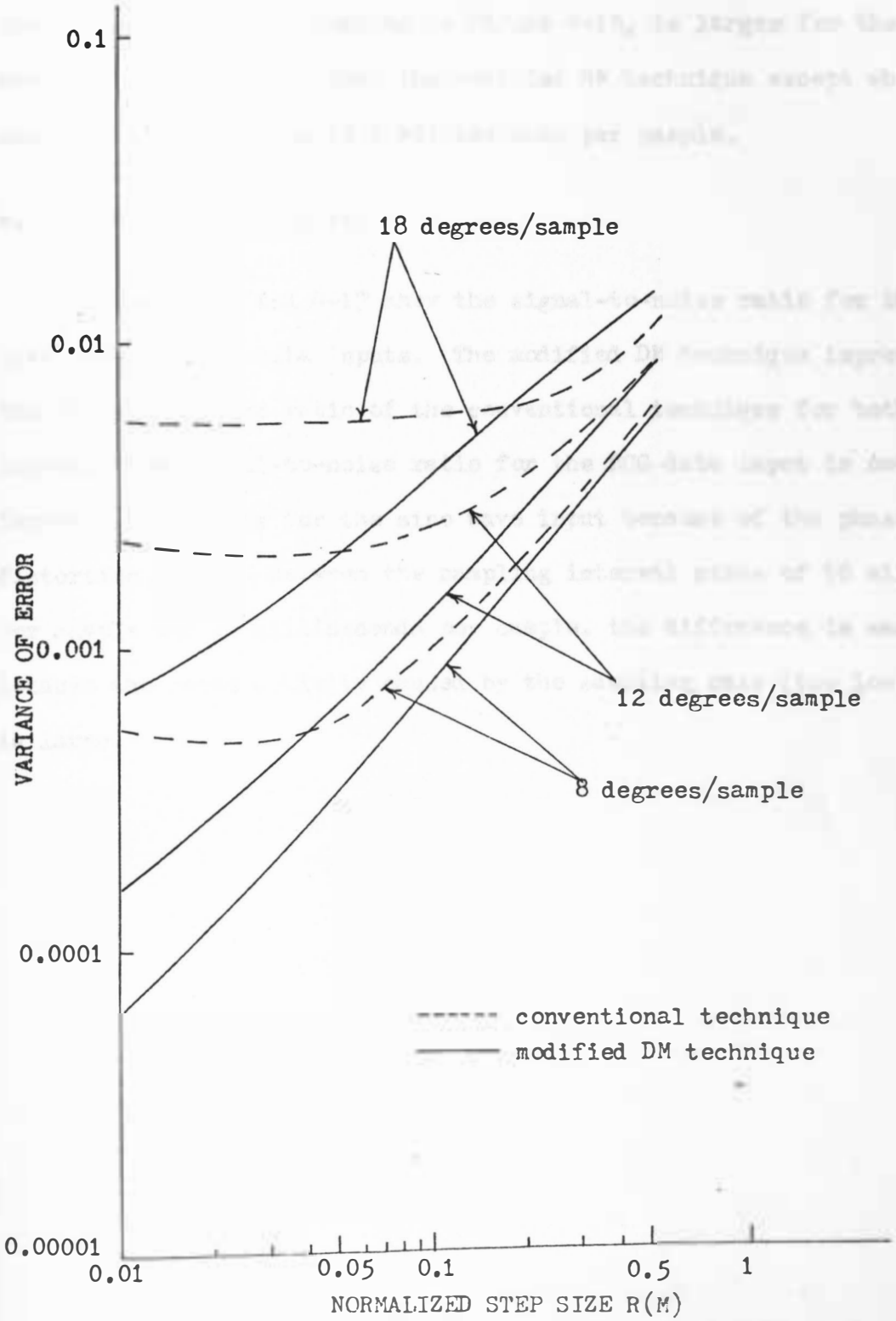


Figure 4-14. Variance of error versus normalized R(M) by the conventional and modified DM techniques for the sine wave input.

the ECG data input, referring to Figure 4-15, is larger for the conventional technique than the modified DM technique except when the sampling interval size is 8 milliseconds per sample.

e. Signal-to-Noise Ratio

Figures 4-16 and 4-17 show the signal-to-noise ratio for the sine wave and ECG data inputs. The modified DM technique improves the signal-to-noise ratio of the conventional technique for both inputs. The signal-to-noise ratio for the ECG data input is not improved as much as for the sine wave input because of the phase distortion noise. Between the sampling interval sizes of 16 milliseconds per sample and 24 milliseconds per sample, the difference is small, because the noise activity caused by the sampling rate (too low) is large.

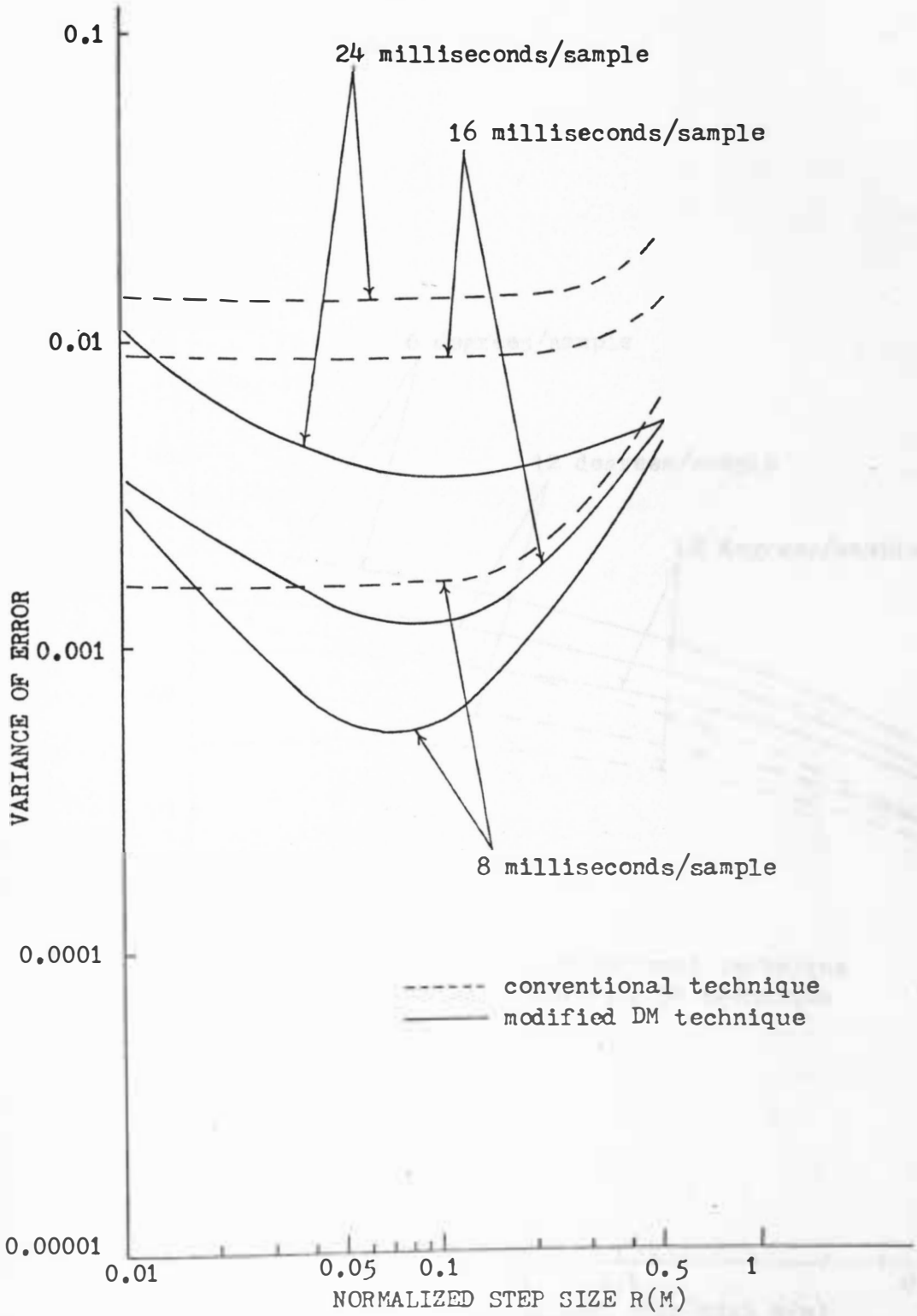


Figure 4-15. Variance of error versus normalized R(M) by the conventional and modified DM techniques for the ECG data input.

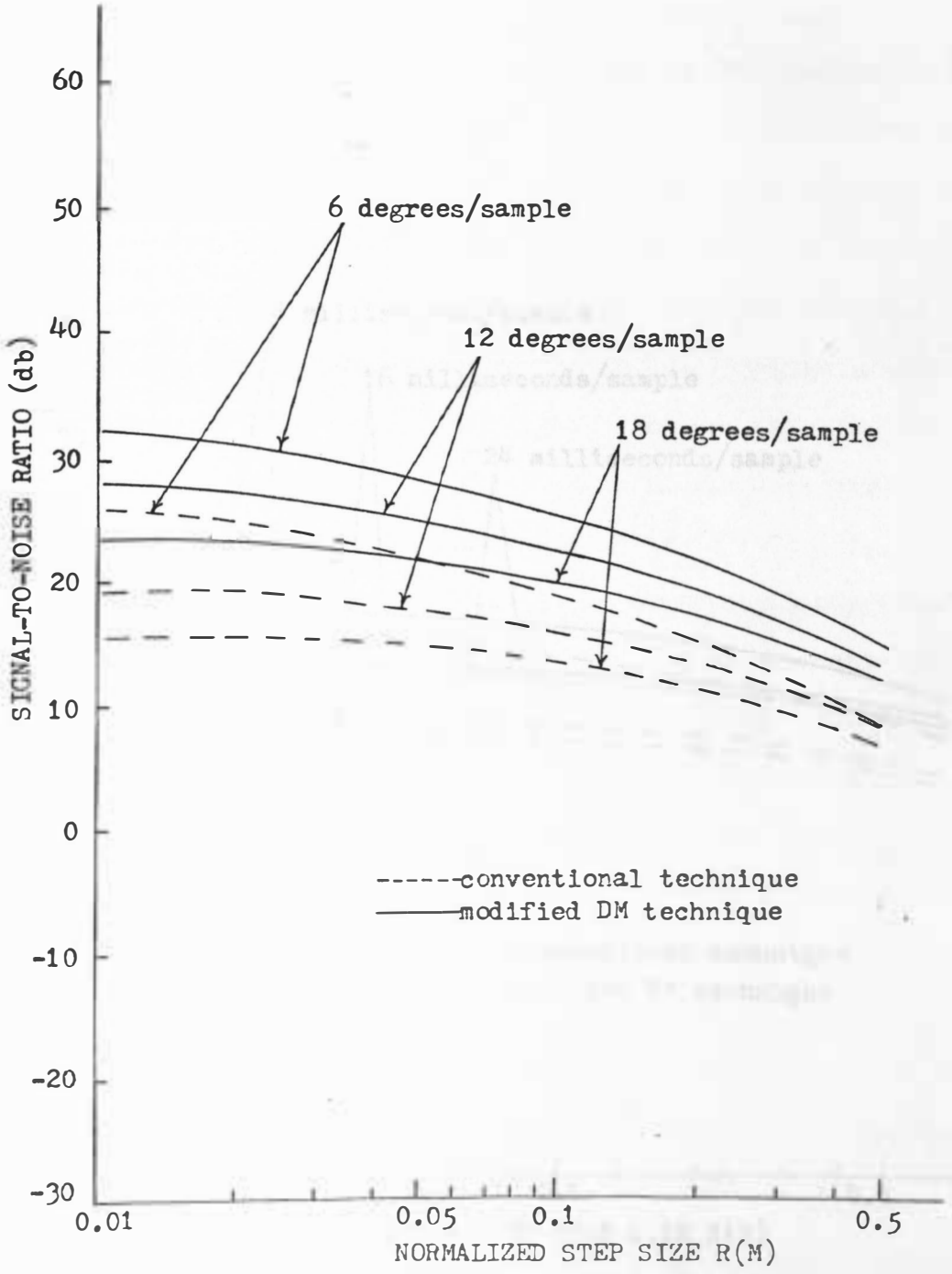


Figure 4-16. Signal-to-noise ratio versus normalized R(M) by the conventional and modified DM techniques for the sine wave input.

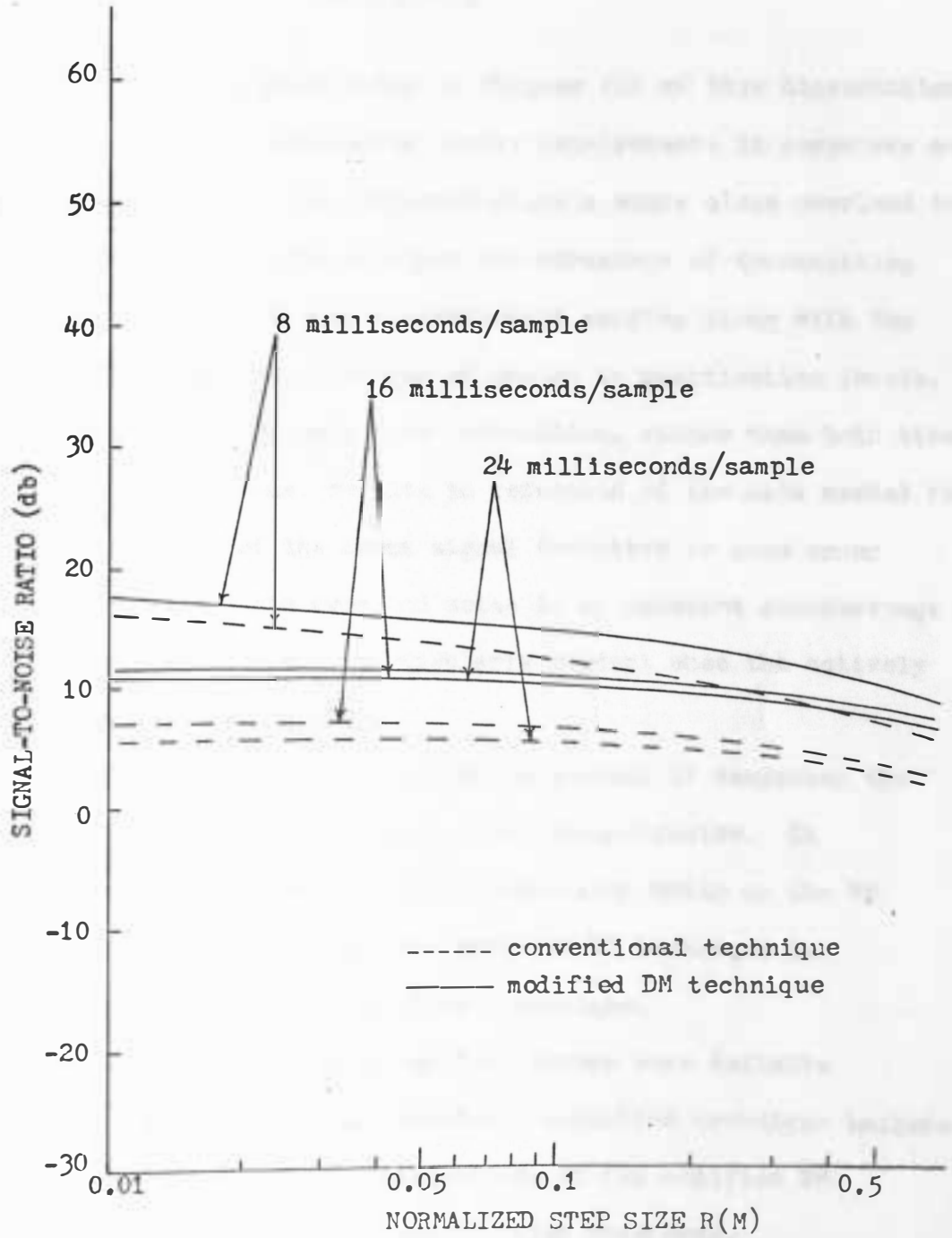


Figure 4-17. Signal-to-noise ratio versus normalized R(M) by the conventional and modified DM techniques for the ECG data input.

# CHAPTER V

## CONCLUSIONS

The DM technique investigated in Chapter III of this dissertation shows possibilities for decreasing memory requirements in computers and data storage systems for low frequency signals where slope overload is minimized. The DM technique provides the advantage of transmitting only the time interval between non-redundant samples along with the sign which determines the direction of change in quantization levels. Thus, the transmission of only time information, rather than both time and amplitude informations, results in reduction of the data needed for faithful reproduction of the input signal (relative to some error criteria). Yet, the slope overload noise is an inherent disadvantage of the DM technique. This is particularly evident when the actively changing signals are processed.

The modified DM technique proposed in Chapter IV decreases the slope overload noise by employing adaptive reconstructor. It maintains the same efficiency or data compression ratio as the DM technique of Chapter III. Thus, the modified DM technique is definitely superior to the conventional technique.

Areas which need more investigations before more definite conclusions can be made on this redundancy reduction technique include:

(1) Investigation of the applications of the modified DM technique to various kinds of input waveforms.

(2) Investigation of a method to reduce or eliminate the phase distortion noise of the modified DM technique.

(3) Investigation of a method to detect the output signal level periodically to maintain the correct waveform continuity between adjacent output data values in case of noise disturbances.

(4) Substantiation of the experimental results of this dissertation through practical system implementation.

## REFERENCES


1. Andrews, C. A., J. M. Davies, and G. R. Schwartz, "Adaptive Data Compression", Proc. IEEE, Vol. 55, March 1967, pp. 267-277.

2. Balakrishnan, A. V., "On the Problem of Time Jitter in Sampling", IEEE Trans. on Information Theory, Vol. IT-8, April 1962, pp. 226-236.

3. Black, H. S., Modulation Theory, D. Van Norstand Company, Inc., 1953, pp. 37-41.

4. Birznieks, U., Computer Simulation of a New Redundancy Reduction Technique, M.S. Thesis, South Dakota State University, 1968.

5. Cutler, C. C., "Scanning the Issue", Proc. IEEE, Vol. 55, March 1967, pp. 251-252.

6. Davisson, D. L., Theory of Data Compression, PhD. dissertation, University of California, Los Angeles, 1969.

7. Downing, J. J., Modulation Systems and Noise, Prentice-Hall, Inc., 1965.

8. Gardenhire, L. W., "Redundancy Reduction--The Key to Adaptive Telemetry", presented at National Telemetering Conference, Los Angeles, California, June 1964.

9. Gardenhire, L. W., "Selecting Sampling Rates", I.S.A. Journal, Vol. II, April 1964, pp. 59-64.

10. Hochman, D. and D. R. Weber, "Adaptive Telemetry--Data Compression", Aerospace Telemetry, Vol. 2, ed. H. L. Stiltz, Prentice-Hall, Inc., 1966, pp. 167-201.

11. Kortman, C. M., "Redundancy Reduction--A Practical Method of Data Compression", Proc. IEEE, Vol. 55, March 1967, pp. 253-266.

12. Kuo, B. C., Analysis and Synthesis of Sampled Data Control Systems, Prentice-Hall, Inc., 1963, pp. 27-28.

13. Liu, B. and T. P. Stanley, "Error Bounds for Jittered Sampling", IEEE Trans. on Automatic Control, Vol. Ac-10, October 1965, pp. 449-454.

14. Medlin, J. E., "Sampled-Data Prediction for Telemetry Bandwidth Compression", IEEE Trans. on Space Electronics and Telemetry, Vol. SET-11, March 1965, pp. 25-36.

15. O'Neal, J. B., Jr., "Delta Modulation Quantizing Noise Analytical and Computer Simulation Results for Gaussian and Television Input Signals", The Bell System Technical Journal, Vol. XLV, January 1966, pp. 117-141.

16. Panter, P. E., Modulation, Noise and Spectral Analysis, McGraw-Hill, Inc., 1965, pp. 679-699.

17. Papoulis, A., "Error Analysis in Sampling Theory", Proc. IEEE, July 1966, pp. 947-955.

18. Sander, D. E., "Reduction of Memory and Data Storage Requirements by an Adaptive Sampling Technique", private communication, October 1967.

19. Schouten, J. F., F. DeJager, and J. A. Greefkes, "Delta Modulation, a New Modulation System for Telecommunication", Philips Technical Review, Vol. 13, 1952, pp. 237-245.

20. Slaughter, J. B., "Quantization Errors in Digital Control Systems", Proc. IEEE, January 1964, pp. 70-74.

21. Stein, S., and Jones, J. J., Modern Communication Principles, McGraw-Hill, Inc., 1967, pp. 196-210.

22. System/360 Scientific Subroutine Package (360A-CM-03X), Version II, Programmer's Manual, International Business Machines Corporation, 1967, pp. 54.

23. Wozencraft, J. M., and Jacobs, I. M., Principle of Communication Engineering, John-Wiley & Sons, Inc., 1965, pp. 285-297.

24. Winkler, M. R., "High Information Delta-Modulation", IRE Convention Record, 1963.

25. Yasuda, Y., H. Inosi, and J. Murakami, "A Telemetering System by Code Modulation: Delta-Sigma Modulation", IRE Transaction on Space Electronics and Telemetry, pp. 204-209, September, 1962.

# APPENDIX A

## ECG TAPE FORMAT

GENERAL: All tape records are written by IBM 1800 computer FORTRAN in un-formatted mode. As a result, all physical tape records are 146 words in length. One word is 16 binary bits. Each physical record contains, at most, 144 words of data. The first word of the physical record is the physical record number within the logical record. The second word of the record indicates the number of words of the physical record used by the logical record.

ECG LOGICAL RECORDS: Each ECG patient record consists of 21 logical records. The first logical record is 16 words long and contains the identification information for the patient record. This record is referred to as the directory record.

LOGICAL RECORD 1:

| | |
|---|---|
| word 1 | Patient I.D. |
| word 2 | Time |
| word 3 | Unused |
| word 4 | Unused |
| word 5 | Day of Year |
| word 6 | RMS Noise |
| words 7-16 | Unused |

Patient I.D. is a 5 digit number. If the last 3 digits are '999', the record is a calibrated record.

Time is a 5 digit number, the first two digits indicate hour, the last 3 digits indicate thousandths of an hour.

Day of year is a 3 digit number indicating the date of the collection.

RMS Noise is the root-mean-square in millivolts present on the telephone line at the time of the data transmission.

LOGICAL RECORDS 2 thru 21:

These logical records contain the digitized ECG data. Each logical record is 320 words long. The 319th word is patient I.D., the 320th word is time. The first 318 words of the logical record consist of 106 sets of readings of each of the X, Y, and Z leads. Data order is X, Y, Z, X, Y, Z, ..... Each piece of data is a binary number ranging between -32768 and +32767. This number can be converted to volts by multiplying by +0.00015259. Each consecutive set of X, Y, Z data points is separated in time by 0.004 seconds.

The end of the tape is indicated by a directory record with all 16 words equal to zero.

# APPENDIX B

## FLOW DIAGRAM OF THE COMPUTER PROGRAM FOR PARAMETER CALCULATION FOR THE MODIFIED DM TECHNIQUE.

The flow diagram in Figure B-1 outlines the computer operations used to calculate mean-square errors and peak errors for the conventional and the modified DM techniques discussed in Chapter IV.

The flow diagram uses standard symbols and format. Variables used in the diagram are defined as:

X = ECG data read from magnetic tape

I = sampling interval size

M = number of quantization levels in the positive half plane

FDR(K) = value of the Kth quantization level

R(M) = quantization step size

YJ = output of the quantizer

YJL = output of the quantizer previous to YJ

YJS = YJL

QCDFSQ = the summation of the squared differences between the input and the reconstructed output data by the conventional technique

QCPKR(M) = the peak error by the conventional technique

ASDIFF = the absolute value of the slope of a sampling interval

LLL = number of subintervals

QRCN = output of the reconstructor

QRCNSV = output of the reconstructor previous to QRCN but not including subinterval outputs

WGT = weighting factor from the calculation of interval size

DFSQ = the summation of the squared difference between the input and the reconstructed output data for the modified DM technique

PKR(M) = the peak error by the modified DM technique

TDWGT = the absolute value of the difference between the input data interval size and the reconstructed output interval size

SNN = the summation of the input data intervals

DELTQT = the summation of the reconstructed output data intervals.

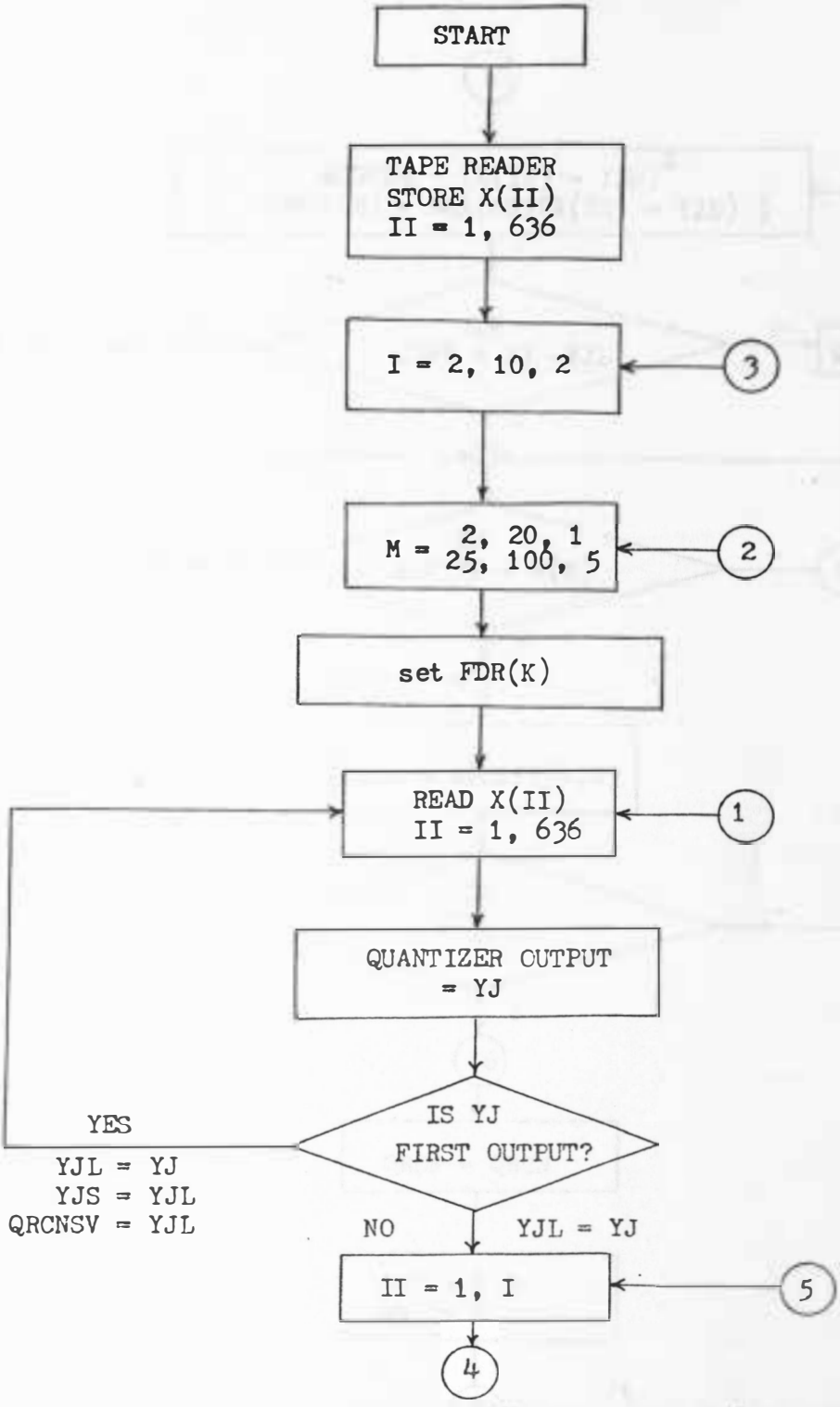


Figure B-1. Flow diagram for computing the M.S.E. and peak error for the modified DM technique.

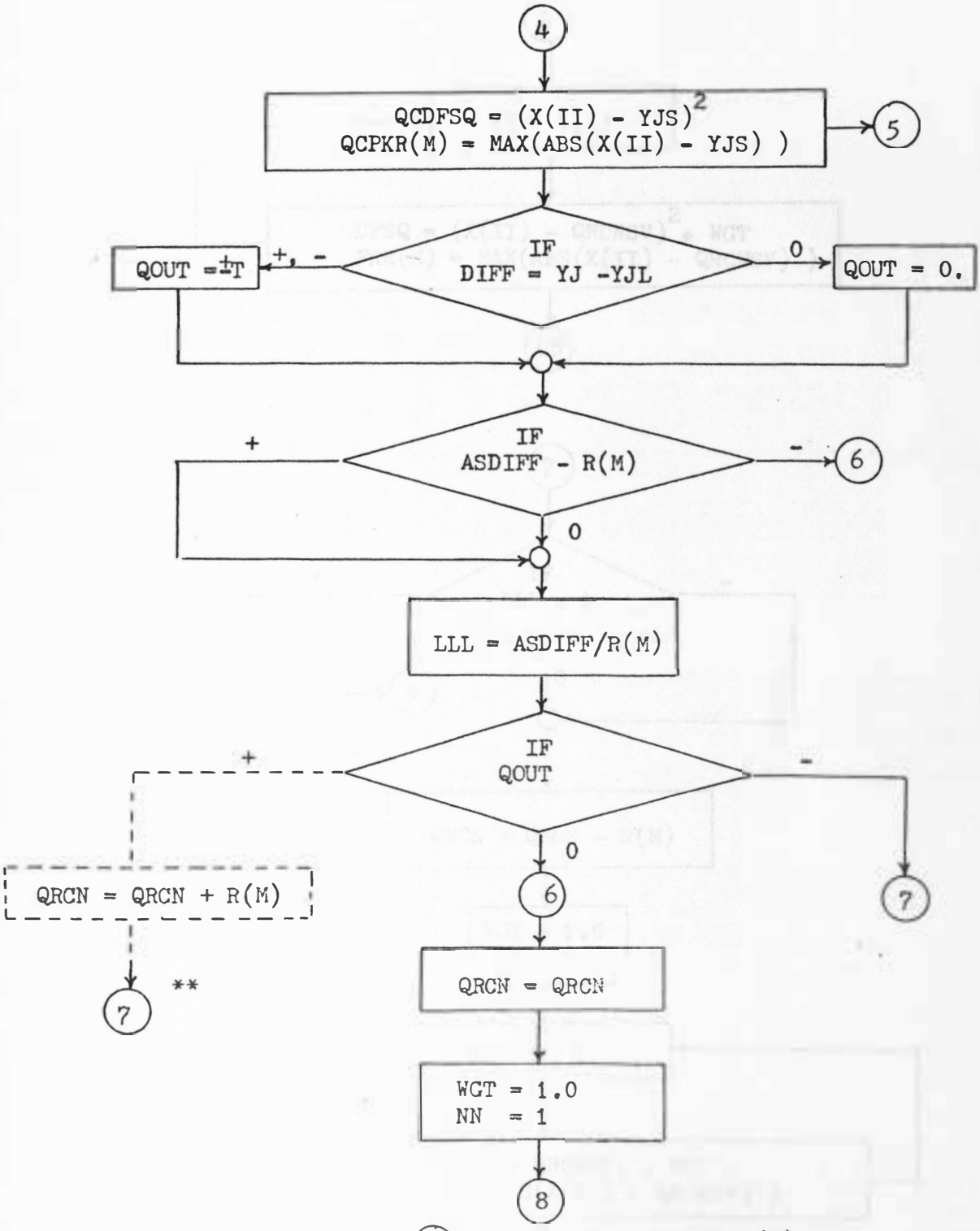


** This loop is same as loop (7) except QRCN = QRCN + R(M)

Figure B-1. (continued)

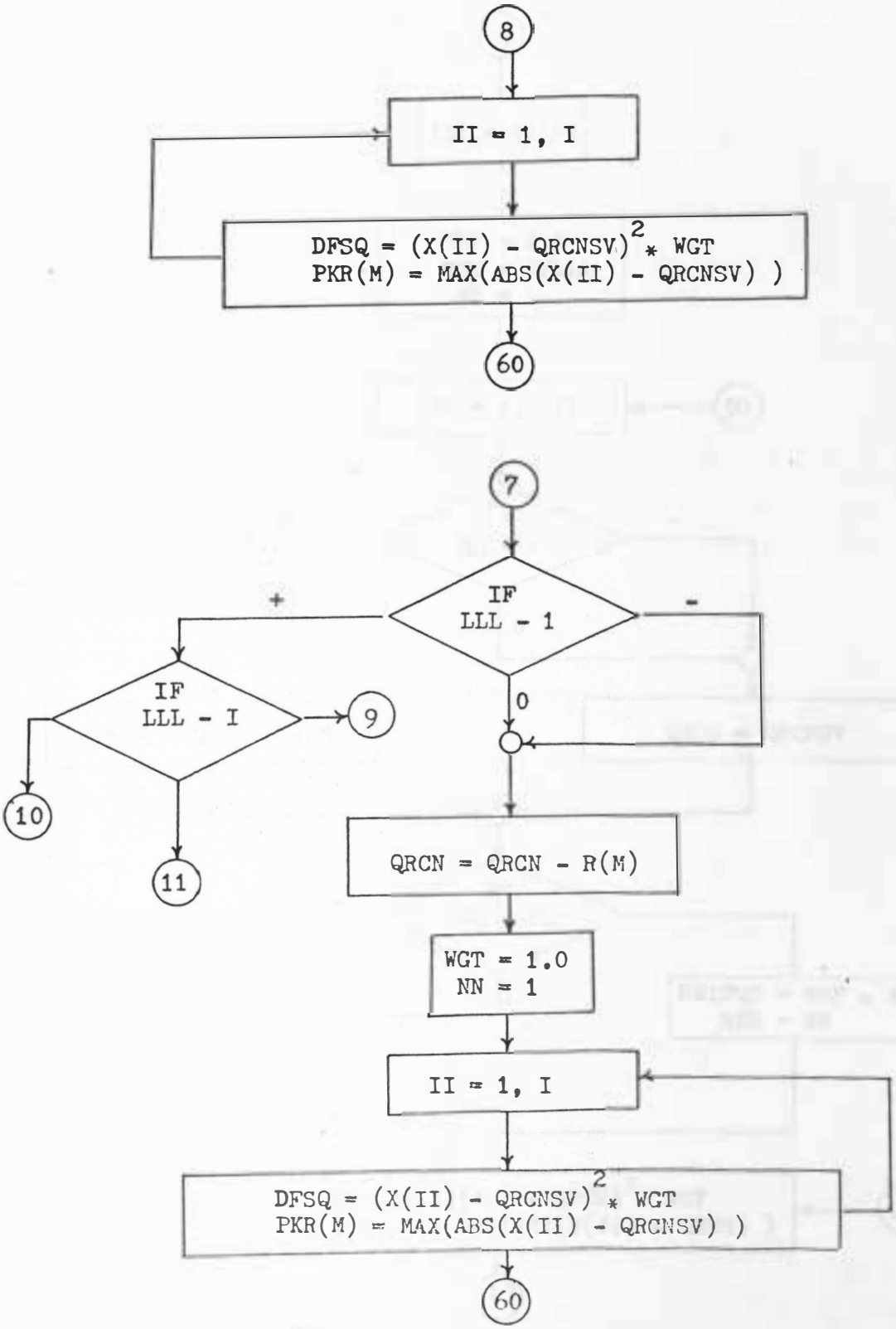


Figure B-1. (continued).

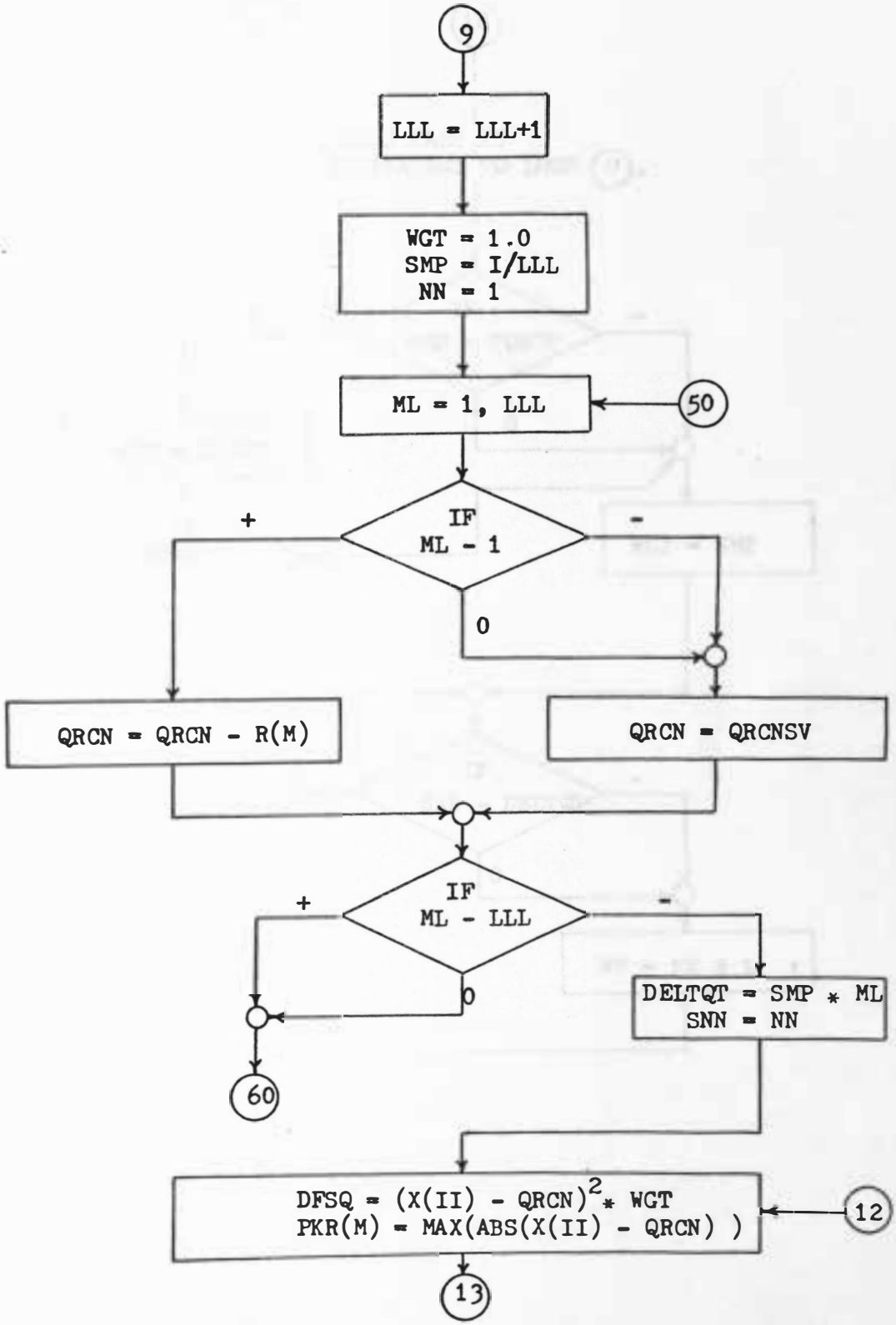


Figure B-1. (continued).

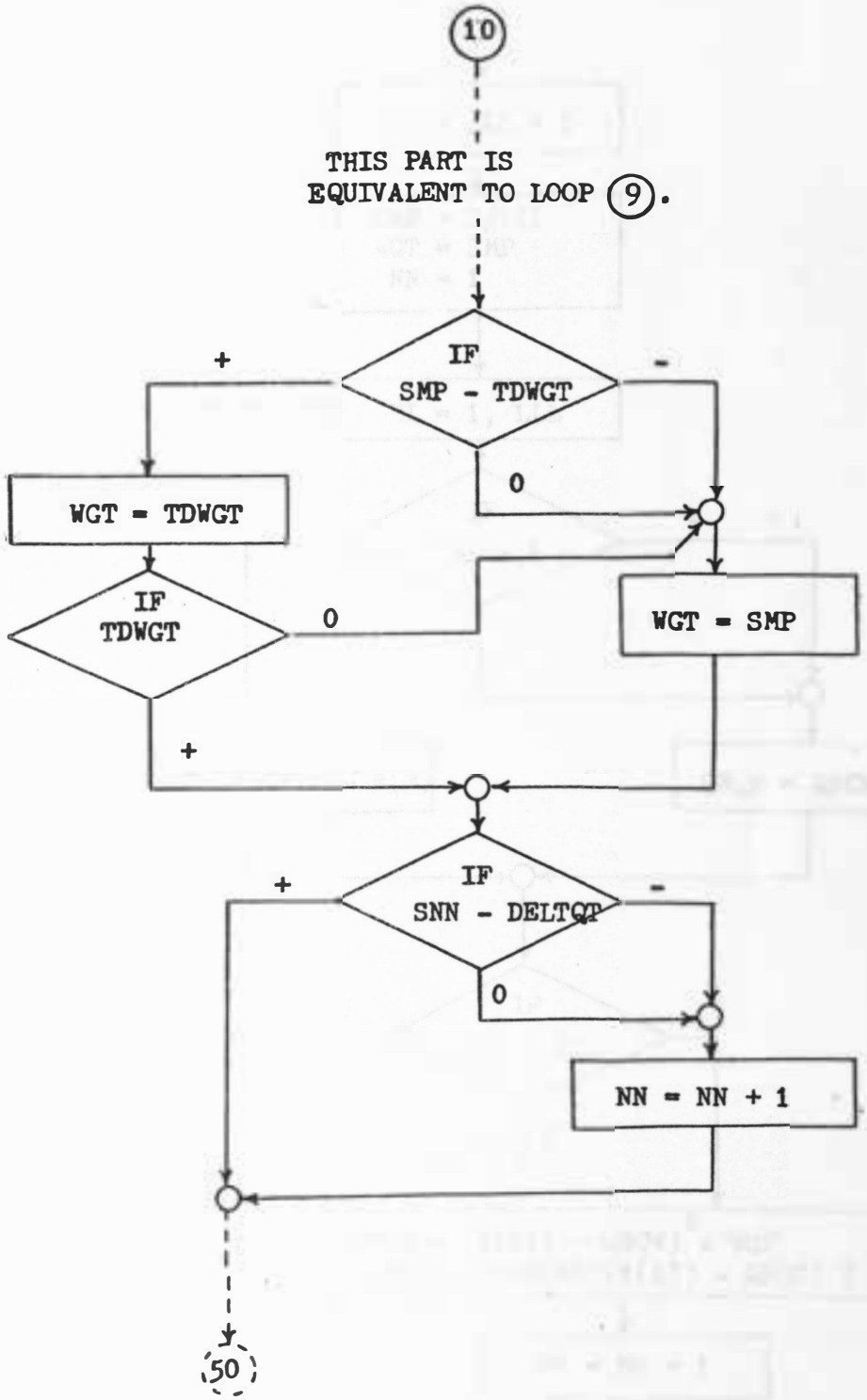


Figure B-1. (continued).

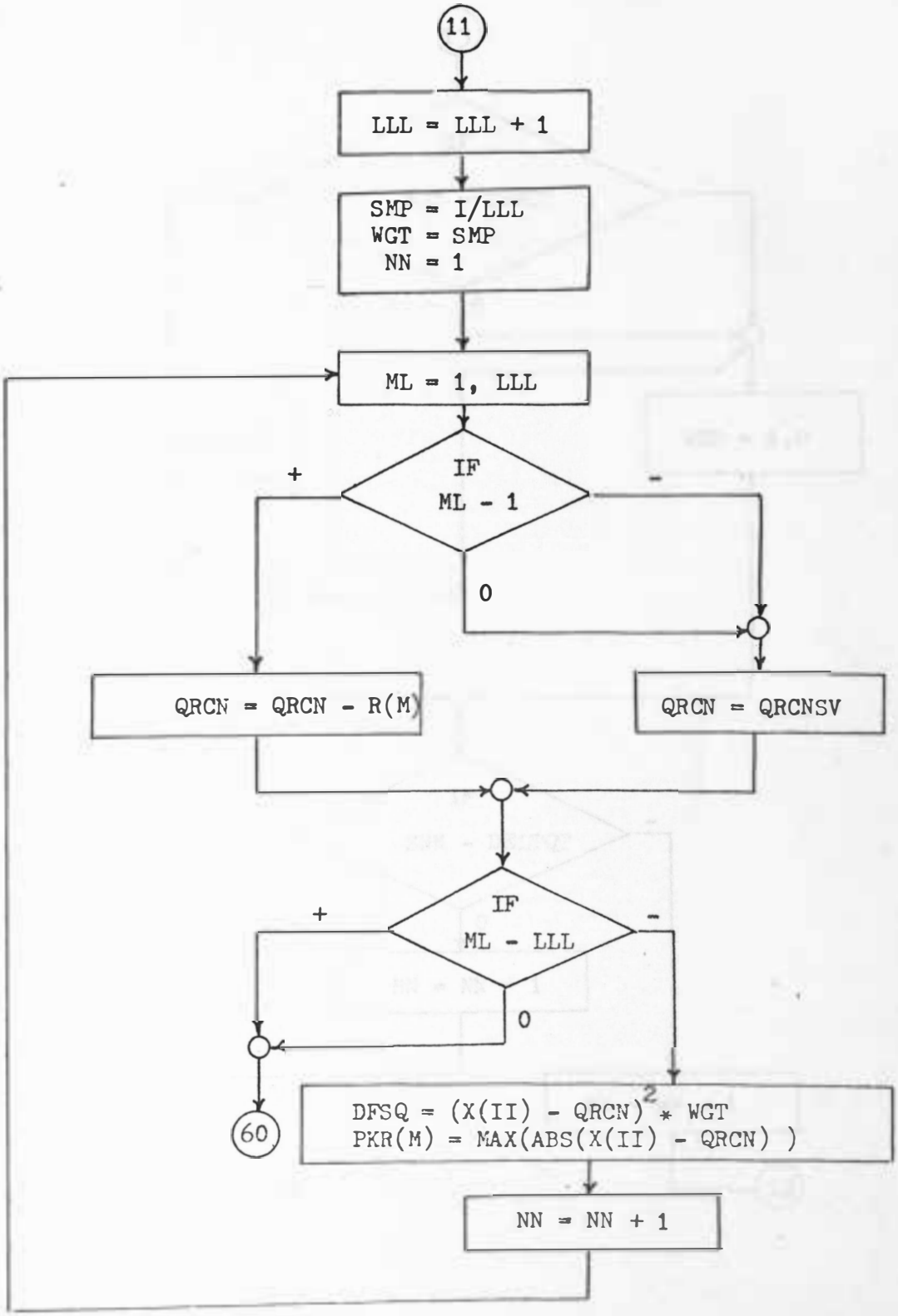


Figure B-1. (continued).

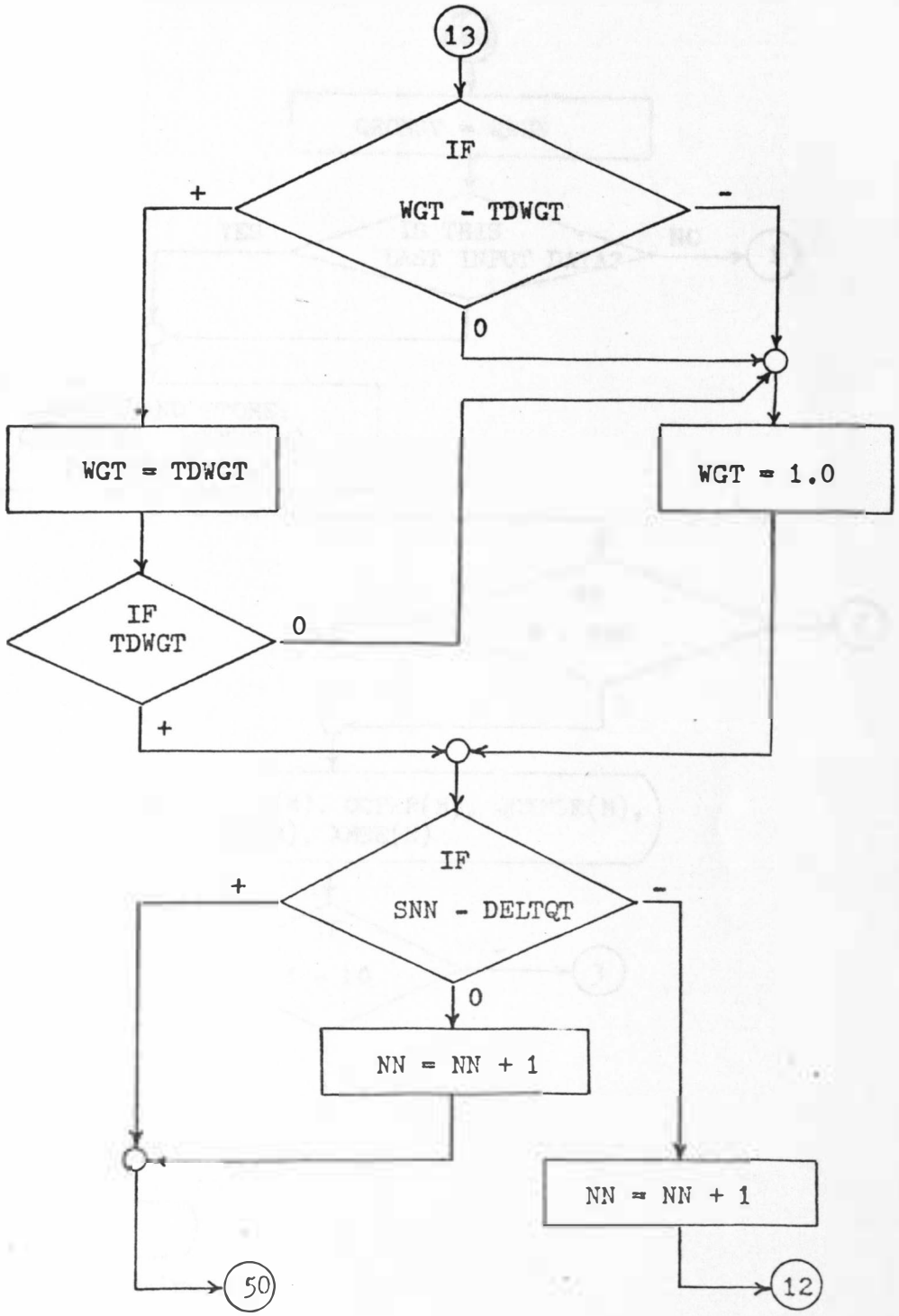


Figure B-1. (continued).

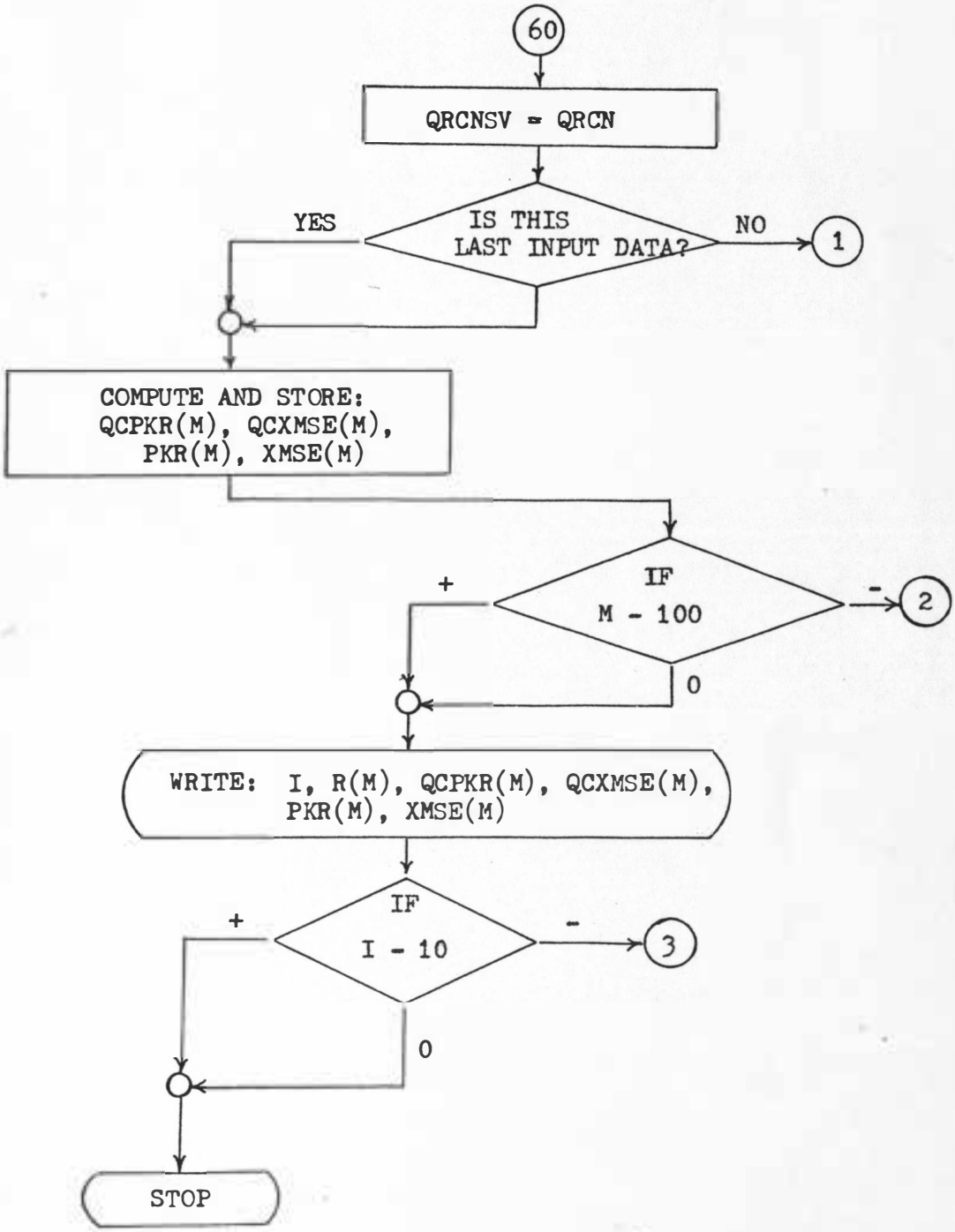


Figure B-1. (continued).